

AD-760 783

HF AND VHF OBLIQUE BACKSCATTER AND  
SCINTILLATION STUDY

Sunanda Basu, et al

Emmanuel College

Prepared for:

Air Force Cambridge Research Laboratories

January 1973

DISTRIBUTED BY:

**NTIS**

National Technical Information Service  
U. S. DEPARTMENT OF COMMERCE  
5285 Port Royal Road, Springfield Va. 22151

HF AND VHF OBLIQUE BACKSCATTER AND SCINTILLATION STUDY

BY  
SUNANDA BASU  
ROBERT L. VESPRINI  
EILEEN MARTIN

EMMANUEL COLLEGE  
400 THE FENWAY  
BOSTON MASSACHUSETTS 02115

Contract No. F19628-71-C-0250

Project No. 414 L



FINAL REPORT

Period Covered: 15 July 1971 through 14 January 1973

January 1973

Contract Monitor: Jules Aarons, Ionospheric Physics Laboratory

Approved for public release; distribution unlimited.

Prepared for

AIR FORCE CAMBRIDGE RESEARCH LABORATORIES  
AIR FORCE SYSTEMS COMMAND  
UNITED STATES AIR FORCE  
BEDFORD, MASSACHUSETTS 01730

Reproduction of this  
NATIONAL TECHNICAL  
INFORMATION SERVICE

AD 760783

Unclassified

Security Classification

DOCUMENT CONTROL DATA - R&D		
(Security classification of title, body of abstract and indexing annotation must be entered when the overall report is classified)		
1. ORIGINATING ACTIVITY (Corporate author) Emmanuel College 400 The Fenway Boston Massachusetts 02115		2a. REPORT SECURITY CLASSIFICATION Unclassified 2b. GROUP
3. REPORT TITLE HF AND VHF OBLIQUE BACKSCATTER AND SCINTILLATION STUDY		
4. DESCRIPTIVE NOTES (Type of report and inclusive dates) Scientific. Final. 15 July 1971-14 January 1973 Approved 20 Apr '73		
5. AUTHOR(S) (First name, middle initial, last name) Sunanda Basu Robert L. Vesprini Eileen Martin		
6. REPORT DATE January 1973	7a. TOTAL NO. OF PAGES 114	7b. NO. OF REFS 13
8a. CONTRACT OR GRANT NO. F19628-71-C-0250	8b. ORIGINATOR'S REPORT NUMBER(S)	
9. PROJECT, TASK, WORK UNIT NOS.	9a. OTHER REPORT NO(S) (Any other numbers that may be assigned this report)	
10. DOD ELEMENT	AFCRL-TR-73-0207	
11. DOD SUBELEMENT		
12. DISTRIBUTION STATEMENT A-Approved for public release; distribution unlimited.		
13. SUPPLEMENTARY NOTES		14. SPONSORING MILITARY ACTIVITY Air Force Cambridge Research Laboratories L.G. Hanscom Field Bedford Massachusetts 01730
15. ABSTRACT The research conducted under this contract was concerned primarily with HF and VHF oblique backscatter observations, made at Plum Island MA, 56° N invariant, over nearly half a solar cycle. The backscatter analysis was performed in two parts. The first part was concerned with the field-aligned irregularities in the E-layer and their association with the ground backscatter echo which are propagated via sporadic E (E <sub>s</sub> ) reflection. It was found that under quiet magnetic conditions the field-aligned echo from E-layer heights (FAE(E)) displays a summer evening maximum in conjunction with the ground E <sub>s</sub> echo. The second part of the study was concerned with the occurrence characteristics of the field-aligned irregularities in the F-layer and their relationship, if any, to the backscatter signal propagating via the F-layer (1F echo). It was found that the field-aligned echo from the F-layer (FAE(F)) was primarily a sunset phenomenon showing strong solar cycle dependence during quiet times, increasing monotonically with the magnetic index until a certain threshold value was reached (Kf <sub>min</sub> = 4) and decreasing beyond that value. The 1F echo was found to be unaffected by the presence of either FAE(F) or E <sub>s</sub> clouds, but was found to be very sensitive function of the F-region parameters. Ray tracings through model ionospheres were used to confirm these hypotheses.		

DD FORM 1473  
1 NOV 66

Unclassified

Security Classification

Unclassified

Security Classification

14.	KEY WORDS	LINK A		LINK B		LINK C	
		ROLE	WT	ROLE	WT	ROLE	WT
	Backscatter Scintillation Aurora Ionosphere Radar						

Unclassified

Security Classification

## ABSTRACT

The research conducted under this contract was concerned primarily with HF and VHF oblique backscatter observations, made at Plum Island MA, 56° N invariant, over nearly half a solar cycle. The backscatter analysis was performed in two parts. The first part was concerned with the field-aligned irregularities in the E-layer and their association with the ground backscatter echo which are propagated via sporadic E ( $E_s$ ) reflection. It was found that under quiet magnetic conditions the field-aligned echo from E-layer heights (FAE(E)) displays a summer evening maximum in conjunction with the ground  $E_s$  echo. The second part of the study was concerned with the occurrence characteristics of the field-aligned irregularities in the F-layer and their relationship, if any, to the backscatter signal propagating via the F-layer (1F echo). It was found that the field-aligned echo from the F-layer (FAE(F)) was primarily a sunset phenomenon/showing strong solar cycle dependence during quiet times, increasing monotonically with the magnetic index until a certain threshold value was reached ( $Kf_t = 4$ ) and decreasing beyond that value. The 1F echo was found to be unaffected by the presence of either FAE(F) or  $E_s$  clouds, but was found to be very sensitive function of the F-region parameters. Ray tracings through model ionospheres were used to confirm these hypotheses.

Finally, the occurrence patterns of scintillations of signals from the geostationary satellite ATS-3 at 137 MHz during magnetic storms was investigated. It was found that at Narssarssuaq the stormtime scintillations showed strong seasonal patterns whereas at Hamilton, where a delayed effect was observed, the seasonal aspect was not so marked. The behavior of the various auroral electrojet indices during the magnetic storms which occurred in 1970 were also studied.

## TABLE OF CONTENTS

	<u>Page</u>
SEASONAL PATTERNS OF AURORAL AND MIDLATITUDE GEOSTATIONARY SATELLITE SCINTILLATIONS DURING MAGNETIC STORMS	4
Figures	8 - 13
References	14
 HF BACKSCATTER STUDY AT 19.4 MHz THROUGH SUBAURORAL IONOSPHERE	
Abstract	16
Table of Contents	17
List of Figures	18
Figures	37 - 55
References	56
 FIELD ALIGNED E- AND F-LAYER BACKSCATTER OBSERVATIONS	
Abstract	61
Table of Contents	62
List of Figures	63
Figures	80 - 110
References	111

Seasonal Patterns of Auroral and Midlatitude  
Geostationary Satellite Scintillations during Magnetic Storms.

Recent analysis of amplitude records of the 137 MHz signal from ATS-3 as observed from Narssarssuaq, Greenland (invariant latitude of the sub-ionospheric point referred to a height of 300 km being  $64^{\circ}N$ ) has shown a very consistent seasonal pattern of scintillations in addition to diurnal and magnetic dependence (Aarons et al., 1972). Sufficient data (September 1968 to March 1972) has been accumulated at Narssarssuaq to justify a statistical study of the seasonal patterns of amplitude scintillation during magnetic storms.

The particular magnetic storms which were chosen for this analysis were those which had a sudden storm commencement (SSC) and were reported by at least eight or more observatories as listed in the Solar Geophysical Data Books, Aeronomy and Space Data Center, Boulder, Colorado. Moreover, since the diurnal pattern as well as the stormtime behavior were also of interest, a program of analysis similar to that used by Mendillo (1971) was utilised for the study. It was found that thirty-two storms during the three and a half year period met all the above requirements.

A similar study of the Sagamore Hill ATS-3 scintillation data was also undertaken to determine seasonal patterns, if any, in the midlatitude ionosphere. The observation period for the

Sagamore Hill Radio Observatory data was from November 1967 to March 1972. In this case thirty-nine storms were found which met all the requirements outlined in the previous paragraph.

The quiet median seasonal patterns for both stations were established by taking all the data in each season which corresponded to a planetary magnetic index of  $K_p = 0$  or 1 and then determining the diurnal distribution of such data. As the two equinoxes showed similar behavior (Aarons et al., 1972) it was decided to divide the year into three seasons, namely the summer (May through August), equinoxes (September, October, March and April), and winter (November through February).

#### Results for Marssarsuaq

The seasonal behavior of scintillations during storms and quiet periods are shown in Figures 1 through 3. Figures 1 and 2, which show, respectively, the summer and equinox behaviors, are somewhat similar. During quiet periods ( $K_p=0,1$ ) in both seasons there is a deep minimum during the daytime and a maximum at 0100 UT (2200 LMT) when the median scintillation indices reach a value as high as 80 per cent. The effect of storms during these two seasons seems to be a marked increase of the daytime scintillations on the day of SSC. On the day after SSC (marked SD2) nighttime scintillations are higher than during the quiet periods. Also the daytime scintillation level is somewhat higher than the quiet day



but lower than the occurrence on SSC day. The second and third days after SSC day (labelled SD3 and SD4) show a scintillation behavior similar to the quiet day pattern. It is to be pointed out that the median quiet day pattern was obtained for one complete day in each season and the same pattern was repeated on the three succeeding days for comparison purposes.

The winter behavior shown in Figure 3 is entirely different from the ones presented in the two previous diagrams. The diurnal pattern during quiet days does not show a marked day to night variation. The daytime level is similar to the other seasons but the night to day index ratio is only 2:1 as compared to Figures 1 and 2 where this same ratio is 7:1. The median stormtime behavior in spite of the scatter shows a similar night to day ratio of 2:1 where now the daytime values are around 50 per cent. The storm effect seems to persist well into the third and fourth days and this is also unlike the behavior in the other two seasons. Thus these three figures show a rather definite seasonal variation of both the quiet and disturbed day scintillation pattern.

#### Results for Hamilton

Three similar diagrams for Hamilton are presented in Figures 4 through 6. There is very little scintillations during quiet periods in any season with the median summer pattern showing no scintillation during the entire 24 hour period. The effect of the

magnetic storms is to increase the nighttime scintillations in all seasons. The effect seems to be most marked in summer when scintillations as high as 50% are observed during the night. The other rather interesting feature of the scintillations during storms at Hamilton seems to be the delayed onset -- the percentage occurrence is greater during the second night after SSC rather than during the night of the actual SSC date. This feature is different from that observed at Narssarssuaq where there is a gradual tapering off of the storm effect.

Further studies utilising the various auroral electrojet indices AE, AL, and AU as defined by Davis and Sugiura (1966) are being made to determine possible causes for determining stormtime and seasonal patterns of scintillation.

x QUIET DAY SI; Kp = 0,1

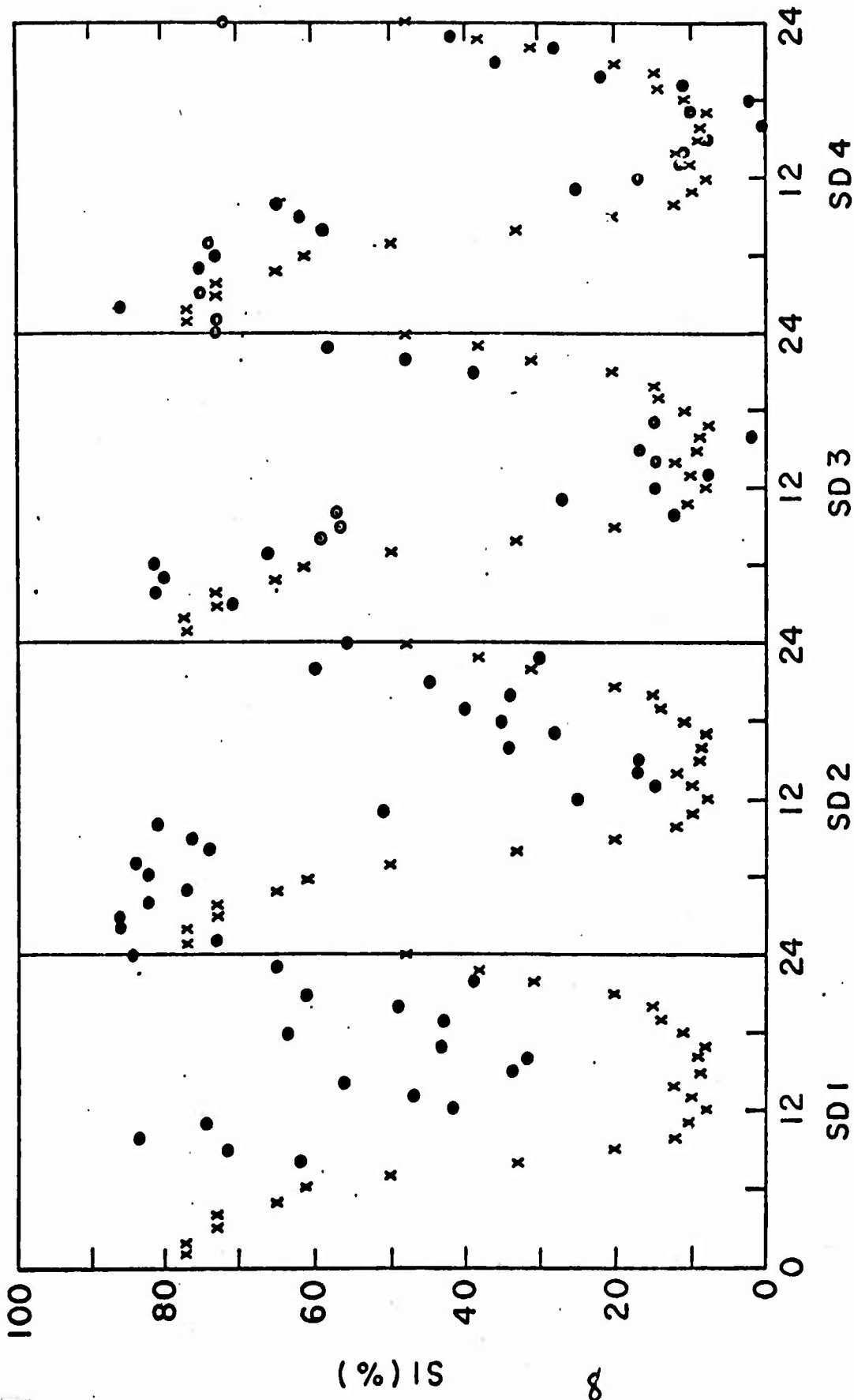
NSSQ

COMMIT

• STORM SI

9 STORMS

OCT 68 - MAR 72



MEDIAN DAILY SI VARIATIONS (UT)

Fig. 1

x QUIET DAY SI ;  $K_p = 0,1$

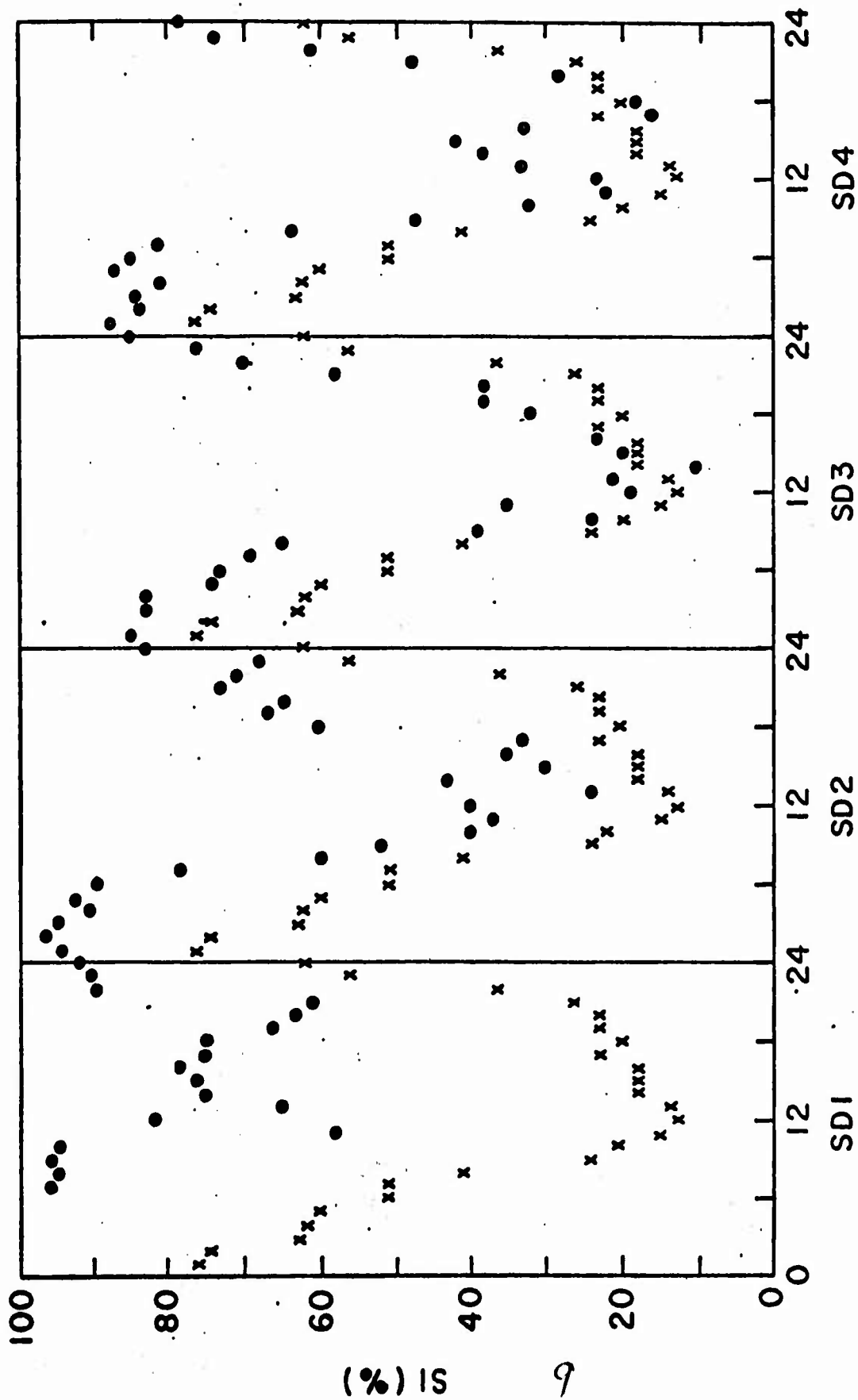
NSSQ

EQUINOX

• STORM SI

13 STORMS

OCT 68 - MAR 72



MEDIAN DAILY SI VARIATIONS (UT)

Fig 2

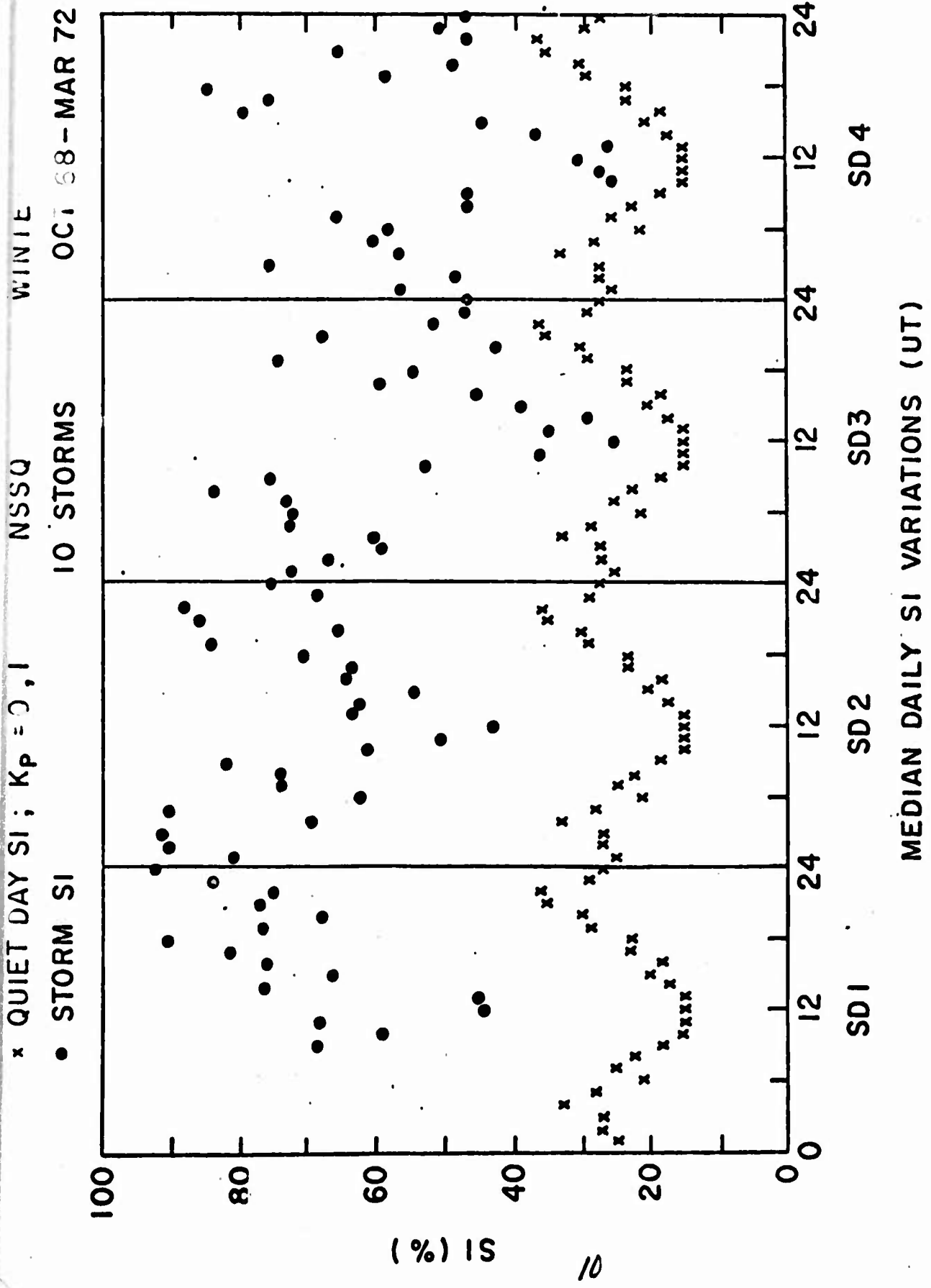


Fig. 3

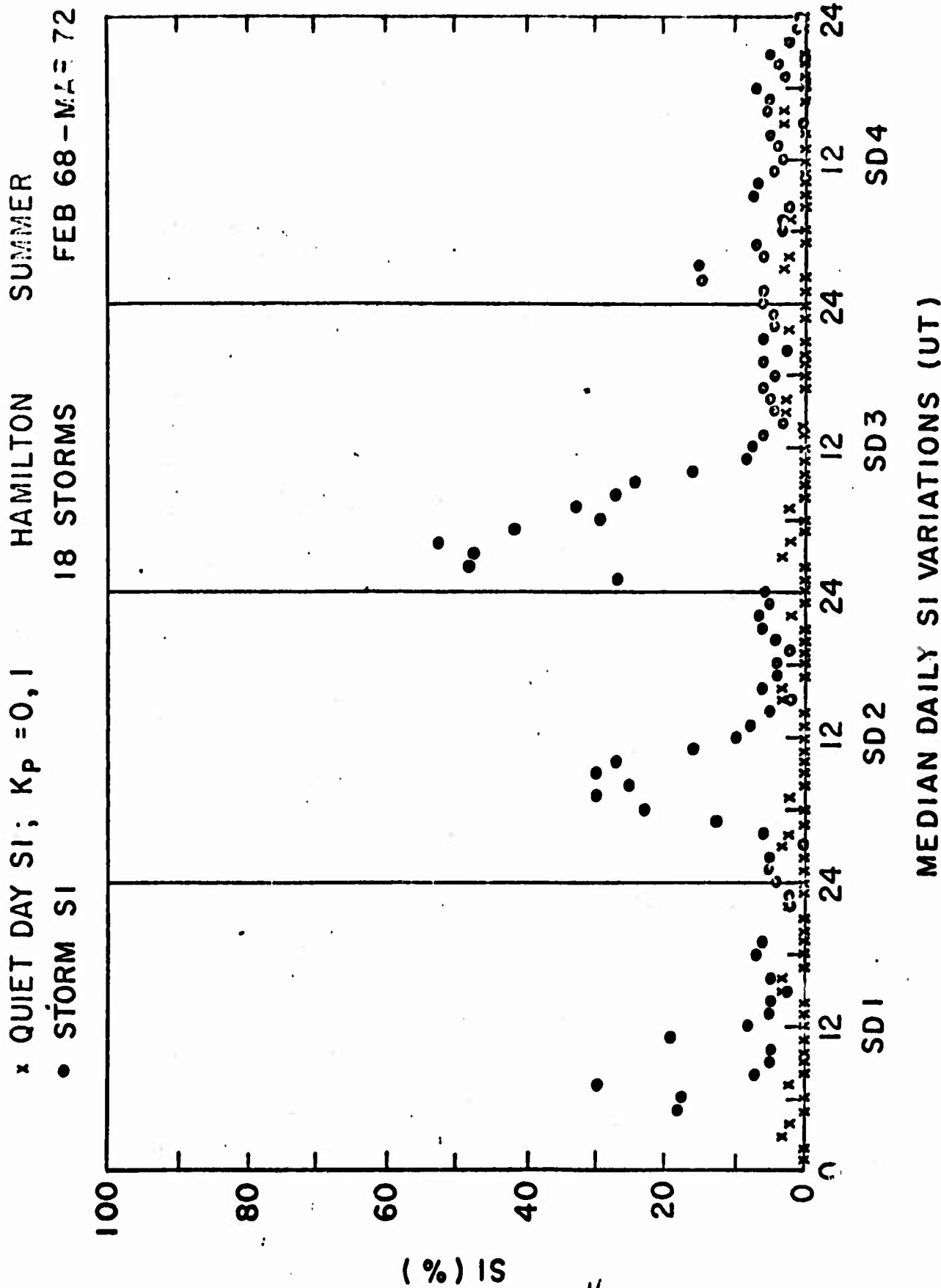


Fig. 4

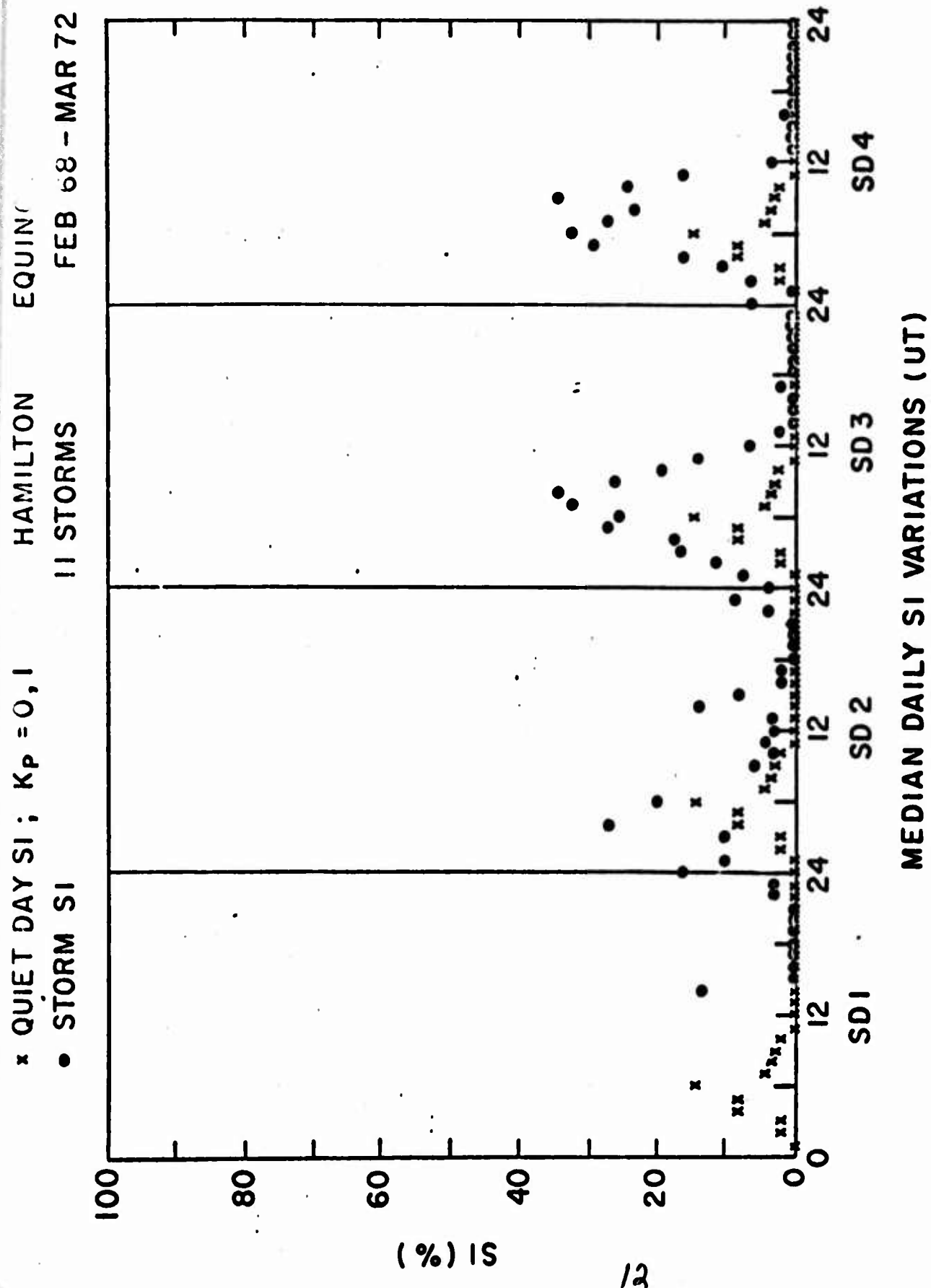
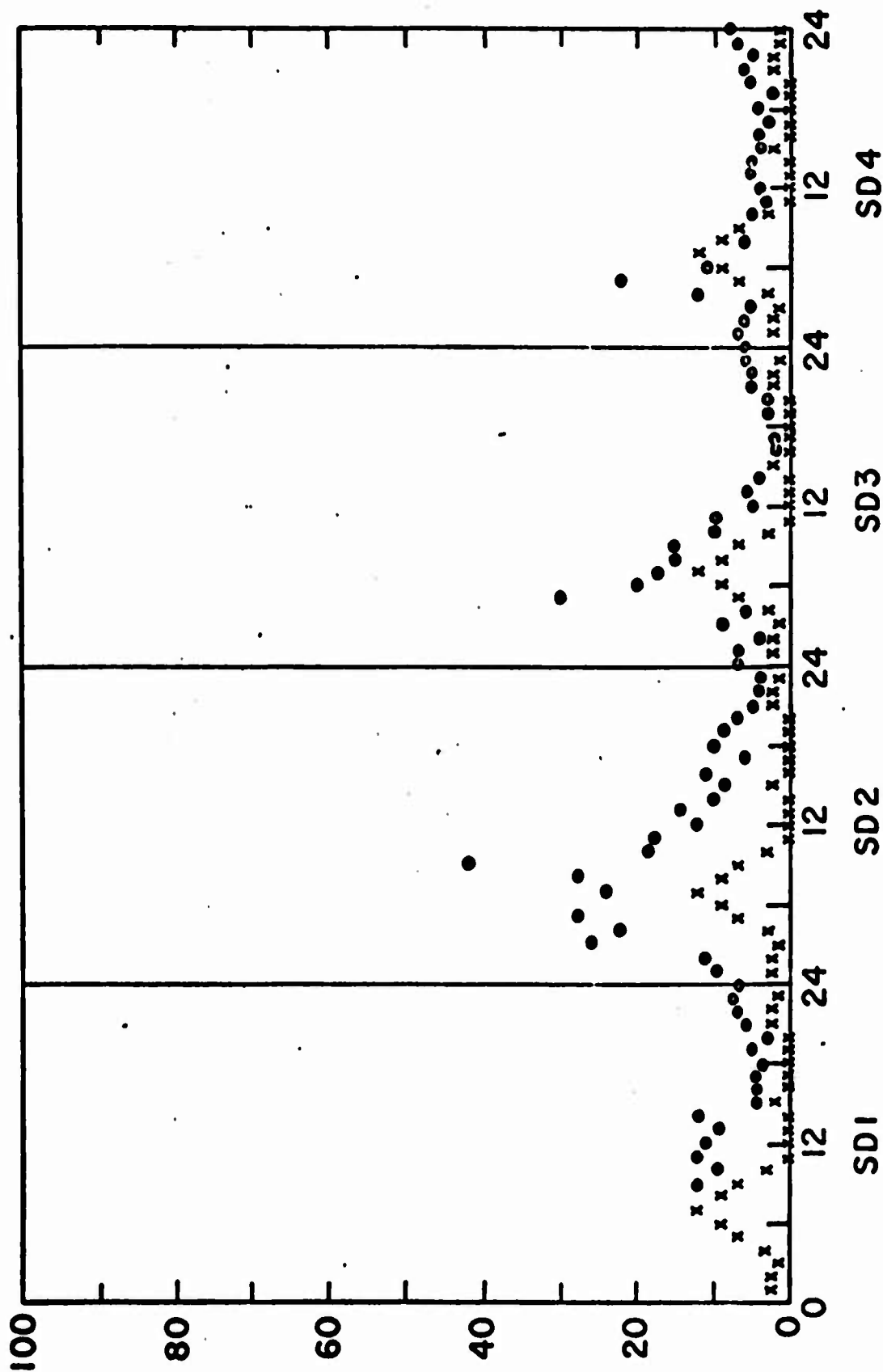


Fig. 5

x QUIET DAY SI;  $K_p = 0,1$       HAMILTON      WINTER  
 • STORM SI      10 STORMS      FEB 68 - MAR 72



MEDIAN DAILY SI VARIATIONS (UT)



### References

- Aarons, J., J.P. Mullen, H.E. Whitney and F. Steenstrup (1972), Seasonal, Diurnal and magnetic dependence of ionospheric scintillation at 64° invariant latitude, Planet Spa. Sci., 20, 957-964.
- Davis, T.N., and M. Sugiura (1966), Auroral electrojet activity index AE and its universal time variations, J. Geophys. Res., 71 785-801.
- Mendillo, M. (1971), Ionospheric total electron content behavior during geomagnetic storms, Nature, 234(45), 23-24.

**HF BACKSCATTER STUDY AT 19.4 MHz THROUGH SUBAURORAL IONOSPHERE**

**by**

**SUNANDA BASU**

**ROBERT L. VESPRINI**

**EMMANUEL COLLEGE  
400 THE FENWAY  
BOSTON, MASSACHUSETTS 02115**

## ABSTRACT

The aim of this study was to determine the effects of direct scatter from field aligned E- and F-layer irregularities, FAE(E) and FAE(F) respectively, as well as scatter from intense  $E_s$  clouds on the 19.4 MHz oblique backscatter signal propagating via the F layer (1F echo). It was found that the direct scatter from field aligned irregularities was weak in nature so that the 1F echo remained unaffected. In fact the presence of the 1F echo was often required to produce FAE(F). The  $E_s$  clouds which were frequently observed during the summer were also found to be non-blanketing so the  $E_s$  reflected echo and the 1F echo could exist simultaneously. However, it was found that the 1F echo was a very sensitive function of F-region parameters and was thus affected by both the seasonal and evening anomalies in F2 ionization at these latitudes. In addition, the changing magnetic declination to the east and west of the station was responsible for an asymmetry in the percentage of the time that the 1F echo was observed by the radar in these general directions.

Finally, the observed occurrence statistics of FAE(E) and FAE(F) presented in Scientific Report No. 1 are discussed in the context of current theories for the formation of these irregularities.

## TABLE OF CONTENTS

1. Introduction
2. Equipment and Data Reduction
3. Nomenclature and Identification of Echoes
4.  $E_s$  Propagation
  - 4.1 Correlation of FAE(E) and  $E_s$  Propagation
5. F-layer Propagation
  - 5.1 Effect of  $E_s$  on F-layer Propagation
  - 5.2 Effect of direct ionospheric scatter on F-layer propagation
  - 5.3 Effect of varying F-region parameters on 1F propagation
6. General Discussion on Formation and Occurrence of Field Aligned Irregularities
  - 6.1 FAE(E)
  - 6.2 FAE(F)
  - 6.3 Conclusion

## LIST OF FIGURES

### Figure

- 1 Percentage occurrence contours of  $E_s$  propagation in the NW quadrant for  $K_{F_r}$  0-3
- 2 Percentage occurrence contours of  $E_s$  propagation in the NE quadrant for  $K_{F_r}$  0-3
- 3 Average diurnal variation of  $E_s$  propagation in the NW quadrant for  $K_{F_r}$  0-3, 1961-1965
- 4 Percentage occurrence contours of  $f_oE_s \geq 5$  MHz for Ottawa
- 5 Percentage occurrence contours of FAE(E) for  $K_{F_r}$  0-3
- 6 Average diurnal variation of FAE(E) when  $E_s$  propagation is present for  $K_{F_r}$  0-3, 1961-1965
- 7 Average seasonal variation of FAE(E) for various ranges of  $K_{F_r}$ , 1961-1965
- 8 Percentage occurrence contours of 1F echo in the NW quadrant for  $K_{F_r}$  0-3
- 9 Percentage occurrence contours of 1F echo in the NE quadrant for  $K_{F_r}$  0-3
- 10 Average diurnal variation of 1F echo occurrence and of FAE(F) occurrence when 1F echo is present for  $K_{F_r}$  0-3, 1961-1965
- 11 Diurnal pattern of the extent of the F-layer irregularity region during quiet magnetic conditions ( $K_{F_r}$  0-3)
- 12 Average diurnal variation of 1F echo occurrence and of FAE(F) occurrence when 1F echo is present for  $K_{F_r}$  4-9, 1961-1965
- 13 Percentage occurrence contours of FAE(F) for  $K_{F_r}$  0-3
- 14 Average seasonal variation of FAE(F) for various ranges of  $K_{F_r}$ , 1961-1965

Figure

- 15      FAE(E) and FAE(F) as a function of  $K_{Fr}$
- 16      Monthly median  $f_oF2$  contours for Winnipeg  
         (Ke ora after Oct 1963)
- 17      Monthly median M(3000)F2 contours for Winnipeg  
         (Kenora after Oct 1963)
- 18      Monthly median  $f_oF2$  contours for St. John's, Newfoundland
- 19      Monthly median M(3000)F2 contours for St. John's,  
         Newfoundland

## 1. INTRODUCTION

The object of this study was to determine the effect of the sub-auroral ionosphere on the propagation of HF signals. The results of an earlier study (Basu and Vesprini, 1972, hereafter to be referred to as Report 1) have shown that the ionosphere at these latitudes is far from uniform with field aligned electron density irregularities existing in the E and F region for a fair percentage of the time. Thus, scattering by these field aligned irregularities may cause a diminution or cut-off of the F-region propagated HF signal. Reflection from intense mid-latitude sporadic E may also have a blanketing effect on HF propagation. Both these factors are considered in this study. In addition to magnetic storm effects the quiet time F region itself is known to exhibit various anomalies such as the evening anomaly and seasonal anomaly in the peak electron concentration of the F2 layer. We have attempted to study the effects of these anomalies on F-layer propagation. Another important parameter which may affect oblique HF propagation is the D-region absorption particularly during magnetic storms. However, no attempt has been made to include absorption effects in this study.

A brief review of current theories for the formation of field aligned irregularities has been presented and the observed statistical occurrence characteristics of these irregularities are discussed in the light of the recently developed physical concepts.

## 2. EQUIPMENT AND DATA REDUCTION

The data for this study were obtained from film records of a continuous series of 19.39 MHz oblique backscatter observations made at Plum Island, MA (42.63°N, 70.82°W and 56° invariant

magnetic latitude) during 1961-65. The data acquisition system as well as the general methods of data reduction have been reported in detail in Report 1.

### 3. NOMENCLATURE AND IDENTIFICATION OF ECHOES

The backscatter records, in general, showed three main classes of echoes in the northern quadrants:

- i) Ground backscatter echoes propagated via sporadic E reflection
- ii) Ground backscatter echoes propagated via F-region reflection
- iii) Direct backscatter from aspect sensitive field aligned irregularities in the E and F layer and which have been designated as FAE(E) and FAE(F) respectively in Report 1.

Since there is considerable confusion in the literature (Croft, 1972) regarding the nomenclature of the various phenomena observed in conjunction with HF propagation, we shall briefly summarize the various terms used in this report to describe the above echoes.

The term  $E_s$  propagation will be specifically used for propagation of signals reflected by an  $E_s$  layer and then scattered by the ground so that the signal retraces its path to the transmitter. It was determined that these diffuse echoes which were obtained at delays of 8-10 msec in the northern quadrants could not be direct returns from the auroral E layer as the antenna system used for this study discriminates against the very low elevation angles (0-1 degree) that would be required to obtain such delays for direct backscatter from the E layer. A similar point has been made by Egan and Peterson (1962). More definite evidence that the  $E_s$  propagation is actually a reflection from  $E_s$  ionization is presented in the next section. Again, it



is not possible for these diffuse echoes to be one-hop F-region propagated groundscatter echoes (to be referred to as 1F echoes); at a frequency of 19.4 MHz 1F echoes occur at much greater delays. Indeed the daytime  $E_s$  echoes are usually accompanied by 1F and sometimes 2F echoes at appropriately greater delays. Besides, the continuous operation of the sounder makes it possible to follow the regular diurnal pattern of 1F echoes as they develop in the morning and decay after sunset. The  $E_s$  echoes on the other hand, are, as their name implies, rather sporadic in nature and are observed for periods of a fraction of an hour to a few hours.

The aspect sensitive field aligned echoes such as those observed by Peterson et al (1955) showed up as much sharper well defined traces on the films. They were predominantly centered in the NW quadrant and were less frequently observed in the NE. The large beamwidth of the antenna ( $\sim 45^\circ$ ) precluded sensitive enough range-elevation displays which could have determined whether these field aligned echoes were themselves discrete or diffuse in nature. Such a distinction was made, among others, by Leadabrand (1961, 1965) working in the VHF and UHF band with narrow beam radars. Thus in the terminology of the IAGA, 1968 classification (Sverdlov, 1971), we cannot distinguish between  $B_1$ ,  $B_2$  and  $B_3$  types of radio aurora. In addition since some of the aspect sensitive echoes are obtained during periods of magnetic calm and hence could not be directly related to auroral disturbances at the latitude ( $\sim 60^\circ$  invariant) of sounding, it was decided to refer to them generally as FAE's rather than radio aurora.

#### 4. $E_s$ PROPAGATION

The occurrence characteristics of  $E_s$  propagation in the NW and NE over the five year period of observation are presented in Figures 1 and 2 for quiet magnetic conditions. There is no

systematic variation of  $E_s$  propagation from one year to another or from one quadrant to another. The only prominent feature is the presence of  $E_s$  propagation during the summer months (May through August) of each year. The diurnal variation during these months shows a morning and an evening peak of occurrence. The evening peak is usually the more intense one when  $E_s$  propagation is observed for as much as 50 per cent of the time. Some occurrence is seen during the winter months in the evening hours, but it is usually present for less than 10 per cent of the time.

The diurnal variation of the occurrence of  $E_s$  propagation over the five years of observation for the NW during quiet magnetic periods is also shown in Figure 3. As in Figure 1, we see the two diurnal peaks of occurrence with the largest peak occurring in the evening. The occurrence of  $E_s$  propagation during magnetic storms is too infrequent for any statistical conclusions to be drawn. This could be due to an actual decrease of  $E_s$  occurrence during storms, as has been reported by various authors, as well as increased D-region absorption during storms which could cut off oblique  $E_s$  propagation since four traversals of the absorbing lower ionosphere are required.

To determine whether this particular type of propagation is indeed a reflection from  $E_s$  clouds to the north of the station,  $fE_s$  occurrence contours from Ottawa were studied. The ionosonde station at Ottawa is very well suited for a comparison of this kind being situated at a slant range of approximately 540 km (E-layer height) at an azimuth of  $330^\circ$  to the observing station. Most of the median delays for the  $E_s$  type propagation correspond to such slant ranges for the  $E_s$  clouds. On a range-elevation display, these slant ranges correspond to elevation angles of 8 to  $10^\circ$ . Thus maximum vertical frequencies of approximately 4.5 to 5 MHz for the  $E_s$  clouds should be able to reflect the observing frequency. Figure 4 shows percentage occurrence contours of  $fE_s \geq 5$  MHz as observed at Ottawa for the years 1961-65. The data for these contours were obtained

from the monthly bulletins of ionospheric data published by the Defence Research Telecommunications Establishment, Ottawa, Canada. The remarkable similarity of Figures 1 and 4 provides convincing evidence for  $E_s$  type propagation observed by the oblique backscatter radar. The diurnal variation of vertical  $E_s$  occurrence at Ottawa (Figure 4) shows the same pattern as that derived from the oblique  $E_s$  propagation (Figure 1). It should be pointed out that Figure 4 represents data taken on all days at Ottawa without discriminating between quiet and disturbed days. However a separate study of the Ottawa  $E_s$  data indicated that magnetically disturbed periods showed less  $E_s$  activity, a fact that had been known earlier and has also been confirmed recently (Whitehead, 1970; Closs, 1971). Hence, Figure 3 generally represents quiet conditions. The exceptionally good statistical agreement between Figures 1 and 4 shows that during periods of quiet magnetic conditions absorption of the oblique rays in the D layer is not strong enough to cut off  $E_s$  propagation.

To prove that the statistical agreement referred to above, is also borne out on a one-to-one basis, the occurrence of  $E_s$  propagation was correlated with the presence of  $E_s$  in the vertical ionosonde data from Ottawa on an hourly basis for a particular month, namely June, 1961. The results show that if  $fE_s \geq 4$  MHz at Ottawa, then the  $E_s$  propagation is observed 80 percent of that time. Considering that the observations were made only once every hour at Ottawa and the oblique sounder was operating continuously, this is a remarkably good correlation.

#### 4.1. Correlation of FAE(E) and $E_s$ Propagation.

The total occurrence statistics of FAE(E) during quiet magnetic periods over the years 1961-65, presented earlier in Report 1, are reproduced in Figure 5 for comparison with the  $E_s$  propagation occurrence, particularly from the NW quadrant. It

should be noted that the time scale is different in Figures 1 and 5. Keeping this in mind, we find that the definite summer evening maximum in FAE(E) is correlated extremely well with the evening maximum of both  $E_s$  propagation and  $fE_s$  at Ottawa. The other diurnal peak in  $E_s$  during the pre-noon hours has no accompanying FAE(E) activity at all. We shall attempt to reconcile these two points in the Discussion. The high association of  $E_s$  with FAE(E) during evening hours is further shown in Figure 6, which represents the percent occurrence of  $E_s$  associated FAE(E) from the NW for the five years of observation during quiet magnetic periods. During 2000 to 0300 hours  $E_s$  propagation is accompanied almost 50 percent of the time by FAE(E).

The occurrence of FAE(E) during magnetically disturbed periods ( $K_{F_r}$  4-9) is statistically insignificant for presentation in the form of contour diagrams as in Figure 5. Instead, this occurrence is presented in the form of average seasonal histograms over the five years of observation, as in Figure 7. The average seasonal behavior for very quiet ( $K_{F_r}$  0,1) and moderate conditions ( $K_{F_r}$  2,3) is also shown for comparison. These seasonal groupings are somewhat different from those presented in Report 1 and are found to be more meaningful in terms of occurrence statistics of  $E_s$ . The predominant summer nighttime maximum, weak secondary maximum in winter, and very low occurrence in the equinoctial months is apparent during both the very quiet and the moderately disturbed magnetic periods. The occurrence pattern of FAE(E) changes drastically when the magnetic field is severely disturbed. During this time, virtually all seasonal differences are wiped out and considerable FAE(E) activity is seen during the daytime. Thus there seems to be a threshold effect for the effects of magnetic disturbances on the formation of field aligned irregularities at E-layer heights. We shall comment on this point further in the Discussion.

## 5. F-LAYER PROPAGATION

The F-layer ground backscatter echoes or 1F echoes form a large fraction of the total data recorded. The echoes obtained at southern azimuths were stronger and more numerous. However, as pointed out earlier, we shall restrict ourselves to echoes obtained from the north. The greater majority of these was obtained at delays of 16-18 msec which corresponds to ground scattering distances of 2400-2700 km. The percentage occurrence contours of this type of echo during magnetically quiet periods are presented in Figures 8 and 9 for the NW and NE respectively. Though the occurrence of ground scatter is appreciably greater in the NE, both diagrams show a very marked solar cycle dependence. Another significant factor in both is the absence of daytime ground backscatter during the summer months - the backscatter appears much later in the day during the afternoon hours in the NE and even later around 1800 hours, in the NW.

### 5.1. Effect of $E_s$ on F-layer propagation

As stated in the Introduction, it was our object to investigate the effects of blanketing, if any, caused by the intense sporadic-E clouds present so consistently during the summer on F-layer backscatter. A quick comparison of Figures 4 and 8 seems to indicate that absence of daytime ground backscatter during the summer may be caused by the presence of  $E_s$ . However, a closer look shows that the evening occurrence of F-layer propagation during this season coincides almost exactly with the evening maximum of  $E_s$  occurrence. Thus the daytime absence of F-layer echoes cannot be attributed to the presence of  $E_s$ , and we have to look for changes in the F-region parameters themselves for an explanation. It is our conclusion, therefore, that  $E_s$  at sub-auroral latitudes does not cause blanketing effects on the 1F mode of propagation. Bates (1969) came to a similar conclusion regarding the 1F mode signal after examining simultaneous records of HF backscatter

at College and the Thule-to-College forward oblique propagation in the auroral zone. In the absence of any amplitude records, we could not determine whether the presence of  $E_s$  causes any fall-off in the echo intensity. However, since F-layer propagation with this low power system could exist simultaneously with the rather intense evening  $E_s$  maximum, our tentative conclusion is that it does not cause any appreciable loss of intensity.

## 5.2. Effect of direct ionospheric scatter on F-layer propagation.

We have seen in Section 4 of this Report that direct ionospheric scatter from the E region, FAE(E), is highly correlated with the presence of  $E_s$  propagation. This lends support to the theory of weak scatter, developed by Booker (1956), in which he postulated that only a small fraction of the incident energy is scattered back towards the radar by the field aligned irregularities which provide discontinuities in the dielectric constant. Again, in the previous section we have seen that the  $E_s$  clouds themselves are of the non-blanketing type. At these latitudes sufficient refraction must be present in the underlying layers to produce aspect sensitivity at F-layer heights. Looking north from the Plum Island radar, the magnetic field direction is so nearly vertical that aspect sensitivity requirements are met close to the reflection level, i.e., when the ray travels horizontally. Thus the existence of the 1F mode becomes an almost necessary condition for the occurrence of direct scatter from the F layer. If the direct scatter and 1F mode echoes occur simultaneously, we can assume that the direct scatter is rather weak. The occurrence of direct scatter is further dependent on another crucial factor, namely, the presence of field aligned irregularities at the latitude of interest at that particular local time.

To study the simultaneous occurrence of the 1F mode of propagation and FAE(F) we constructed Figure 10. This diagram shows the diurnal variation of the occurrence of the F-layer

echo over 5 years of observation as well as the percentage of the time that FAE(F) accompanied the F-layer echo. Figure 10 shows that the hours of greatest F-layer echo occurrence are accompanied by a negligible percentage of FAE(F), whereas the evening hours with rapidly tapering 1F echo occurrence are those which are accompanied by FAE(F) for 25 to 50 percent of the time. This diurnal variation during quiet times can be immediately explained in terms of the irregularity region obtained from scintillation measurements as shown in Figure 11 (Aarons and Allen, 1971) which shows that the low latitude scintillation boundary approaches  $60^\circ$  invariant at 1700 hours local time. This is precisely the time beyond which an appreciable FAE(F) activity is observed. Thus if irregularities are present, then it is possible to have simultaneous FAE(F) and 1F echoes.

During disturbed times the equatorward scintillation boundary is found to move southwards. Thus it is quite possible from boundary concepts to expect irregularities and hence FAE(F) activity. Figure 12 shows the diurnal variation of hours of 1F echo as well as the percentage of the time that this 1F echo was accompanied by FAE(F). That the FAE(F) is present simultaneously for 30 percent of the time the 1F echo is present proves that direct scatter from the F-region irregularities is weak in nature and the limiting factor in Figure 10 was the absence of irregularities. Comparing Figures 10 and 12 and noting that the number of  $K_{F4-9}$  samples is only 10% of the number of  $K_{F0-3}$  samples, we find a tremendous increase of FAE(F) activity during magnetic storms in the hours when F-layer propagation is simultaneously present.

For the sake of completeness, as well as a one-to-one comparison with Figure 8, we have reproduced from Report 1 the FAE(F) occurrence contours obtained over the 5 years of observation in the NW quadrant during quiet times in Figure 13. The sunset peak of occurrence and solar cycle dependence is very clearly displayed. The diurnal, seasonal, and magnetic effects

are also very clearly depicted in Figure 14. It is interesting to note the increase of echo occurrence with increasing magnetic index in each season excepting the summer. The explanation for this is the generally observed fact that summer magnetic storms at midlatitudes are usually accompanied by a decrease of  $f_oF2$ , whereas the opposite is the case in winter (Matsushita, 1959; Maeda and Sato, 1959). Although Figure 14 generally shows increase of FAE(F) with each range of magnetic index, an earlier study (Report 1) showed that FAE(F) increased monotonically with  $K_{F_r}$  until  $K_{F_r}=4$  and then decreased thereafter, attaining complete cut off for  $K_{F_r} \geq 7$ . The complete cut off for  $K_{F_r} \geq 7$  shows that severe magnetic storms in any season are accompanied by a decrease in  $f_oF2$  at these latitudes as is the case at high latitude stations for even moderate storms. In contrast FAE(E) showed uniformly high activity for  $K_{F_r}$  ranging from 6 to 9. These results are reproduced in Figure 15.

It is our conclusion that direct ionospheric scatter does not affect F-layer propagation. Rather, F-layer propagation is often required to produce FAE(F) at locations where direct orthogonality between the ray-path from the radar and the geomagnetic field is not achieved for straight line propagation.

### 5.3. Effect of varying F-region parameters on 1F propagation.

It was pointed out previously that the disappearance of F-layer propagated echoes during the summer, as shown in Figures 8 and 9, was probably caused by the seasonal variation of the F-region parameters and not due to blanketing effects of  $E_s$  ionization. The two most important parameters affecting F-layer propagation are its critical frequency  $f_oF2$ , and the true height of maximum ionization  $h_mF2$ . However, the true height analysis of ionograms is not carried out on a routine basis and hence the maximum usable frequency factor of the F2 layer for a distance of 3000 km,  $M(3000)F2$ , was used to obtain relative variation of the true height between one time



and another. It has been shown by Shimazaki (1955) that for most electron density profiles the height of the maximum electron density is approximated by  $h_p F2 = 1490 / M(3000)F2 - 176$ . Thus the variation of  $M(3000)F2$  indicates the trend in the variation of  $h_p F2$  - the lower values of  $M(3000)F2$  corresponding to higher values of  $h_p F2$  and vice-versa.

The ionosonde stations to the NW and NE of Plum Island are Winnipeg (49.9°N, 97.4°W) and St. John's (47.6°N, 52.7°W), respectively, and their data are considered to represent ionospheric F2-layer conditions in these two directions. Hence contours of the monthly median  $f_o F2$  and  $h_p F2$ , calculated from the  $M(3000)F2$  factor by Shimazaki's relation, were drawn for both stations using DRTE(Ottawa) Canadian data books. These are shown in Figures 16 through 19. Systematic differences are found between the  $f_o F2$  contours of the two quadrants - the median critical frequency to the NE always being higher than that of the NW at a particular hour, usually by at least 0.5 MHz. This higher critical frequency is responsible for the higher percentage of the time that F-layer propagation is present to the NE. Looking at the  $h_p F2$  contours we find that the summer daytime values are the highest of any season in addition to being accompanied by the lowest values of  $f_o F2$ . This particular combination of high  $h_p F2$  and low  $f_o F2$  is responsible for the disappearance of F-layer propagation in the daytime. However, it reappears in the evening when the  $f_o F2$  is higher and the  $h_p F2$  is lower. The solar cycle variation is manifested by a decrease of  $h_p F2$  from 1961 to 1964. However, this favorable trend is more than compensated for by an accelerated decrease of  $f_o F2$  with the declining solar cycle, so that we observe a general decrease of F-layer propagation. A separate empirical study is underway to determine particular combinations of  $f_o F2$  and  $h_p F2$  which will yield the observed percentage of F-layer propagation.

We thus conclude that the F-region parameters themselves are crucial in determining the extent of F-layer propagation.

We have observed that in a particular quadrant the F-layer propagation varies with time of day, season, and sunspot number. This is largely dictated by the variable shape of the  $f_oF2$  vs. time curves as a function of season. We find from Figure 16 that the winter  $f_oF2$  vs. time curves show a single midday maximum which is greater than the  $f_oF2$  at any other season. This is the seasonal anomaly. The summer and equinox months on the other hand show an evening peak which is usually greater than the midday value. This is generally referred to as the evening anomaly. Strobil and McElroy (1970) made computations for a latitude of  $43^\circ N$  under sunspot minimum conditions and found that most of the seasonal variations as well as the evening anomaly could be explained by altering the atmospheric composition, specifically that of  $O/O_2$ , keeping the aggregate oxygen mass constant, at a base level of 120 km. Thus, contrary to general expectations, neutral winds are not the direct cause of the seasonal anomaly (Rishbeth, 1968).

Neutral winds, however, are largely responsible for the other noteworthy feature that has emerged from these observations, namely, the greatly enhanced F-layer propagation in the NE as compared with the NW. The two ionosonde stations chosen to represent conditions in these general directions are St. John's (NE) and Winnipeg (NW). These stations, though similar in latitude, differ in magnetic declination. St. John's has the rather large westerly declination of  $27^\circ W$  whereas Winnipeg has a declination of  $10^\circ E$ . The difference in F2-layer behavior at places of similar latitude but opposite declination has been discussed in a recent review on thermospheric winds by Rishbeth (1972) and also by Kohl et al (1969). These authors conclude that wind effects can account for the dependence of the diurnal F2-layer variations on declination, that had been suggested previously by Eyring (1963). Thus we find that factors such as changes in atmospheric composition and neutral winds indirectly control F-layer propagation.

## 6. GENERAL DISCUSSION ON FORMATION AND OCCURRENCE OF FIELD ALIGNED IRREGULARITIES

### 6.1. FAE(E)

The statistical results of the occurrence of FAE(E) in this study extending over half a solar cycle seem to agree well with Forsyth's (1969) recent paper on the occurrence of radio aurora over a full solar cycle. He finds a consistent summer maximum throughout the solar cycle. However, the diurnal variation of radio aurora shows a daytime maximum as opposed to the nighttime maximum that is observed at Plum Island. It should be noted that Forsyth's paper was based on forward scatter measurements made at 40 MHz between a transmitter located at Greenwood and receiver located at Ottawa on an east-west line. As indicated earlier, the oblique backscatter observations reported in this study sound the ionosphere over Ottawa for E-region heights. Thus the two sets of measurements refer to ionospheres at almost the same invariant latitude, but located possibly a few hundred km apart in the east-west direction. Referring to the earlier paper by Collins and Forsyth (1959), it becomes evident that the daytime summer maximum reported by Forsyth must be caused by the S-type scatter (classified as  $A_4$  by IAGA, 1968) which is weakly aspect-sensitive and is not correlated with magnetic disturbances. This type of irregularity when existing at the zenith at Ottawa is reported as  $E_s$  and gives rise to the  $E_s$ -type propagation that is so consistently observed during the summer daytime under quiet conditions. Forsyth also makes the comment that even if the daytime occurrences are eliminated, the summer maximum still remains - a fact which is adequately borne out by our observations.

The current thinking (Unwin and Knox, 1971) is to explain radio aurora, i.e., aspect-sensitive high latitude disturbances strongly related to magnetic storms, in terms of either Farley's (1963) 'ion-acoustic instability' or the 'drift-gradient instability' developed by Simon (1963) and Hoh (1963). Unwin and Knox (1971) further show that the B1 or diffuse type of

radio aurora is probably due to the ion-acoustic instability, whereas the B2 and B3 (discrete) types are probably due to the drift-gradient instability. These authors also point out that the condition for the onset of the latter type of instability is inversely proportional to the square of the wavelength thus making an HF system very sensitive for its detection. An order of magnitude estimate shows that an electric field of 1 mv/m may be adequate for causing this kind of instability at HF and this value is well within the range that can be accounted for by normal ionospheric winds. Thus the drift gradient instability could be one of the possible causes for the formation of FAE(E) during magnetically quiet and moderately disturbed times. The ion-acoustic instability, on the other hand, requires a threshold electric field of the order of 30 mv/m even at HF. It may be reasonable to expect fields of this order at E-region heights for quite disturbed conditions ( $K_{\text{p}} > 4$ ) at approximately  $60^\circ$  invariant latitude. Thus the FAE(E) observed during strong disturbances could very well have been caused by this instability (Gadsden, 1967; Moorcroft, 1972).

Goodwin (1965) found Booker's theory (1965) of scattering to be adequate for the explanation of his 16 MHz data and the same argument may be valid for this 19 MHz data obtained during quiet times in the presence of non-auroral  $E_s$ . This non-auroral  $E_s$  provides as high a background ionization as do irregularities occurring in the aurora. These irregularities in electron density which are elongated along the magnetic field are supposed to be randomly distributed, and are caused by atmospheric turbulence. Recent measurements of nighttime and twilight wind profiles from chemical trails have shown that turbulence once initiated maintains itself for 30 percent of the time at altitudes below 110 km (Rosenburg and Zimmerman, 1972). Booker assumed the blobs of ionization to be gaussoid in form. Later measurements (Chesnut et al, 1968) have shown that the gaussoid model is not a good one for representing radio aurora, and it is Bates' view (1969) that Booker's scattering theory is general and does indeed apply in most cases; rather it is the gaussoid model that does not apply.

## 6.2. FAE(F)

The percentage occurrence contours of FAE(F) show that during quiet periods they are primarily a sunset phenomenon. During disturbed periods, however, they are found to occur more frequently in the daytime, in addition to their sunset occurrence. It is to be emphasized that their diurnal peak of occurrence should be interpreted in terms of their aspect sensitivity requirements which in this case is dependent on refraction due to underlying ionization. If the probing HF radar had been at a somewhat lower geomagnetic latitude, such as that at Brisbane, the diurnal peak would have occurred closer to midnight when the irregularities are found to be most predominant from scintillation measurements (Aarons et al, 1969). Such were indeed the findings with a 16 MHz radar situated at Brisbane (Matthew, 1961). This led Bates (1969) to suggest that statistical studies of any given type of echo (e.g., E-scatter or F-scatter) are not too meaningful because the same scattering region gives different answers when viewed from different locations. However, it is quite correct to suggest that near-sunset conditions are conducive to the formation of field aligned irregularities in the mid-latitude ionosphere, whereas during the daytime, conditions are relatively unfavorable. Bates (1971) has shown that slant-F echoes were seen on a one-to-one basis whenever the vertical incidence F-layer traces were spread at College. At that station, which is well within the auroral oval, these slant-F echoes were present much of the time between roughly 1600 and 0600 LT. Slant-F echoes were, however, observed only occasionally at Palo Alto, California during 1964. Plum Island, being at an intermediate latitude, should show intermediate occurrence. Bates comes to the conclusion that the slant-F echoes are produced by highly aspect-sensitive backscatter from field aligned irregularities in the F layer. It is thus quite reasonable to assume that the oblique backscatter sounder will show

FAE(F) activity when spread-F conditions are reported by relevant ionosondes. Positive correlations between spread-F and FAE(F) were reported by various authors (Herman, 1966 and various authors quoted therein). However most authors also report the presence of spread-F without corresponding FAE(F) activity, thus showing that the vertical ionosonde is a more sensitive detector of irregularities than a backscatter sounder (Au, 1970). Bates (1971) and Au(1970) found sufficiently good agreement between the existence of irregularities producing FAE(F) and the scintillation boundary (Aarons, et al, 1969) to invoke the same mechanism for the formation of the irregularities. Very recently Kelley and Mozer (1971) have found evidence of turbulent electrostatic fields whose daytime and nighttime equatorward boundary agree extremely well with that determined by Aarons and Allen (1971). Kelley and Mozer were making in situ low frequency vector electric field measurements from orbiting satellites at a height of 400 km. It is interesting to note that these signals showed significant peaks when the spacecraft was in the statistical auroral oval as defined by Feldstein (1966). Kelley and Mozer quote a peak intensity at 12 Hertz of 1 mv/m · hertz<sup>1/2</sup>. However, without knowing the spectral characteristics over the entire bandwidth it is difficult to compare this value with other quoted dc field measurements.

The existence of electrostatic fields and plasma density gradients in the ionosphere are known to give rise to a unique type of instability known alternatively as 'cross-field instability' or 'drift-gradient instability' which can result in the growth of ionization density irregularities that are aligned along the earth's magnetic field. It will be recalled that this type of instability has been invoked for the explanation of the B2 and B3 types of radio aurora at E-layer heights (Unwin and Knox, 1971). Reid (1968) considered the formation of field aligned irregularities in the F-region due to this mechanism and Au(1970) later extended his calculations for a station at the dip pole. From these calculations, it is evident

that the dynamo region of the ionosphere is quite likely to be unstable in the presence of moderate electric fields to the growth of irregularities with scale sizes in the range from a few tens of meters to a few kilometers. Conduction of the small-scale electrostatic fields associated with this instability up the magnetic field lines can give rise to the growth of irregularities of corresponding scale sizes in the F-region. However, the theory is still on a rather tentative footing and no rigorous theory of formation of field aligned echoes seems to have yet been formulated.

### 6.3. Conclusions

While the physics of the origin of the irregularities are in the process of being developed, the morphology of the irregularity region is clear. Irregularities exist in the region hatched in Figure 11. With the acceptance of this model, the geometry of the probing radar becomes the all important factor with the propagation angle and the local ionospheric parameters forming the basis for the occurrence statistics. Knowledge of the diurnal pattern of the irregularity region, and the intensity within the irregularities across the auroral zone and the polar cap is being expanded by high latitude observations as well as by observations near the scintillation boundary. With statistics such as shown in this paper, it should be possible, given the morphology and the height and critical frequency of the F2 layer, to work out occurrence statistics for field aligned echoes in the F region.

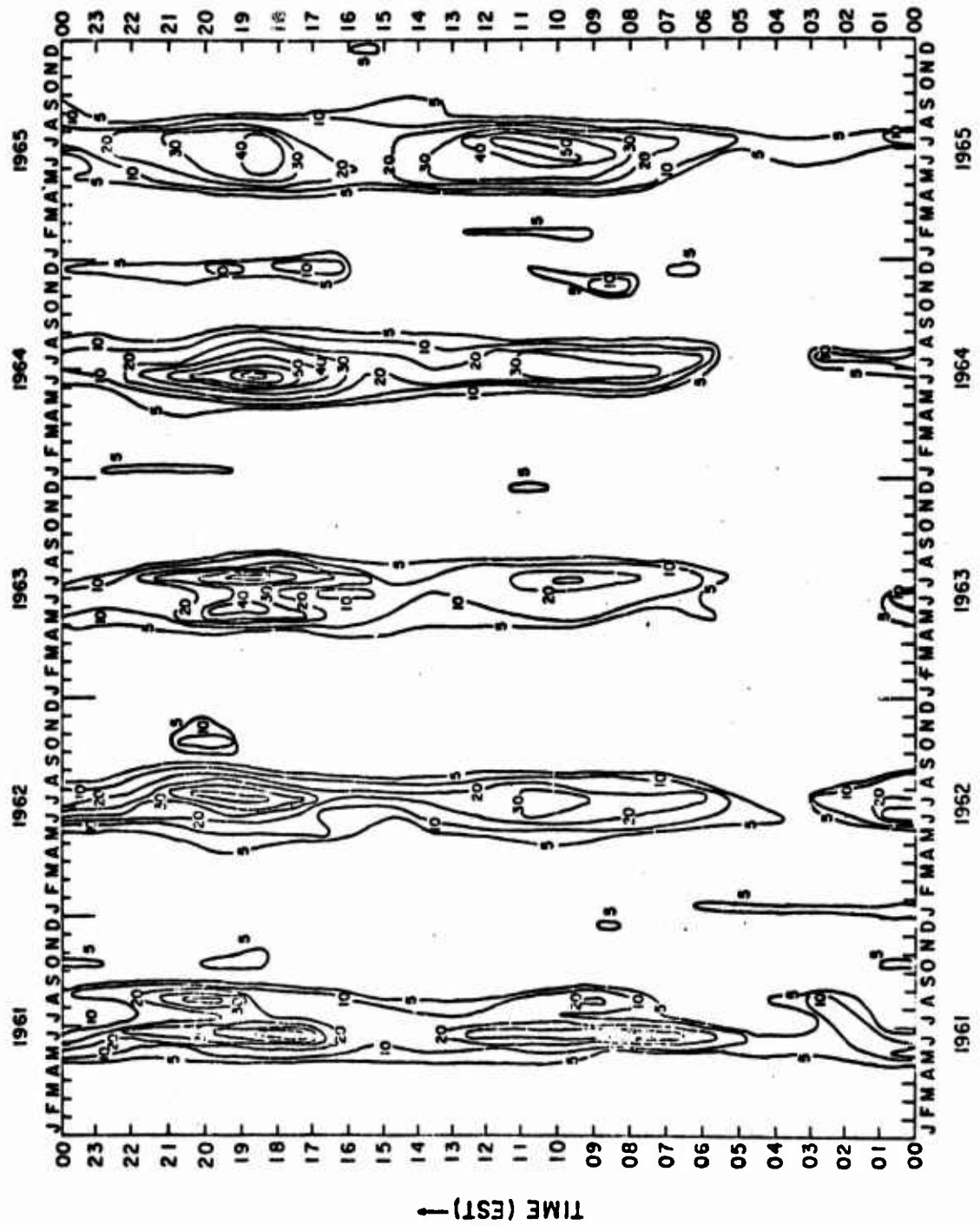


FIG. 1. PERCENTAGE OCCURRENCE CONTOURS OF  $E_s$  PROPAGATION IN THE NW QUADRANT FOR  $K_{F0-3}$



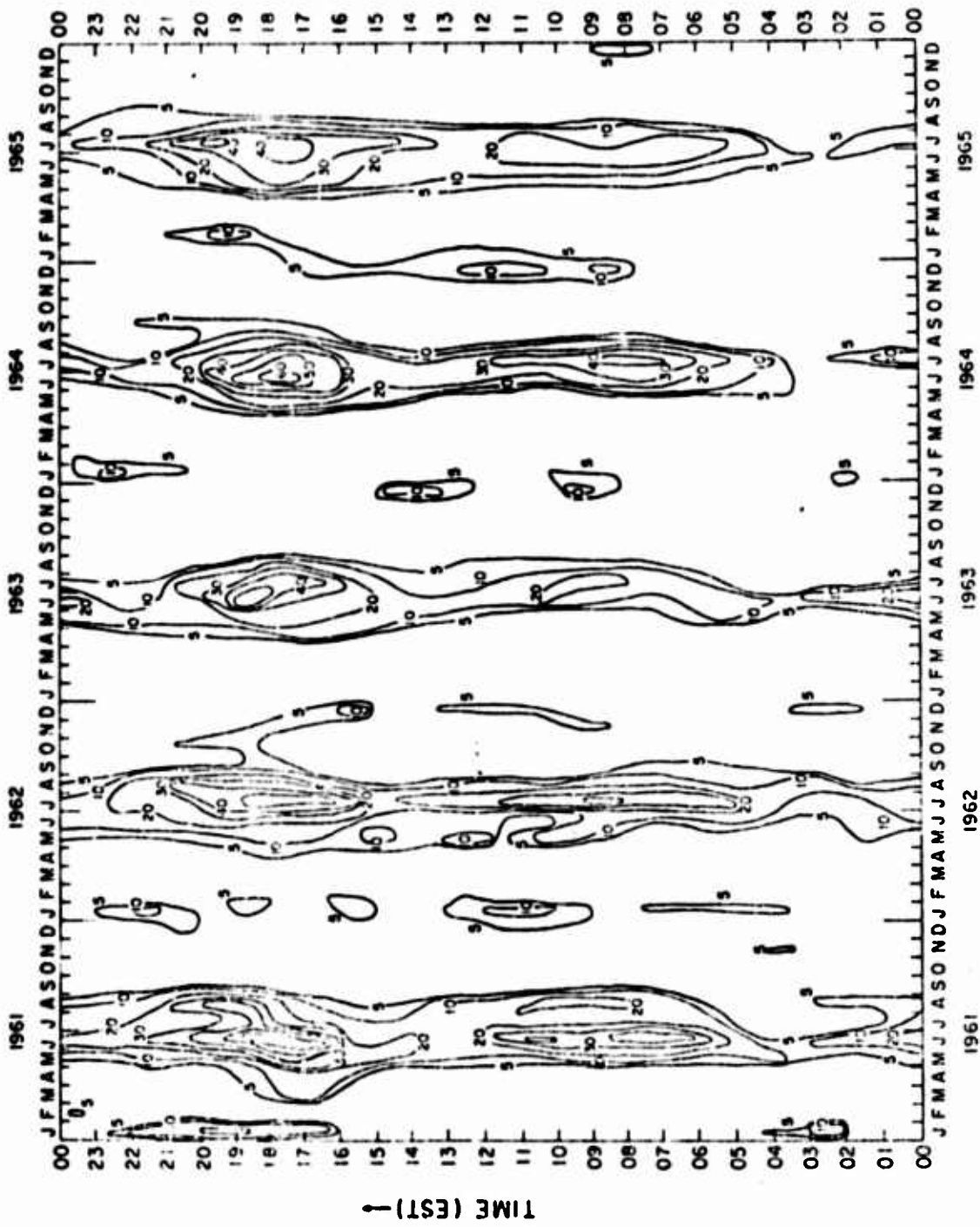


FIG. 2. PERCENTAGE OCCURRENCE CONTOURS OF  $E_s$  PROPAGATION IN THE NE QUADRANT FOR  $K_{fr}$  0-3

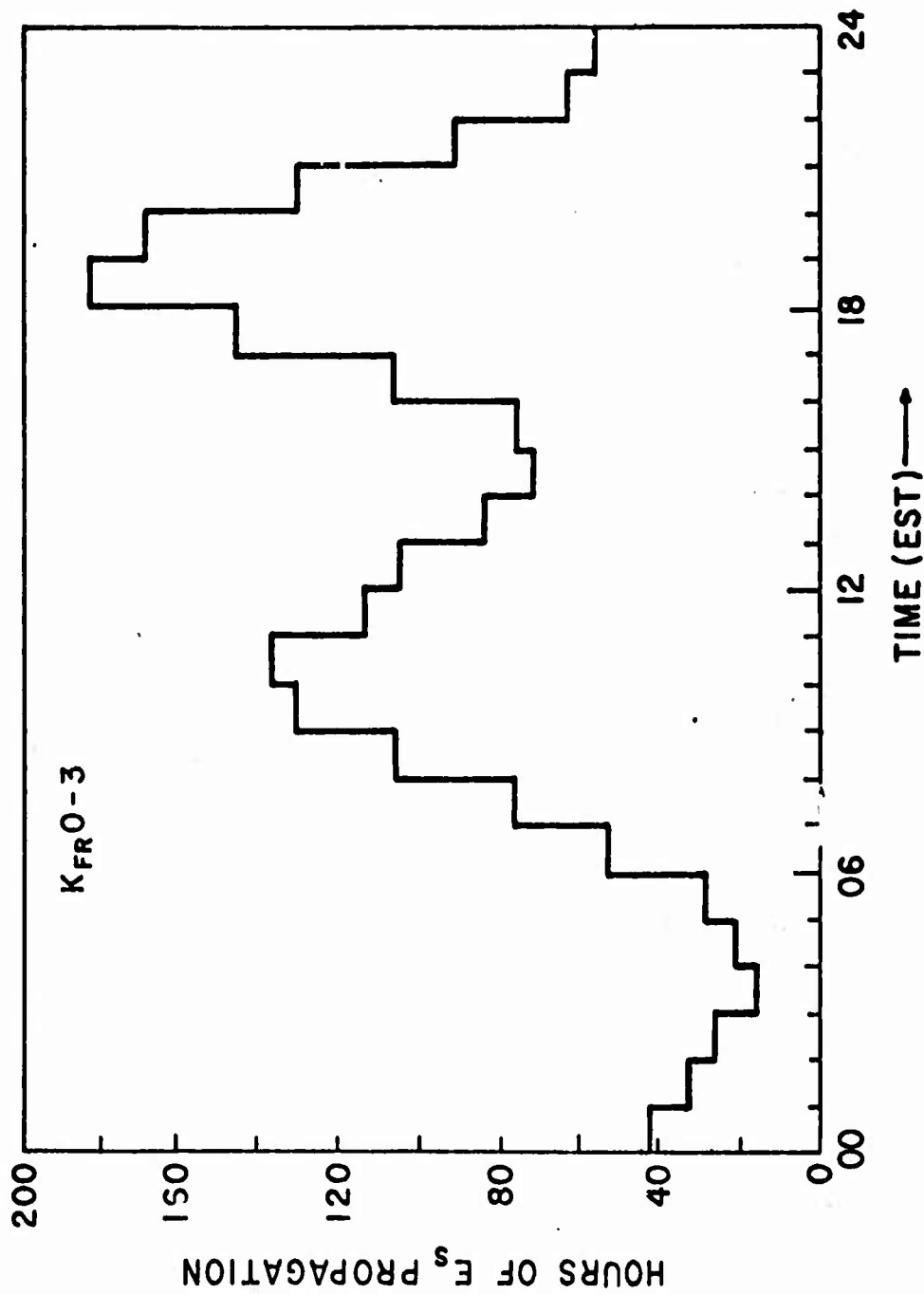


FIG. 3. AVERAGE DIURNAL VARIATION OF  $E_s$  PROPAGATION  
IN THE NW QUADRANT FOR KFR 0-3, 1961-1965

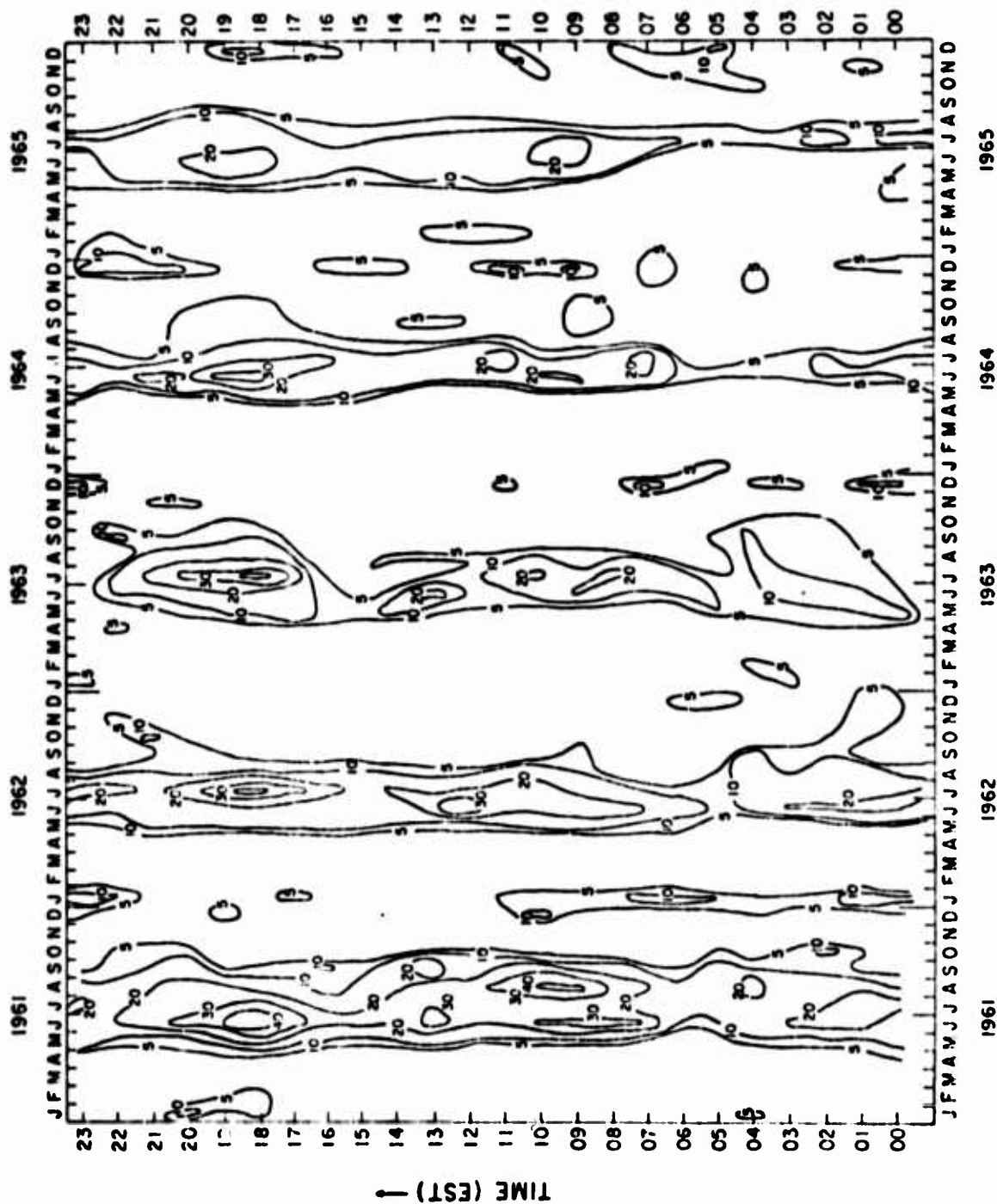


FIG. 4. PERCENTAGE OCCURRENCE CONTOURS OF  $f_o E_s \geq 5$  MHz FOR OTTAWA

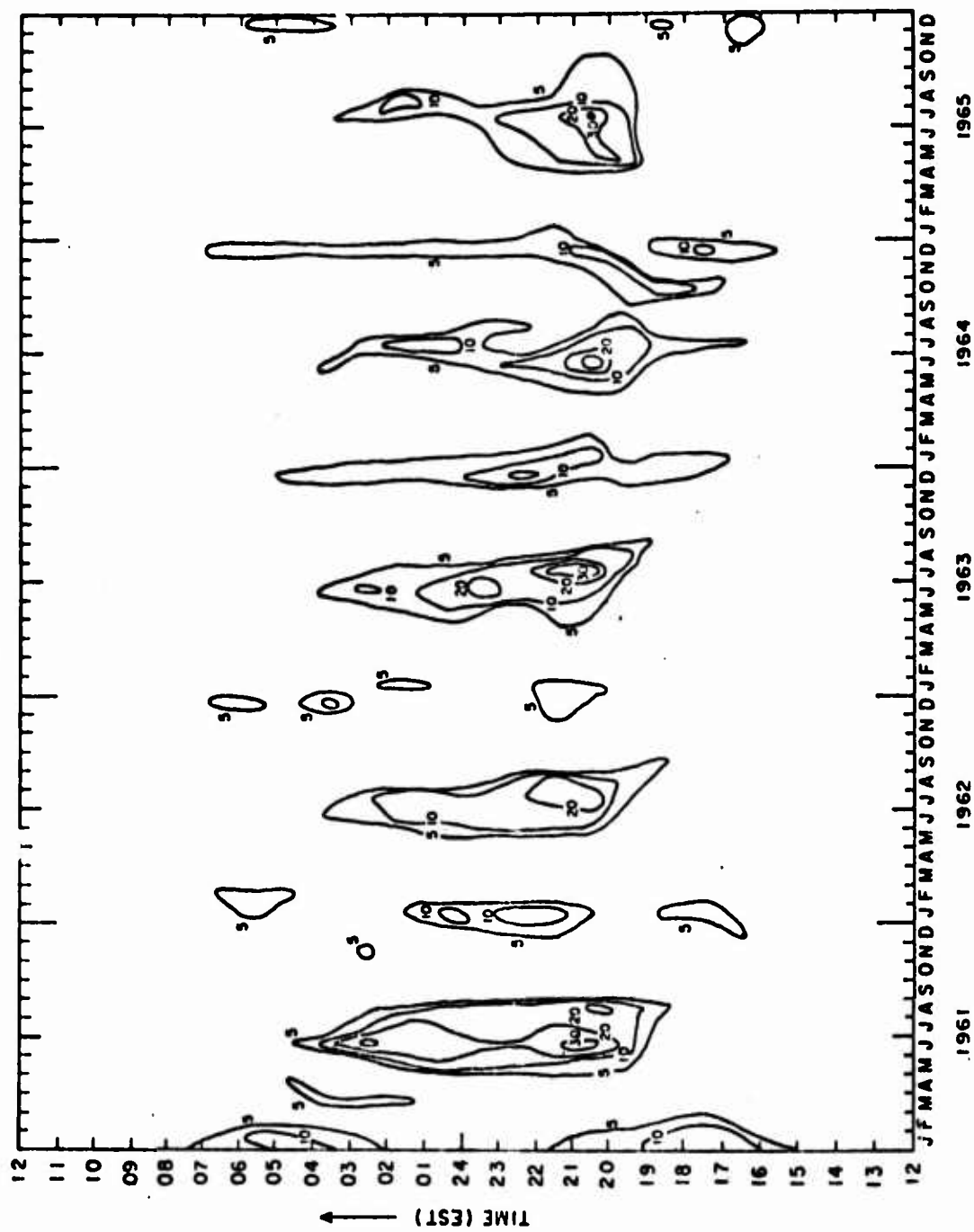


FIG. 5. PERCENTAGE OCCURRENCE CONTOURS OF FAE(E) FOR KFR 0-3

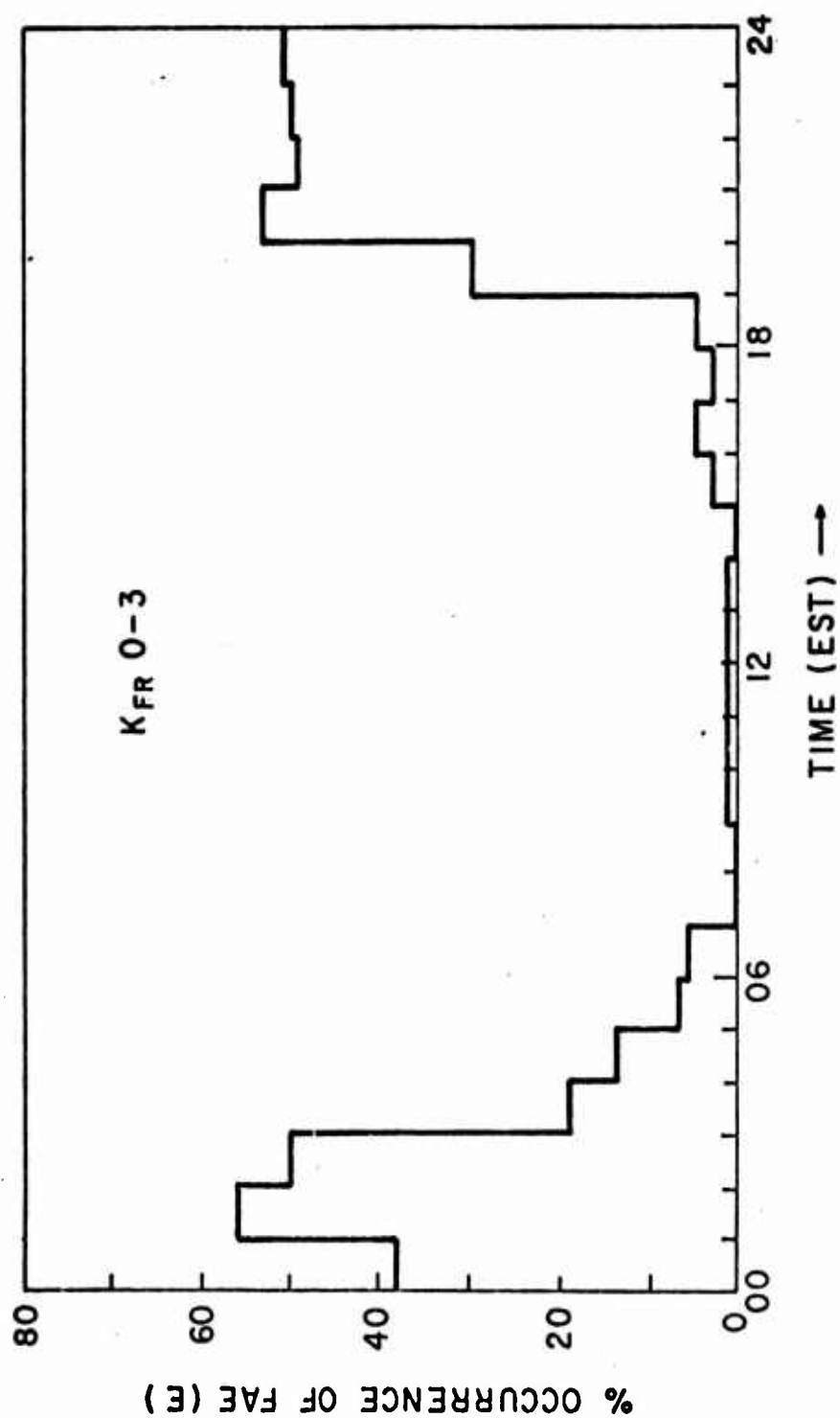


FIG. 6. AVERAGE DIURNAL VARIATION OF FAE(E) WHEN  $E_s$  PROPAGATION IS PRESENT FOR  $K_{FR}0-3$ , 1961 - 1965

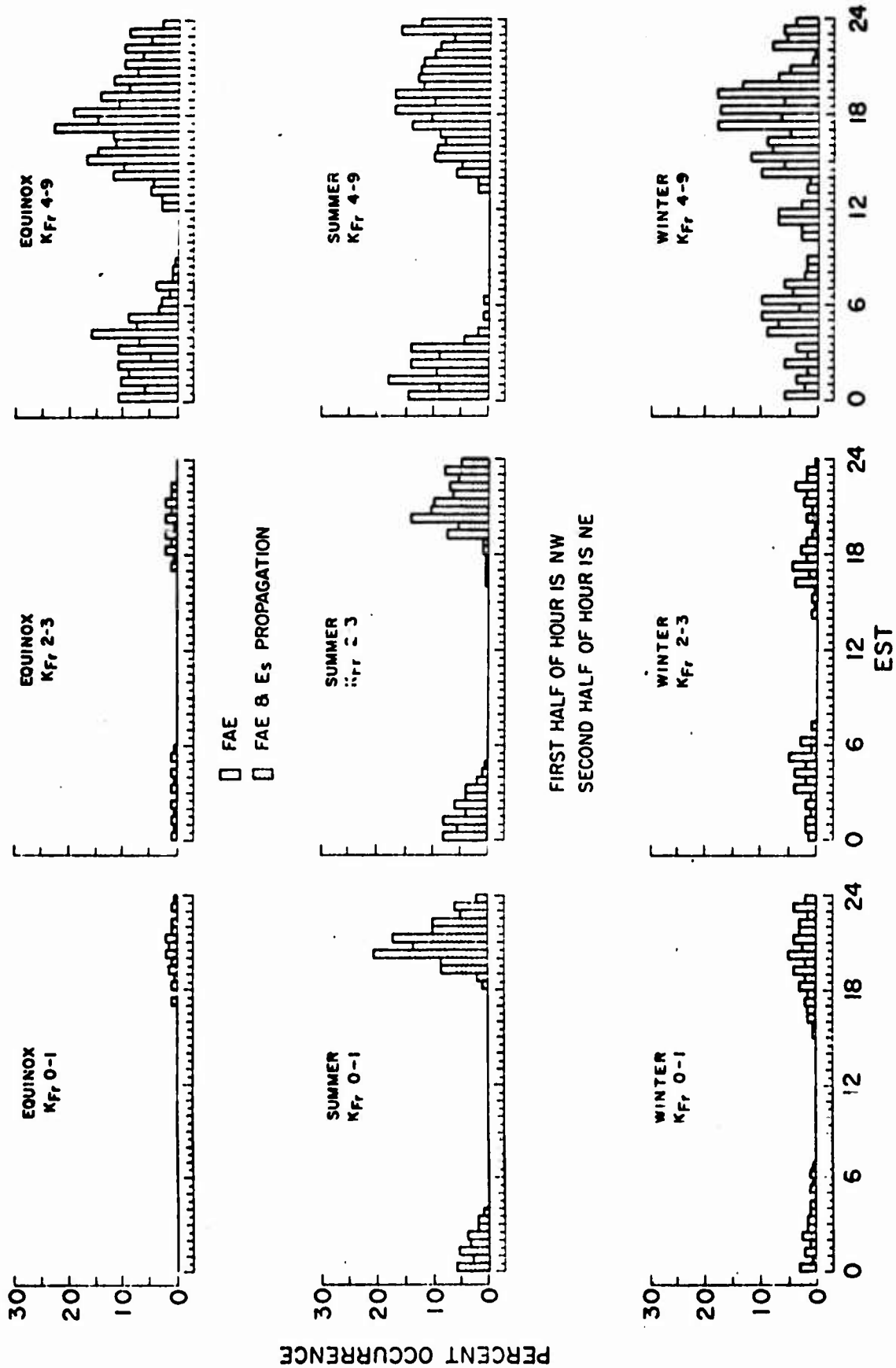


FIG 7. AVERAGE SEASONAL VARIATION OF FAE(E) FOR VARIOUS RANGES OF KFr. 1961-65.

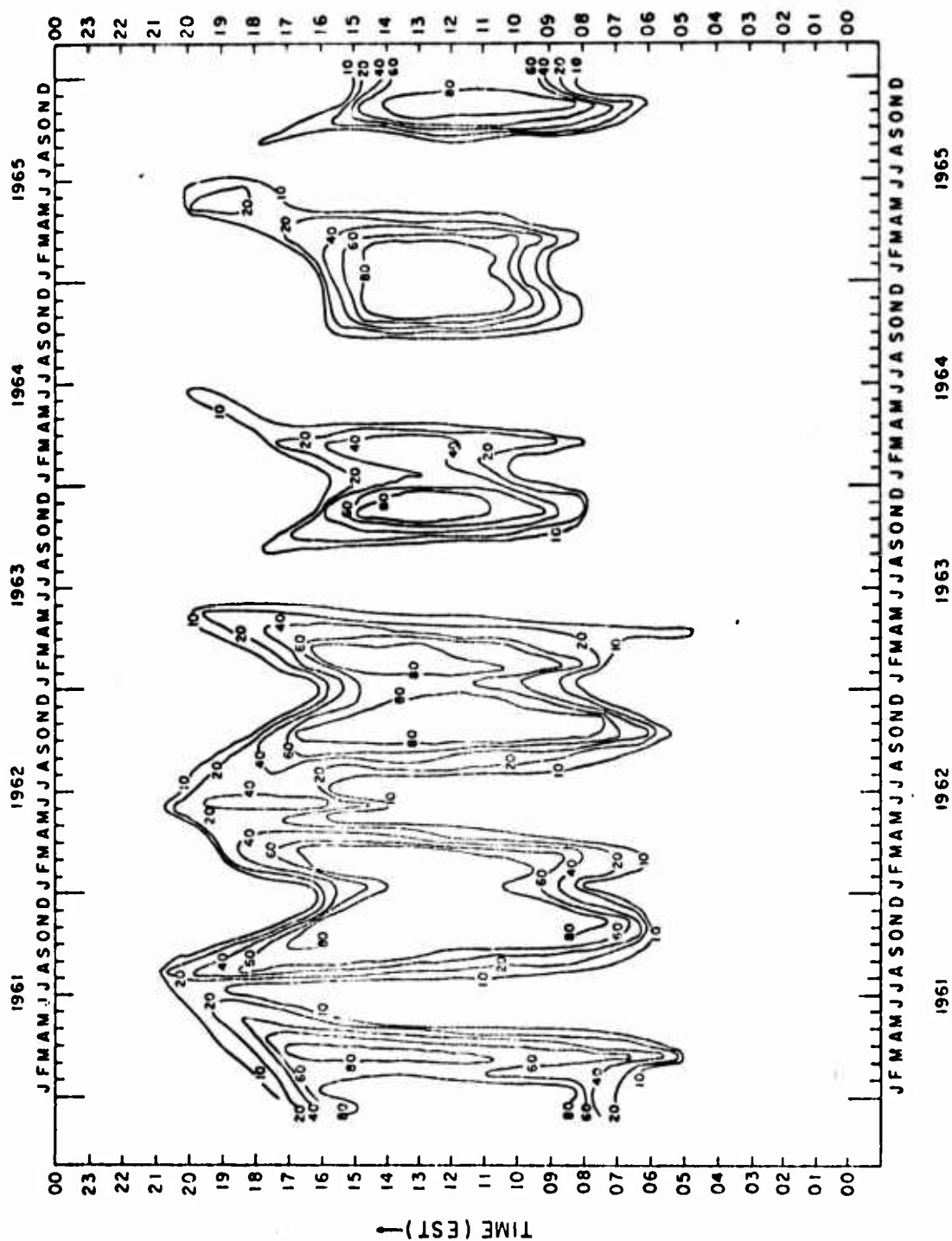


FIG. 8. PERCENTAGE OCCURRENCE CONTOURS OF 1F ECHO IN THE NW QUADRANT FOR KFR 0-3

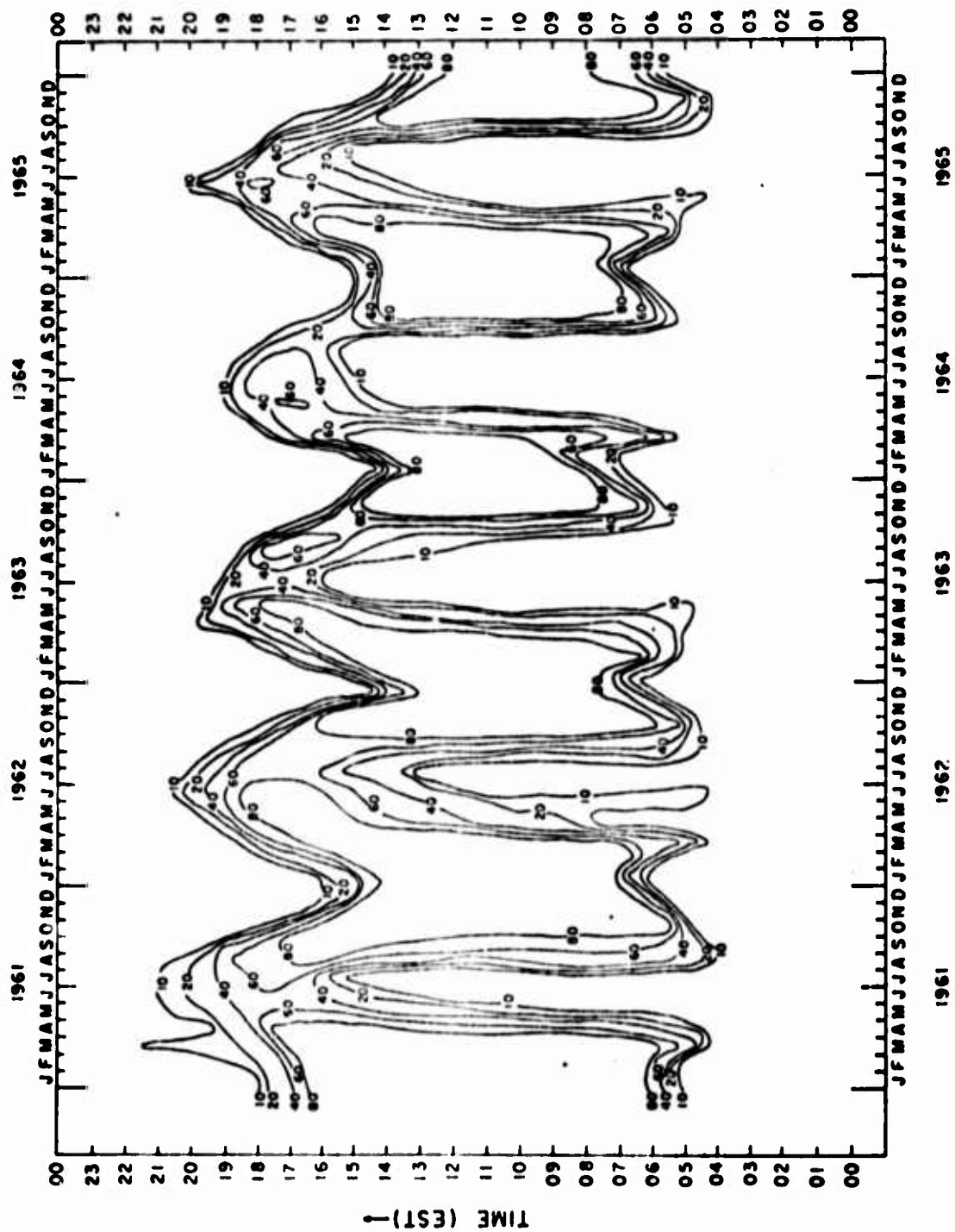


FIG. 9. PERCENTAGE OCCURRENCE CONTOURS OF IF ECHO IN THE NE QUADRANT FOR KFR 0 - 3



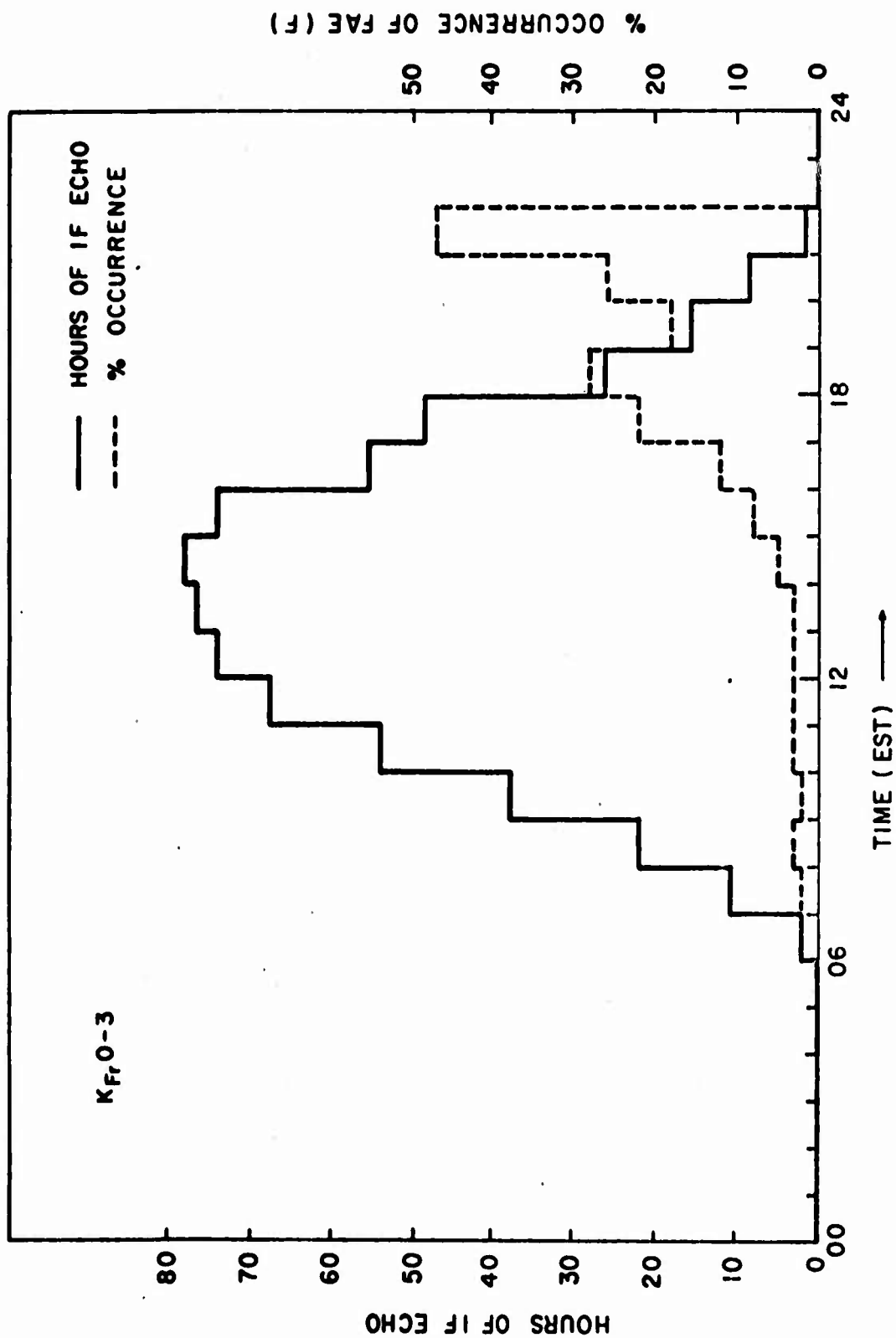


FIG. 10. AVERAGE DIURNAL VARIATION OF IF ECHO OCCURRENCE AND OF FAE(F) OCCURRENCE WHEN IF ECHO IS PRESENT FOR K<sub>FR</sub> 0-3, 1961 - 1965

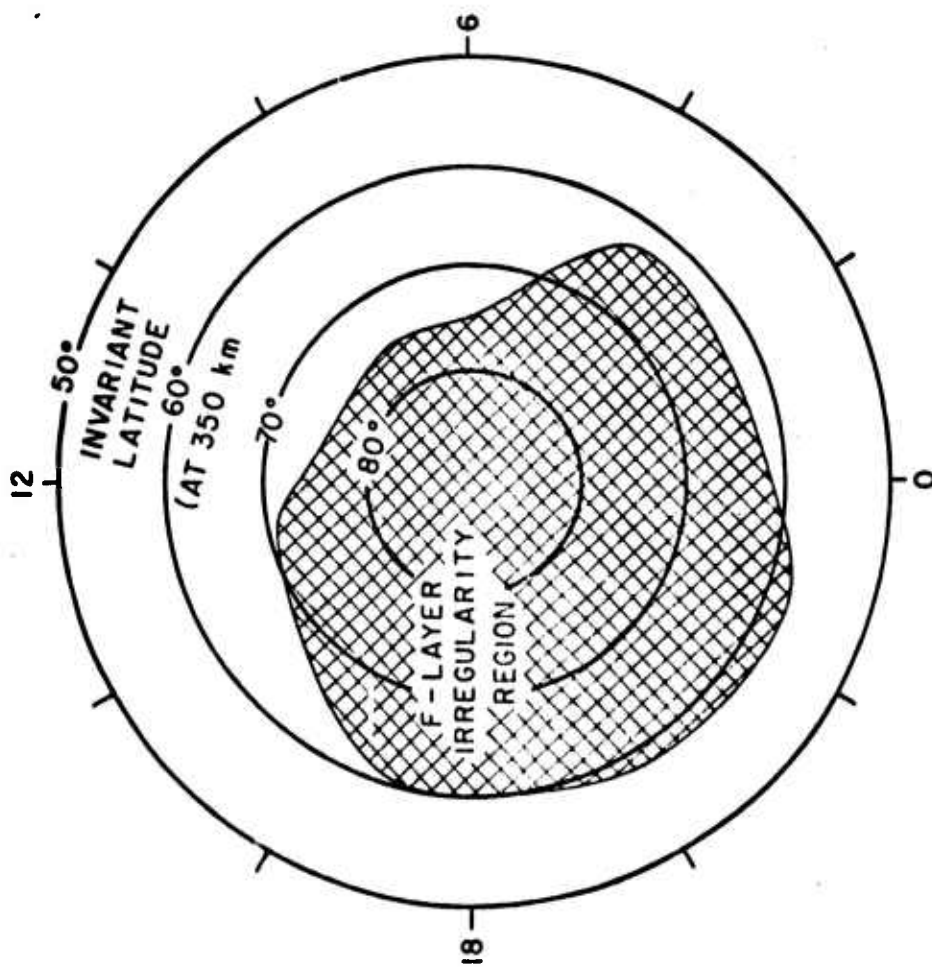


FIG. II. DIURNAL PATTERN OF THE EXTENT OF THE F-LAYER IRREGULARITY REGION  
DURING QUIET MAGNETIC CONDITIONS ( $K_{F10-3}$ )

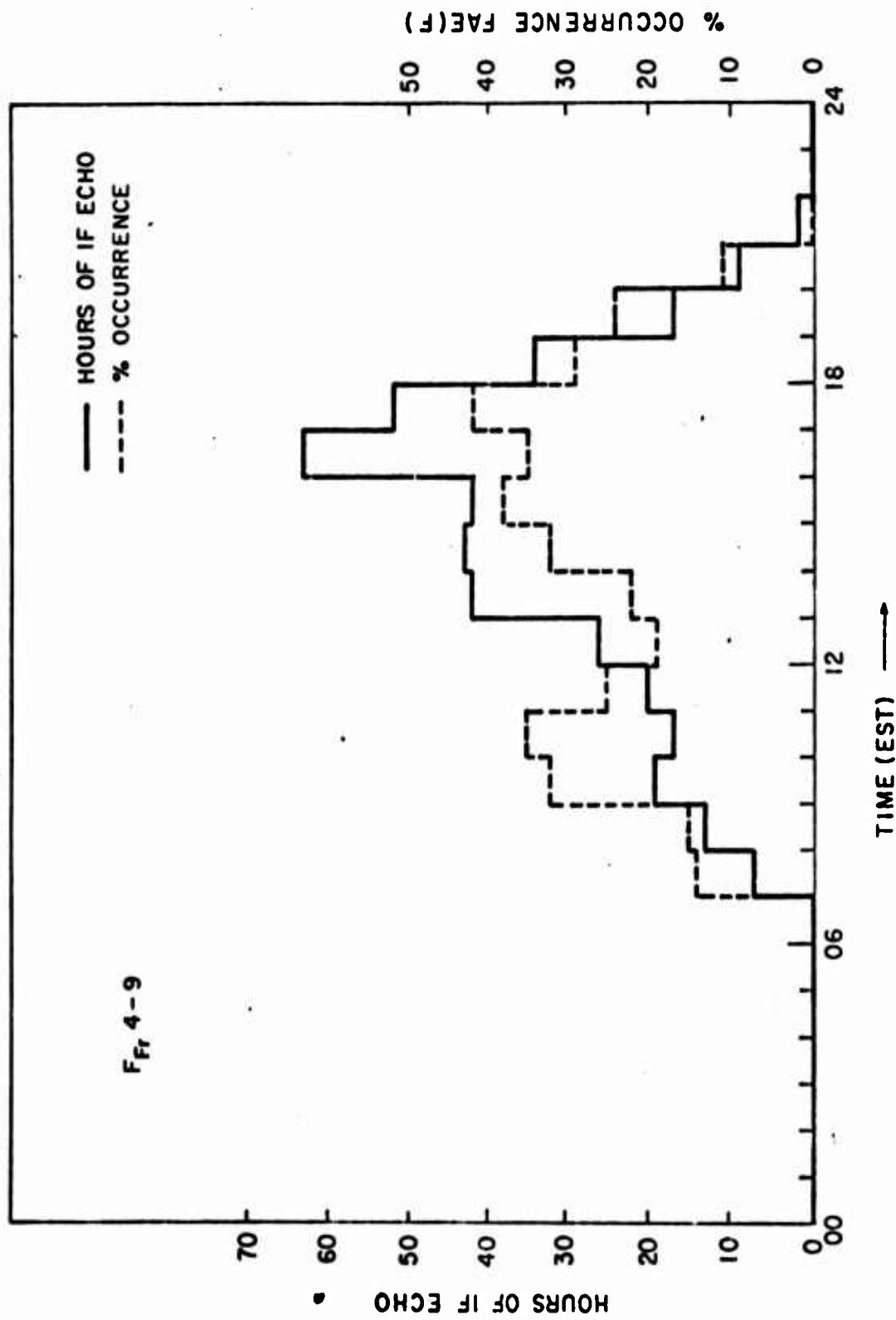
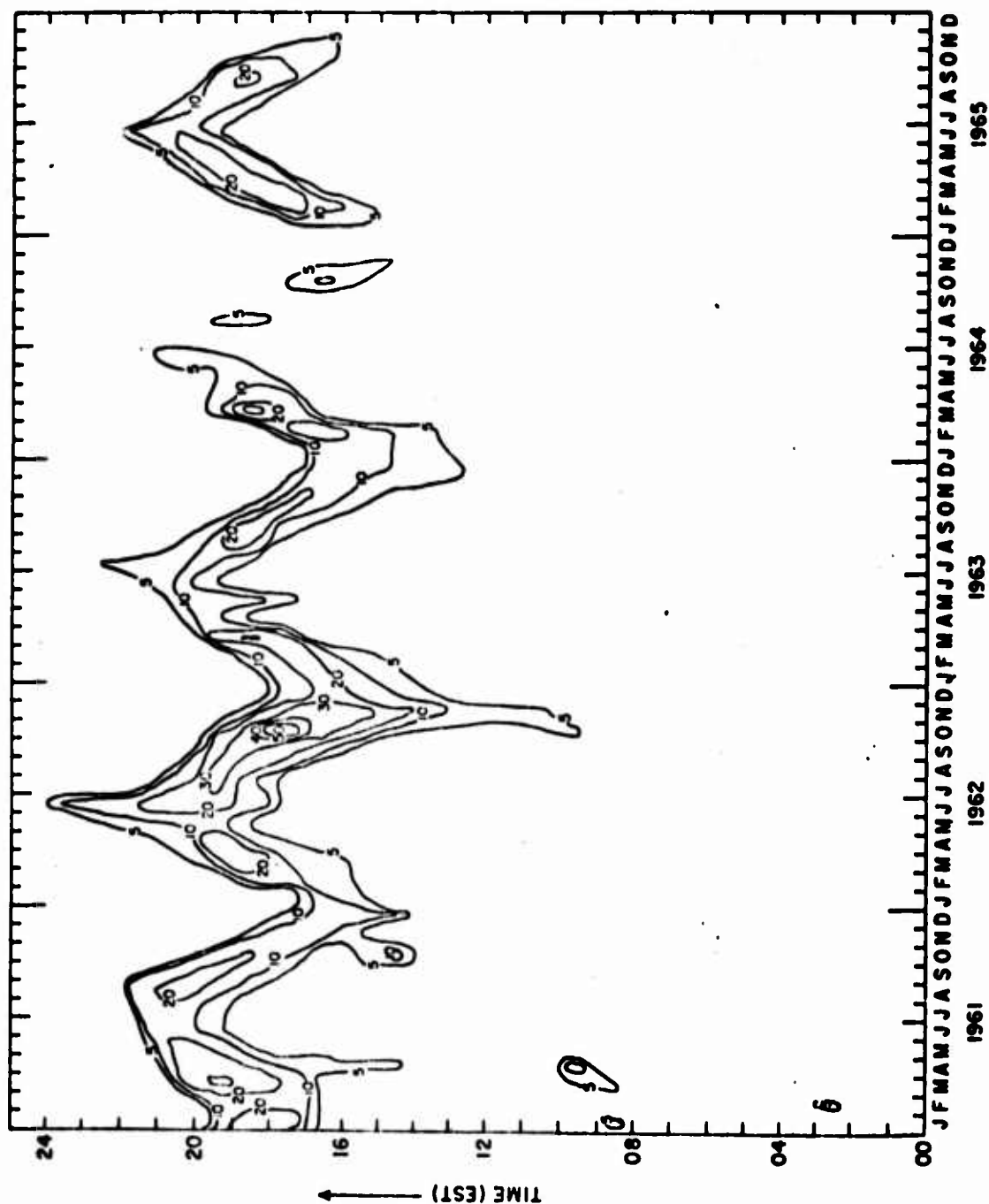


FIG. 12. AVERAGE DIURNAL VARIATION OF IF ECHO OCCURRENCE AND OF FAE(F) OCCURRENCE WHEN IF ECHO IS PRESENT FOR K<sub>Fr</sub> 4-9, 1961-1965



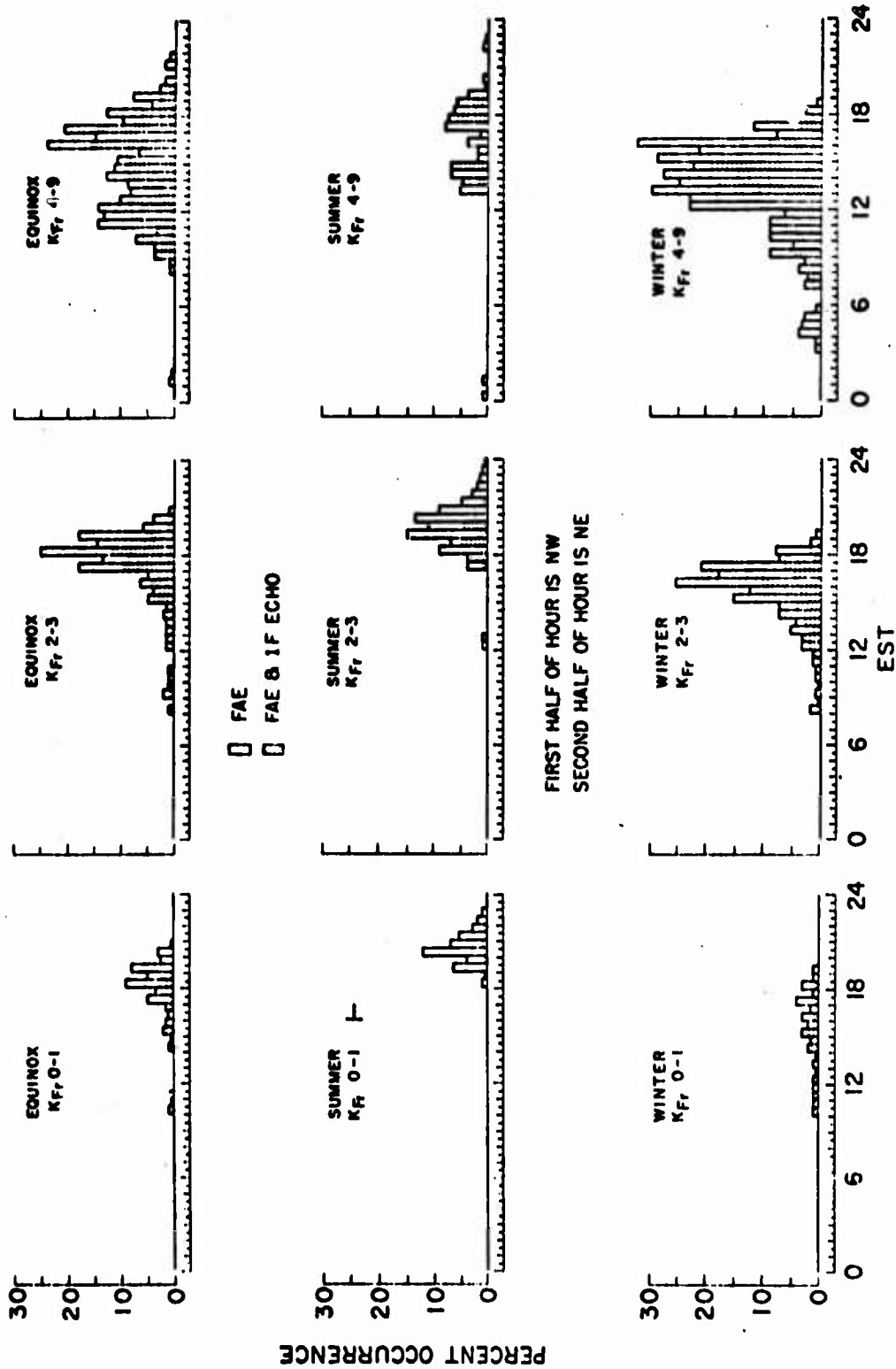


FIG. 14. AVERAGE SEASONAL VARIATION OF FAE (F) FOR VARIOUS RANGES OF  $K_{Fr}$ . 1961-65.

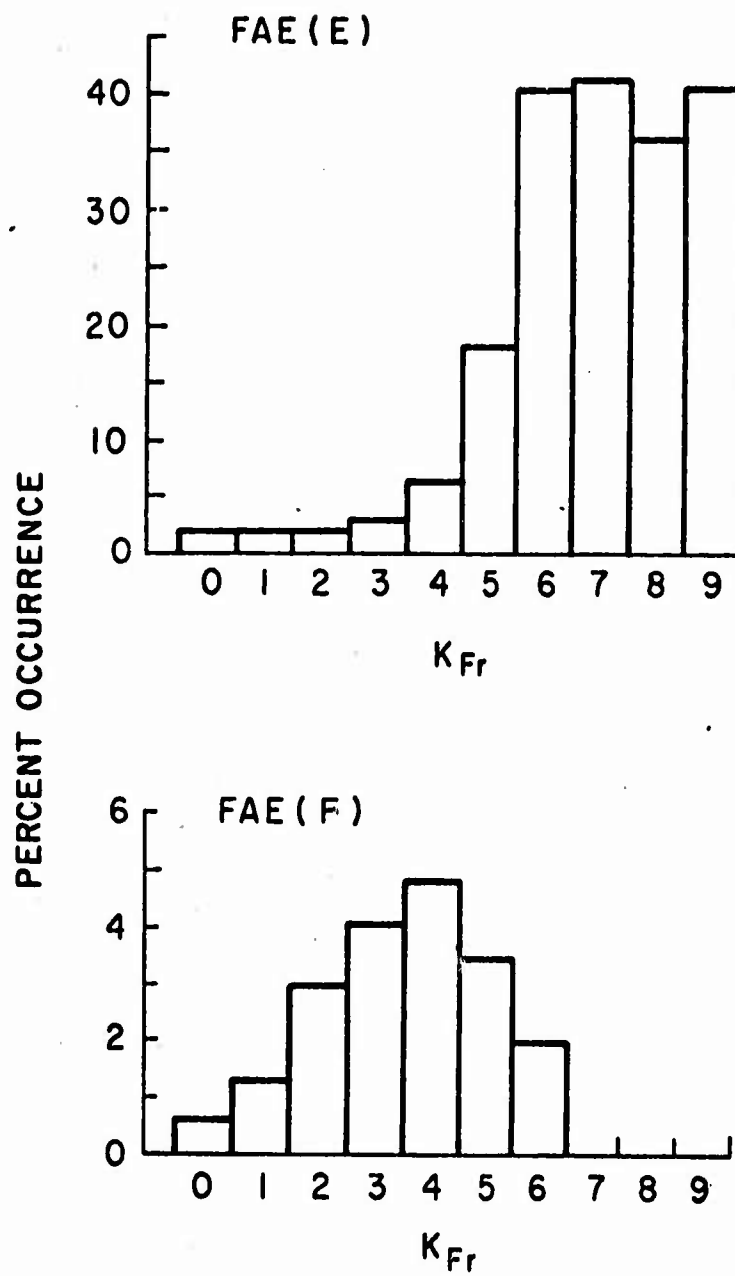


FIG. 15. FAE (E) AND FAE (F) AS A FUNCTION OF  $K_{FR}$

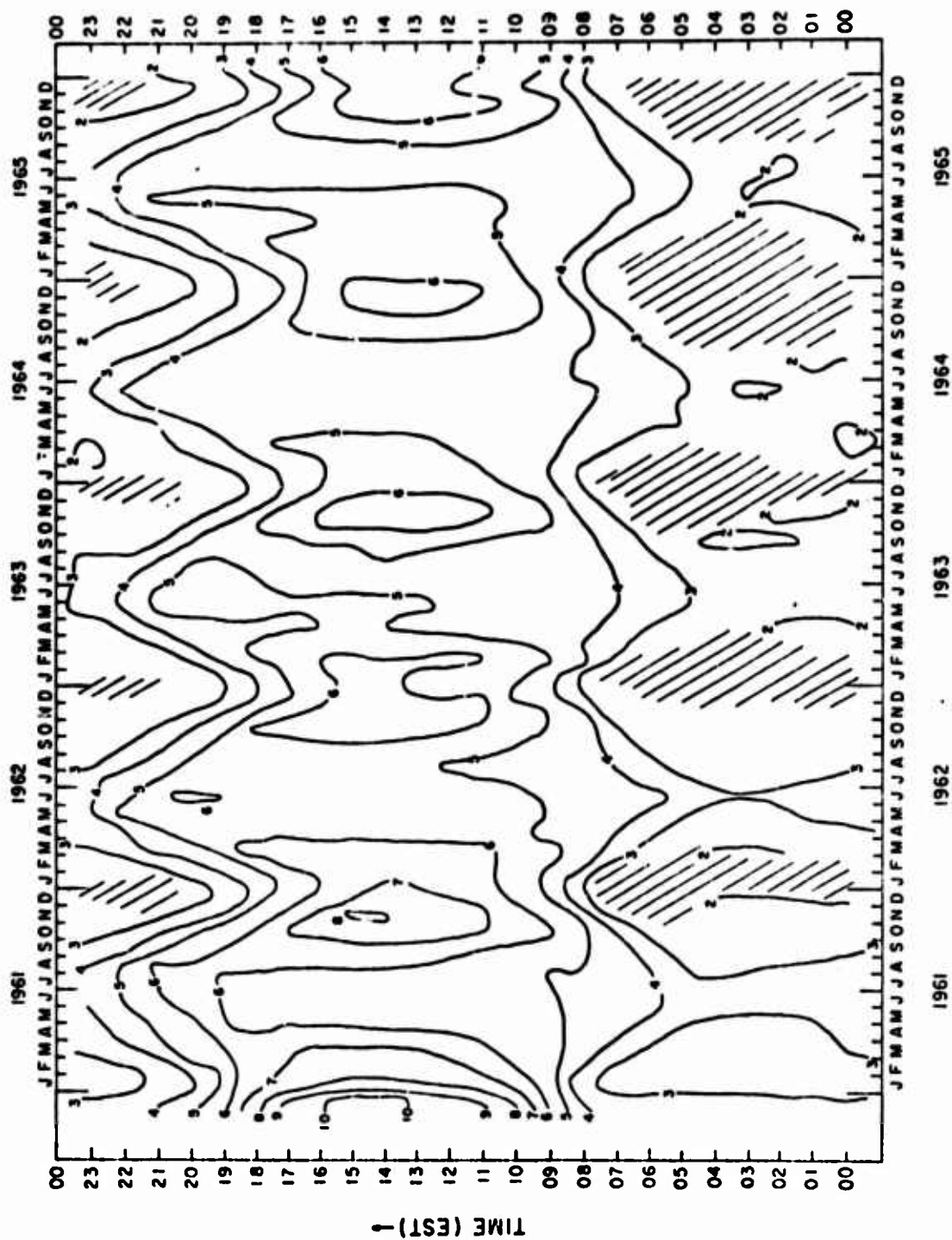


FIG. 16. MONTHLY MEDIAN  $f_0F_2$  CONTOURS FOR WINNIPEG ( KENORA AFTER OCT. 1963 )

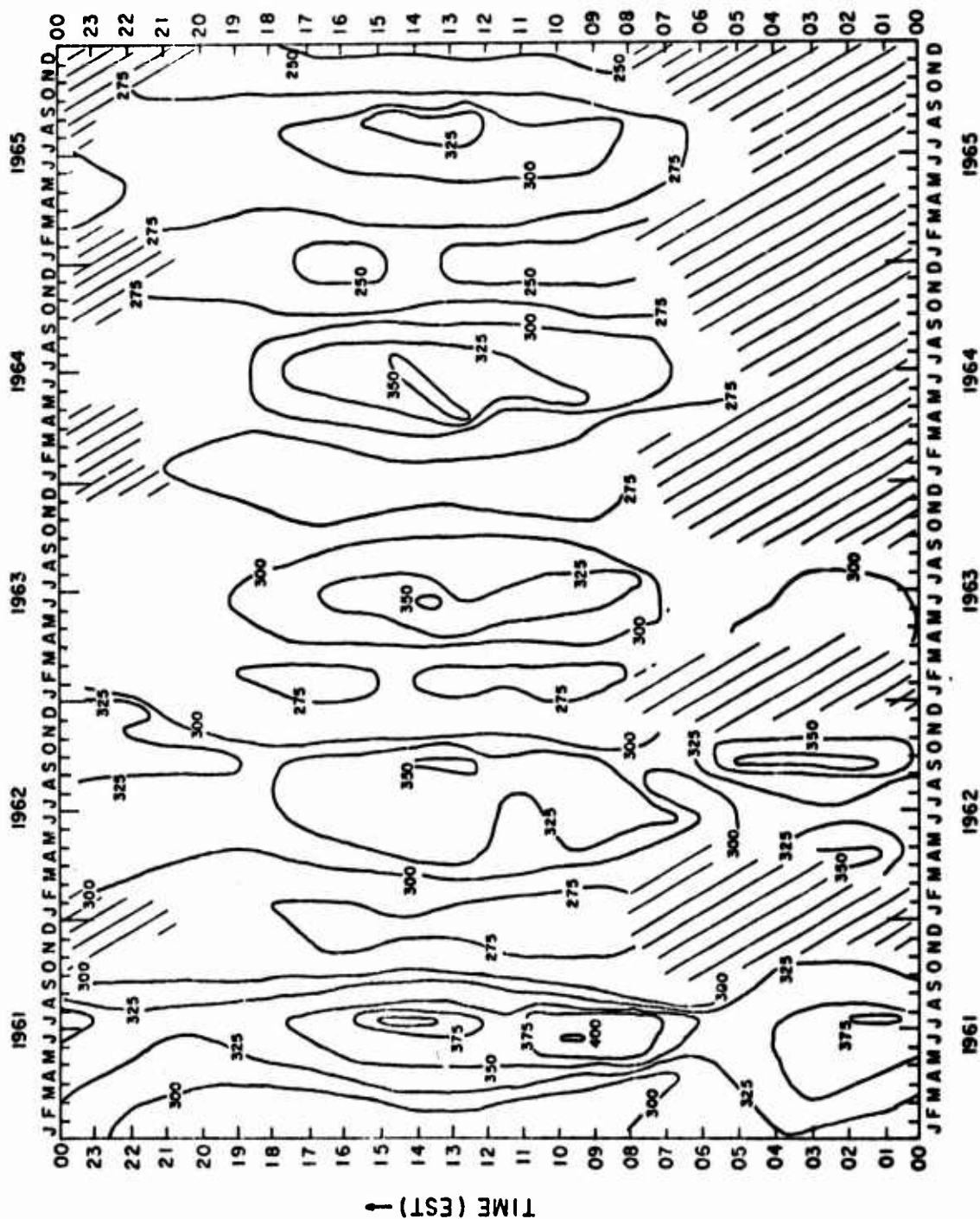


FIG. 17. MONTHLY MEDIAN M(3000)F<sub>2</sub> CONTOURS FOR WINNIPEG (KENORA AFTER OCT. 1963)



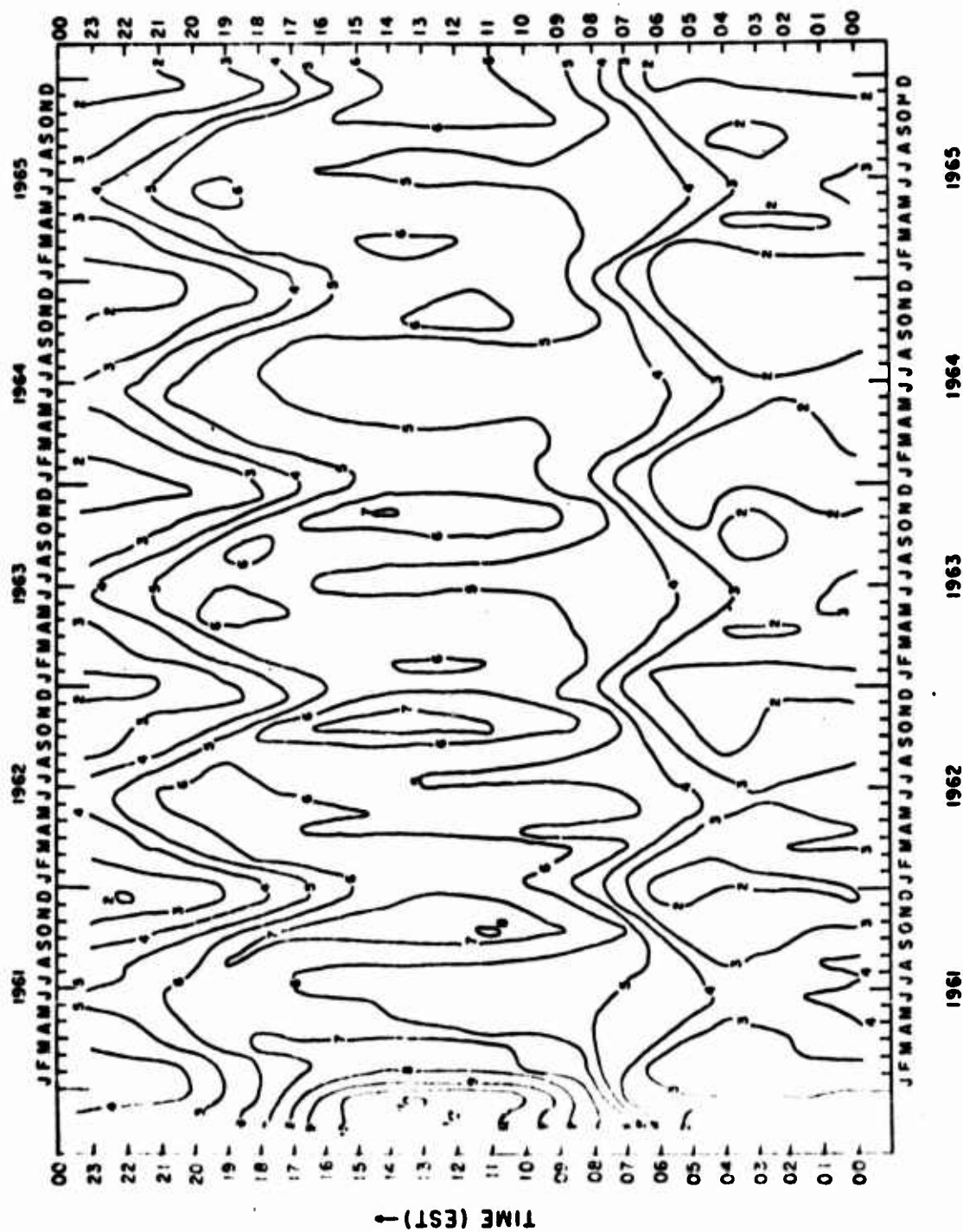


FIG. 18. MONTHLY MEDIAN  $f_0F_2$  CONTOURS FOR ST. JOHN'S, NEWFOUNDLAND

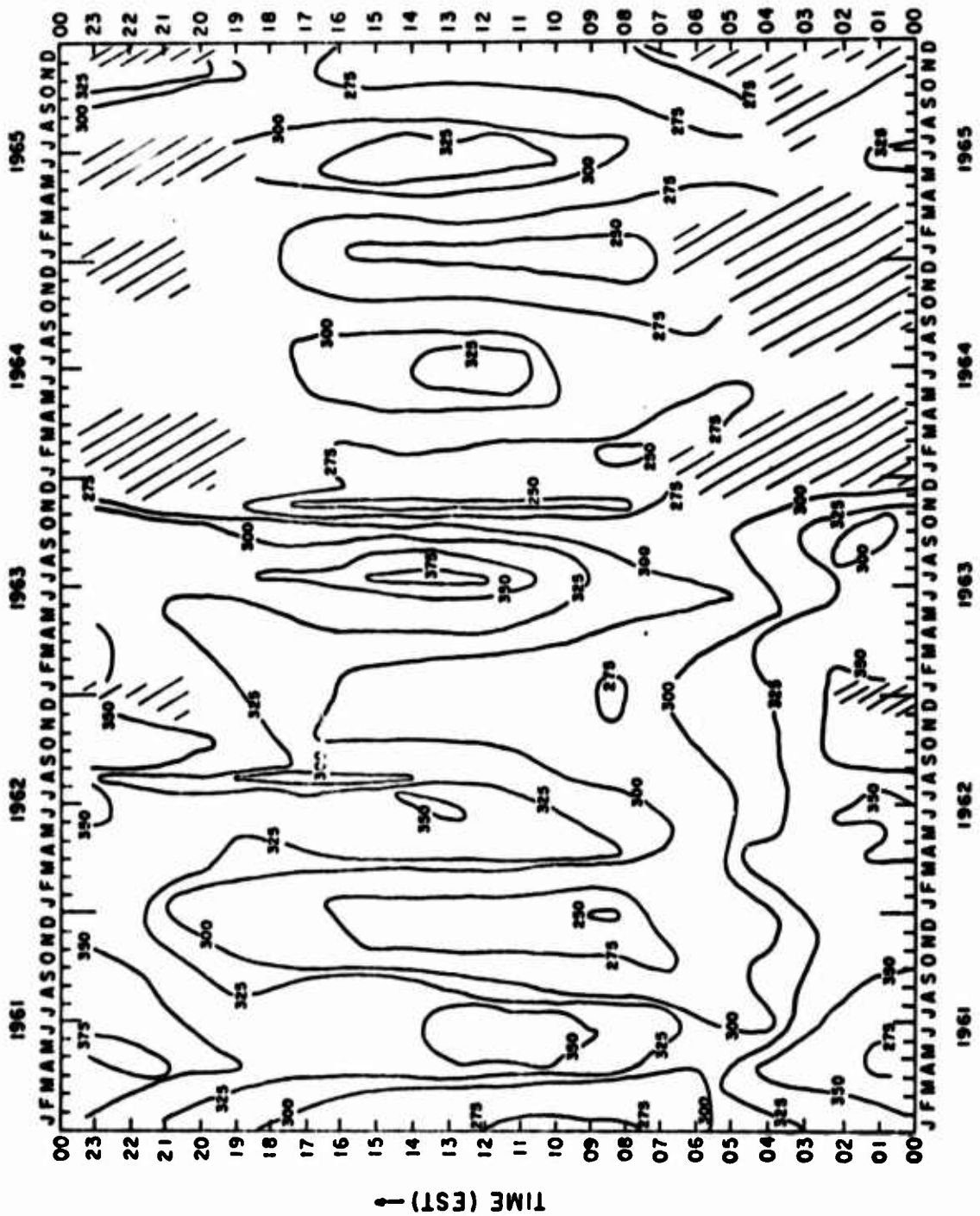


FIG. 19. MONTHLY MEDIAN  $M(3000)F_2$  CONTOURS FOR ST. JOHN'S, NEWFOUNDLAND

## REFERENCES

- Aarons, J., J.P. Mullen, and H.E. Whitney, "The Scintillation Boundary", J. Geophys. Res., 74, 884, 1969.
- Aarons, J., and R.S. Allen, "Scintillation Boundary during Quiet and Disturbed Magnetic Conditions", J. Geophys. Res., 76, 170, 1971.
- Au, W.W.L., "The Morphology of Backscatter from F-layer Field-Aligned Irregularities at Mid- and High-Latitudes and the Generation of these Irregularities", Research Report 70/16-35, Contract IIV-3816-0966, Washington State University, Pullman, Washington, March, 1970.
- Basu, Sunanda and R.L. Vesprini, "Field Aligned E- and F-Layer Backscatter Observations", Scientific Report 1, Contract AF19628-71-C-0250, Emmanuel College, Boston, MA, January, 1972.
- Bates, H.F., "HF Propagation Characteristics through Auroral Ionosphere", Final Report, SRI Project 7539, Purchase Order 211-000480-T1926, Stanford Research Institute, Menlo Park, California, May, 1969.
- Bates, H.F., "The Aspect Sensitivity of Spread-F Irregularities", J. Atmos. Terr. Phys., 33, 111, 1971.
- Booker, H.G., "A Theory of Scattering by Non-isotropic Irregularities with Application to Radar Reflections from the Aurora", J. Atmos. Terr. Phys., 8, 204, 1956.
- Chesnut, W.G., J.C. Hodges, and R.L. Leadabrand, "Auroral Backscatter Wavelength Dependence Studies", Final Report, SRI Project 5535, Contract AF30(602)-3734, Stanford Research Institute, Menlo Park, California, 1968.
- Closs, R.L., "Sporadic E and Geomagnetic Activity", J. Geophys. Res., 76, 7000, 1971.
- Collins, C., and P.A. Forsyth, "A Bistatic Radio Investigation of Auroral Ionization", J. Atmos. Terr. Phys., 13, 315, 1959.

- Croft, T.A., "Sky-Wave Backscatter; A Means for Observing Our Environment at Great Distances", *Rev. Geophys. Space Phys.*, 10, 73, 1972.
- Egan, R.D., and A.M. Peterson, "Backscatter Observations of Sporadic E" in *Ionospheric Sporadic E*, Pergamon Press, England, 1962.
- Eyrfrig, R.W., "The Effect of the Magnetic Declination on the F2 Layer", *Annales de Geophysique*, 19, 102, 1963.
- Farley, D.T., "A Plasma Instability Resulting in Field Aligned Irregularities in the Ionosphere", *J. Geophys. Res.*, 68, 6083, 1963.
- Feldstein, Y.I., "Peculiarities in the Auroral Distribution and Magnetic Disturbance Distribution in High Latitudes Caused by the Asymmetrical Form of the Magnetosphere", *Planet. Space Sci.*, 14, 121, 1966.
- Forsyth, P.A., "The Rate of Occurrence of VHF Radio-Aurora over an Eleven-Year Period", *J. Atmos. Terr. Phys.*, 31, 313, 1969.
- Gadsden, M., "On the Association of 'Auroral' Radar Echoes with the Aurora", *Planet. Space Sci.*, 15, 693, 1967.
- Goodwin, G.L., "Some Aspects of Direct Backscatter Echoes from Sporadic-E", *J. Atmos. Terr. Phys.*, 27, 777, 1965.
- Herman, J.R., "Spread F and Ionospheric F-Region Irregularities", *Rev. Geophys.*, 4, 255, 1966.
- Hoh, F.C., "Instability of Penning-Type Discharges", *Phys. Fluids*, 6, 1184, 1963.
- Kelley, M.C., and F.S. Mozer, "A Satellite Survey of Vector Electric Fields in the Ionosphere at Frequencies from 10 to 500 Hertz, 1. Isotropic, High Latitude, Low Frequency Emissions", *Space Sciences Laboratory Series 12, Issue 34*, Contract N00014-69-A-0200-1015, December 1971.
- Kohl, H., J.W. King, and D. Eccles, "An Explanation of the Magnetic Declination Effect in the Ionospheric F2-Layer", *J. Atmosph. Terr. Phys.*, 31, 1011, 1969.

- Leadabrand, R.L., "A Note on the Disposition of Auroral Ionization in Space", J. Geophys. Res., 66, 421, 1961.
- Leadabrand, R.L., "Electromagnetic Measurements of Auroras", in Auroral Phenomenon, Stanford University Press, U.S.A., 1965.
- Maeda, K.I., and T. Sato, "The F-region during Magnetic Storms", Proc. of the IRE, 47, 232, 1959.
- Matsushita, S., "A Study of the Morphology of Ionospheric Storms", J. Geophys. Res., 64, 305, 1959.
- Matthew, E.H., "Preliminary Survey of Results of Observations of Field-Aligned Irregularities from Brisbane", Scientific Report 4, Contract AF64(500)-9, Radio Research Station, University of Queensland, Brisbane, November, 1961.
- Moorcroft, D.R., "Radio-Auroral Aspect Sensitivity and the Two-Stream Instability", J. Geophys. Res., 77, 765, 1972.
- Peterson, A.M., G.G. Villard, Jr., R.L. Leadabrand, and P.B. Gallagher, "Regularly-Observable Aspect-Sensitive Radio Reflections from Ionization Aligned with the Earth's Magnetic Field and Located within the Ionospheric Layers at Middle Latitudes", J. Geophys. Res., 60, 497, 1955.
- Reid, G.C., "The Formation of Small-Scale Irregularities in the Ionosphere", J. Geophys. Res., 73, 1627, 1968.
- Rishbeth, H., "On Explaining the Behavior of the Ionospheric F-region", Rev. Geophys., 6, 33, 1968.
- Rishbeth, H., "Thermospheric Winds and the F-region", J. Atmosph. Terr. Phys., 34, 1, 1972.
- Rosenberg, N.W., and S.P. Zimmerman, "Ionospheric Winds and Viscous Dissipation", Radio Science, 7, 377, 1972.
- Shimazaki, T., "World-Wide Daily Variations in the Height of the Maximum Electron Density in the Ionospheric F2-layer", J. Rad. Res. Labs, 2, 85, 1955.
- Simon, A., "Instability of a Partially Ionized Plasma in Crossed Electric and Magnetic Fields", Phys. Fluids, 6, 382, 1963.

- Strobel, D.F., and M.B. McElroy, "The F2 layer at Middle Latitudes", Planet. Space Sci., 18, 1181, 1970.
- Sverdlov, Yu. L., "New Terminology in the Field of Study of the Effect of Radio Wave Scattering on Auroral Inhomogeneities", Geomagn. Aeron., 11, 492, 1971.
- Unwin, R.S., and F.B. Knox, "The Morphology of VLF Radio Aurora at Sunspot Maximum, 4, Theory", J. Atmos. Terr. Phys., 30, 25, 1968.
- Unwin, R.S., and F.B. Knox, "Radio Aurora and Electric Fields", Radio Science, 6, 1061, 1971.
- Whitehead, J.D., "Production and Prediction of Sporadic E", Rev. Geophys. Space Phys., 8, 65, 1970.

**FIELD ALIGNED E- AND F-LAYER BACKSCATTER OBSERVATIONS**

**by**

**SUNANDA BASU**

**ROBERT L. VESPRINI**

**EMMANUEL COLLEGE  
400 THE FENWAY  
BOSTON, MASSACHUSETTS 02115**

## ABSTRACT

In a reanalysis of the HF (19 MHz) backscatter data from Plum Island MA, the occurrence of field aligned echoes from the E and F layers, called FAE(E) and FAE(F) respectively, was studied in detail. From this site, direct orthogonality with the magnetic field can be achieved only at E-layer heights, whereas refraction is necessary for the F layer. FAE(E) during quiet magnetic conditions ( $K_{F2}0-3$ ) is a nighttime phenomenon with a definite maximum during the summer, when it is accompanied by groundscattered  $E_s$ . A weaker maximum is observed in the winter. Geomagnetic activity increases the occurrence of FAE(E) when no seasonal control is evident. During quiet magnetic conditions, FAE(F) are confined primarily to sunset hours. The equinoxes show more activity than the solstices, and the FAE(F) are generally accompanied by F-layer supported groundscatter echoes. FAE(F) shows a positive correlation with solar cycle. The incidence of FAE(F) increases monotonically with  $K_{F2}$  until a threshold value is reached ( $K_{F2} \geq 4$ ), beyond which the depletion in the background ionization causes it to decrease, with complete cut-off for  $K_{F2} \geq 7$ .

In the next scientific report, the occurrence characteristics of various groundscattered echoes will be presented and these will be used to explain qualitatively the observed characteristics of FAE.



## **TABLE OF CONTENTS**

- 1. Introduction**
- 2. Equipment**
- 3. Data Reduction**
- 4. Data Presentation**
  - 4.1 Occurrence of FAE(E)**
  - 4.2 Occurrence of FAE(F)**
- 5. Range Distribution of FAE**
- 6. Average Seasonal Behavior of FAE**
- 7. FAE as a Function of Magnetic Activity**
- 8. Solar Cycle Dependence of FAE**
- 9. Summary and Conclusions**
  - 9.1 FAE(E)**
  - 9.2 FAE(F)**
- 10. Future Work**

## LIST OF FIGURES

### Figure

- 1a Propagation angle contours for Plum Island MA at 110 km height
- 1b Propagation angle contours for Plum Island MA at 300 km height
- 2 Backscatter from field aligned irregularities at E-layer heights for  $K_{F_r}$  0-3 during 1961
- 3 Backscatter from field aligned irregularities at E-layer heights for  $K_{F_r}$  0-3 during 1962
- 4 Backscatter from field aligned irregularities at E-layer heights for  $K_{F_r}$  0-3 during 1963
- 5 Backscatter from field aligned irregularities at E-layer heights for  $K_{F_r}$  0-3 during 1964
- 6 Backscatter from field aligned irregularities at E-layer heights for  $K_{F_r}$  0-3 during 1965
- 7 Average E-layer backscatter for each month for  $K_{F_r}$  4-9 during the period 1961-1965
- 8 Backscatter from field aligned irregularities at F-layer heights for  $K_{F_r}$  0-3 during 1961
- 9 Backscatter from field aligned irregularities at F-layer heights for  $K_{F_r}$  0-3 during 1962
- 10 Backscatter from field aligned irregularities at F-layer heights for  $K_{F_r}$  0-3 during 1963
- 11 Backscatter from field aligned irregularities at F-layer heights for  $K_{F_r}$  0-3 during 1964
- 12 Backscatter from field aligned irregularities at F-layer heights for  $K_{F_r}$  0-3 during 1965
- 13 Average F-layer backscatter for each month for  $K_{F_r}$  4-9 during the period 1961-1965
- 14 Range distribution of FAE's during the spring season, 1961-1965

## Figure

- 15 Possible multi-hop propagation modes and direct scatter from field aligned irregularities in the E and F layers
- 16 Range distribution of FAE's during the summer season, 1961-1965
- 17 Range distribution of FAE's during the fall season, 1961-1965
- 18 Range distribution of FAE's during the winter season, 1961-1965
- 19 Diurnal pattern of the range distribution of FAE's for 1961
- 20 Diurnal pattern of the range distribution of FAE's for 1964
- 21 Percentage range distribution of all FAE occurrence for 1961 & 1964
- 22 Average seasonal behavior of FAE(E) during magnetically quiet and disturbed periods, 1961-1965
- 23 Average seasonal behavior of FAE(F) during magnetically quiet and disturbed periods, 1961-1965
- 24 FAE(E) as a function of magnetic index  $K_{F_r}$
- 25 FAE(F) as a function of magnetic index  $K_{F_r}$
- 26 Percentage occurrence contours of E-layer echoes for  $K_{F_r}$  0-3 for 1961-1965
- 27 Percentage occurrence contours of F-layer echoes for  $K_{F_r}$  0-3 for 1961-1965
- 28 Mean Zurich sunspot numbers for 1961-1965

## 1. INTRODUCTION

A continuous series of fixed frequency oblique backscatter observations was conducted at the Plum Island site ( $42.63^{\circ}\text{N}$ ,  $70.82^{\circ}\text{W}$ ) of the Sagamore Hill Radio Observatory between January 1961 and December 1965. The primary objective of this program was to study the field aligned irregularities in the ionization density at both E-layer and F-layer heights. These irregularities are responsible for the auroral clutter which affects the performance of HF, and even VHF and UHF, high latitude radars whose purpose is to detect and track aircraft and missiles (Leadabrand, 1964). A preliminary analysis of a part of this data has been presented by Malik and Aarons (1964) in which they noted the frequent occurrence of auroral echoes over a three year period. A more recent analysis of the data has been made by Aarons (1971).

Studies of radar echoes from field aligned irregularities have been made for many years. However, studies of the field aligned E-region irregularities (to be henceforth referred to as FAE(E)) have been more numerous as indicated in the review articles by Booker (1960), Chamberlain (1961) and Bowles (1964). This is primarily because it is possible to achieve direct orthogonality at E-layer heights from most mid-latitude and sub-auroral stations. The condition that the earth's magnetic field be perpendicular to the probing radar signal, also referred to as the aspect sensitivity requirement, is a necessary condition for sufficient backscatter to occur. Recent work (Bates, 1971) has shown that the intensity of the backscattered signal falls off 5-6 dB per degree off orthogonality.

The detection of field aligned F-region irregularities (FAE(F)) from most mid-latitude stations, however, will require sufficient refraction in the underlying layers to achieve orthogonality at F-layer heights. In order that the amount of refraction be adequate, frequencies in the HF range have to be used. The geometrical situation for the Plum Island site is shown in

Figures 1a and 1b. The aspect sensitivity requirements are directly met at 110 km, whereas the lowest propagation angle achieved at F-layer heights is  $100^\circ$  for straight line propagation. Thus the refraction in the underlying layers has to bend the ray by at least  $10^\circ$  to meet the orthogonality criterion at a height of 300 km. The interpretation of the F-layer echoes should thus be viewed in this context; namely, the absence of echoes need not necessarily mean the absence of irregularities but could be due to insufficient refraction, such as under nighttime conditions.

## 2. EQUIPMENT

The data used for this study were obtained from film records of a 19.39 MHz sounder located at Plum Island, Massachusetts ( $56^\circ$  invariant latitude). A low powered 1 kw peak-power radar was used with a pulse length of 1 millisecond and a repetition frequency of 10/sec. The pulses were transmitted by a horizontal three-element Yagi antenna placed  $0.6\lambda$  above ground and rotating at the rate of one revolution every eight minutes. The receiver band width was 1 kc. The resulting data were recorded on compressed time-scale film as well as on the range azimuth (PPI) type frames. The maximum range on the sweep was 3750 km taken in 750 km steps. Field aligned echoes, both FAE(E) and FAE(F), and sporadic-E and F-layer propagated ground scatter signals were read from the film and recorded on graphs. These graphs also recorded the azimuth of the various returns and their respective delays.

## 3. DATA REDUCTION

For the purpose of this report, the information present in the graphs referred to above was put into digital form. The

basic procedure was to record on punch cards the duration of the FAE and average delay, correct to the nearest millisecond for each hour of the day. The azimuth of these echoes, i.e., obtained from either the NW or NE quadrant, was also recorded. The quadrant behavior, however, is to be treated with caution due to the broad beamwidth (about  $45^\circ$ ) of the antenna used. When FAE's were observed, it was noted from the graphs whether sporadic-E or F-layer supported groundscatter was simultaneously present in the same quadrant. Results were recorded on the cards. The 3-hour magnetic activity index  $K_{F_r}$  obtained from Fredericksburg, Virginia or Fort Belvoir, Virginia was also put on these cards. It is to be mentioned that Fredericksburg is a few degrees to the south of the station whereas the FAE's are obtained from the north. However, Fredericksburg is in the same longitude zone as the observing site and this is considered important in the separation of diurnal and magnetic activity dependence of FAE's. The hours in which there was equipment failure were excluded from the analysis.

The punch cards were first sorted by range to distinguish between FAE(E) and FAE(F). It was found - and range scatter plots will also show this - that echoes which were obtained with delays less than six milliseconds (msec) were E-layer echoes. Any echoes obtained at greater ranges are presumed to be either direct F-layer echoes or a combination of multi-hop propagation and field alignment. Each of these two broad categories are then subdivided according to the  $K_{F_r}$  index. A range of  $K_{F_r}$  from 0-3 is considered to represent average quiet conditions, whereas  $K_{F_r}$  ranging from 4-9 represents disturbed conditions. Later sorting on the basis of  $K_{F_r}$  alone will justify this grouping.

The data, after being divided into the four categories mentioned above, were sorted to yield the percentage occurrence in each hour for a particular month. This is an actual percentage of occurrence obtained by dividing the number of hours the FAE was present in that particular hour of the month by the total

number of samples available for the same month. Other groups, such as that working at Washington State University (Keck and Hower, 1968) have used a definition whereby an occurrence of FAE for more than 5 minutes in an hour is considered to be an occurrence for the whole of that hour. Thus it is difficult to compare occurrence statistics among various groups of workers.

#### 4. DATA PRESENTATION

The behavior of the FAE's observed at Plum Island throughout the years 1961-65 is presented in the form of a series of histograms showing the diurnal variation of their percentage occurrence. We shall discuss the characteristics of each type of echo separately.

##### 4.1 Occurrence of FAE(E)

The occurrence of FAE(E) for the five years of observation is shown in Figures 2 through 7. Each diagram represents 12 months of data. The first half of each hour represents percentage occurrence of echoes obtained from the NW quadrant in that entire hour, whereas the second half represents the echoes from the NE quadrant for that same hour. The shading within the occurrence blocks shows the fraction of time for which sporadic-E supported groundscatter was simultaneously present. Figures 2 through 6 represent individual months for quiet conditions, whereas Figure 7 represents average disturbed months over the five years of observation, the samples being statistically insignificant for each month separately. The number of samples in Figures 2 through 6 range from a low of 18 (when there were many disturbed periods) to a maximum of 31. The month of December 1965 has about half as much data as the other months because the observations were terminated in the middle of the month. Equipment failure occurred very rarely. Figure 7,

even though an average over 5 years, has a similar number of samples in each block except for a few daytime blocks when there are less than ten samples.

The first obvious pattern of the quiet day FAE(E) is its occurrence in the evening, nighttime, and early morning hours. There is virtually no daytime FAE(E). There is a greater incidence during the solstices than during the equinoxes, with the summer maximum being higher than that in the winter. The winter months, having a longer period of darkness, show echo activity more uniformly distributed over a longer period of time than do the summer months. The increased occurrence during the solstice period is usually accompanied by increased sporadic-E supported propagation occurring simultaneously. This leads us to believe that there is a high degree of field-alignment in the sporadic-E patches that appear to the north of the station during the evening hours of the summer and winter months. The equinoctial periods are characterized by little or no occurrence at all, and very little of the FAE(E) that is present is accompanied by the sporadic-E type propagation so common in the summer. Thus there is a distinct seasonal dependence as well as diurnal dependence of quiet time FAE(E). One other obvious feature in these diagrams is the greater incidence of echo activity from the NW as compared to the NE. This asymmetry becomes self-explanatory when the geometry of the station as shown in Figure 1 is taken into consideration. Since the magnetic pole is to the NW of the station, a much greater degree of field alignment is possible in that direction.

Figure 7, representing the average monthly behavior of FAE(E)'s over the five years of observation during magnetically disturbed conditions ( $K_{F_r}$  4-9), shows many features which are different from the quiet time behavior. A uniformly higher nighttime percentage occurrence is obtained throughout the year, thus obliterating any seasonal differences. In addition, much more daytime activity is evident in the afternoon hours. The



summer and winter months, even though they have greater echo activity, have much less supporting sporadic-E propagation. This suggests that periods of magnetic activity tend to inhibit the formation of sporadic E. A similar E-W asymmetry is somewhat reduced, leading us to believe that during periods of greater magnetic activity the irregularities have a greater density and are received by a broad beam angle antenna at all northern azimuths.

#### 4.2 Occurrence of FAE(F)

The characteristics of the field aligned F-layer echoes are discussed in this section. This is a more complex phenomenon than the E-layer backscatter where orthogonality considerations are universally met. The monthly percentage occurrence curves are presented in Figures 8 through 13 following the same general procedure as for the FAE(E). The only difference is that the shading in this case represents the fraction of time for which the FAE(F) were accompanied by F-layer propagated groundscatter. This gives us an idea of the amount of refraction available to produce orthogonality at F-layer heights. The most obvious feature of the quiet day histograms (Figures 8-12) is the sunset peak of occurrence of these echoes. The peak is present throughout the year, but the equinoxes show more activity than the solstices. It must be remembered that there is a great deal of FAE(E) during the solstices which reduces the energy reaching F-layer heights.

A closer look at the diagrams shows that the peak echo activity shifts with the time of sunset - the peak occurs earlier in winter and much later in summer, a fact already pointed out by Malik and Aarons (1964). The supporting groundscatter pattern follows the echo pattern, and it is the gradual decrease of the groundscatter later in the evening that is responsible for the tapering off seen in the echo activity. This will be more clearly seen in the groundscatter contour

diagrams to be presented in a later report. From scintillation boundary concepts (Aarons and Allen, 1971), we know that the late evening and midnight hours are precisely those during which we expect an increased probability of finding F-layer field aligned irregularities at the latitudes of interest. However, the decay in underlying ionization at these hours makes it impossible for the ray to achieve orthogonality at the higher heights.

Some daytime backscatter is evident, almost all of it entirely supported by groundscatter. This shows that during the daytime refraction is adequate, but the absence of irregularities is the usual limiting factor. It is interesting to note that there is hardly any daytime backscatter activity during the summer which is probably due to the high incidence of  $E_s$ . We shall see later that most of the daytime FAE(F) observed have large delay times. There is a great deal of year-to-year variability in the occurrence statistics - in general the higher sunspot years showing greater activity.

The average behavior of the disturbed day FAE(F) is shown in Figure 13. As in Figure 7, each month represents the mean over five years of observation. There is an increase in the daytime backscatter throughout the year except during the summer months. There is also a shift in the sunset peak towards earlier hours of the afternoon. We shall further discuss the disturbed day features later in the report.

## 5. RANGE DISTRIBUTION OF FAE.

The range distribution of FAE's is presented in Figures 14 and 16 through 18 on an individual seasonal basis to determine, if possible, the most probable ranges for FAE(E) and FAE(F). The diagrams include backscatter from both quiet and disturbed days in each season. The seasons are defined such that spring

represents Feb-Apr; summer, May-July; fall, Aug-Oct; and winter, Nov-Jan. The ordinate represents the total number of hours of backscatter echo obtained with delays ranging between 2 and 25 msec. It is to be emphasized that these are not percentage occurrence curves, but each seasonal curve shows the total number of hours of echo obtained in a particular season out of a possible maximum of roughly  $90 \times 24 = 2160$  hours. The graphs are not shown as histograms in order to facilitate the superposition of data obtained during the five consecutive years.

Each seasonal curve clearly shows a maximum around 3-4 msec delay and again around 7-9 msec delay with a distinct minimum at 5 msec. Thus it is quite reasonable to assume that the echoes represented by delays less than 6 msec are FAE(E), whereas the echoes obtained at delays  $\geq 6$  msec originate in the F layer. The range corresponding to each millisecond is 150 km for free space propagation. Referring to Figure 1a, we find that for an E-layer height of 110 km, delays of 3-4 msec correspond to elevation angles of  $6^\circ$ - $10^\circ$ , and for azimuths centered around magnetic north, these delays correspond to propagation angles ranging between  $89^\circ$ - $91^\circ$ . A direct comparison with Figure 1b is unjustified for the F-layer echoes, as considerable refraction makes the ray paths deviate greatly from idealized straight line paths on which this diagram is based. In addition, there is a much greater variability in the height of the F layer.

The long range field aligned echoes, though only a small fraction of the regular FAE(F), show certain interesting features. All the seasons show small peaks around 13-14 msec, another close to 18-19 msec, and a very small one near 22-23 msec. The first two of these roughly correspond to a 2F1E mode and a 3F2E mode respectively, in terms of their observed delay as shown in Figure 15. It should be noted that for the 2F1E mode the field alignment is in the E layer, whereas for the 3F2E mode the field alignment is in the F layer. Later diagrams will show that these long range echoes are observed

only in the daytime when there is sufficient ionization in the E layer and the F layer. The possibility of observing such modes of propagation has been demonstrated by Agy (1971) using ray tracings through a model high-latitude ionosphere. The radar used being of low power, these modes have the added advantage of a minimum number of traversals through the absorbing D region.

Figures 16 through 18 show similar characteristics for the three other seasons. Figure 16 which represents summer conditions is somewhat different in as much as no long-range echoes are observed. The decrease in F-layer activity may be attributed to two causes: (1) the summer decrease in  $f_oF2$  which decreases refraction and (2) the high incidence of sporadic E which severely decreases the energy reaching F-layer heights. Figure 18 representing winter conditions has only four graphs superposed on it since winter 1965 was not complete, observations having been stopped in the middle of December. The interesting point to note on this graph is the relatively large peak at 22 msec which is probably due to the ground supported 3F mode with field alignment in the F layer as shown in Figure 15. The winter  $f_oF2$  being the highest and  $f_oE$  being the lowest of any season in the year, conditions for observing such a mode should be most favorable in the winter.

To show the diurnal variation of the range of echoes in any given year, the day was divided into 3 different time periods: a daytime period between 0600 and 1800 hours, a sunset and pre-midnight period between 1800 and 2400 hours, and finally the post-midnight period between 0000 and 0600 hours. The resulting graphs for the years 1961 and 1964 are shown in Figures 19 and 20. All the long-range echoes are confined to the daytime period, the evening hours show both E-layer and F-layer activity, whereas the post-midnight period shows only E-layer activity. It is interesting to note that the horizon for an altitude of 300 km is represented by a distance of approximately 2000 km which corresponds to a delay of 13 msec.

As such, all the activity in the evening hours can be explained in terms of direct reflections from the E and F layers, and those in the post-midnight period from the E layer alone. The daytime long-range echoes are, however, obtained from distances far beyond the northern horizon where the probability of encountering daytime irregularities is much enhanced. The year 1964 (Figure 20) shows reduced long range echo activity because of the reduced solar activity being indicated by the very low sunspot numbers (Figure 28). The percentage of all echoes obtained with a particular delay are shown in Figure 21 for the years 1961 and 1964. The other years, with sunspot numbers intermediate to those of these two years, have comparable behavior. In order to get an idea of the total occurrence of backscatter, it should be mentioned that backscatter occurred for only 6% of the time throughout 1961, and of all the occurrence noted, only 5% was of the long range kind, i.e., with delays greater than 13 msec.

## 6. AVERAGE SEASONAL BEHAVIOR OF FAE

The average seasonal behavior of FAE(E) during both quiet and disturbed magnetic periods is shown in Figure 22. The quiet periods represent approximately 400 hours of data while the disturbed periods range from 25 to 100 hours with the majority of time-blocks ranging between 40-60 hours. As pointed out earlier, the increased occurrence of FAE(E) during magnetic storms is very prominent in all four seasons. In addition to the increased evening and nighttime occurrence, there is a great deal of daytime occurrence. In fact, virtually all the daytime occurrence during these five years is during disturbed periods. The other interesting feature is the decrease of simultaneous  $E_s$ -supported propagation that accompanies the increase of FAE(E)'s during storms. This suggests that magnetic storms

inhibit the formation of  $E_s$  clouds. However, an influx of charged particles at E-layer heights is responsible for the enhanced FAE(E) (Paulikas, 1971).

A similar diagram for FAE(F) is shown in Figure 23. Here, too, we find the same obvious increase with increased magnetic activity, except during the summer where the opposite seems to be true. The summer storms at these latitudes are usually followed by a large depletion of the F layer (Mendillo et al, 1969), and this reduced ionization seems to be responsible for the decreased FAE(F). There is some daytime occurrence of high backscatter even during quiet days. As a matter of fact, all the long-range backscatter ( $\geq 13$  msec) shown in Figures 14, 17, and 18 were obtained during quiet periods. There is an increase of daytime backscatter during disturbed periods but they are all of the direct-F kind. It seems that during any magnetic storm situation there is some depletion of the bottom-side F layer as well as increased absorption which is adequate to block out the long-range echoes.

## 7. FAE AS A FUNCTION OF MAGNETIC ACTIVITY

We have seen that generally both FAE(E) and FAE(F) increase with magnetic activity. So far, however, we have considered two ranges of activity only. To study in detail the dependence of backscatter on the level of magnetic activity, the FAE data was sorted according to the  $K_{F_r}$  index. The result for the case of E-layer irregularities is shown in Figure 24a, in which the percentage occurrence of echoes is plotted as a function of  $K_{F_r}$ . The data represents the entire five year period under consideration, and the number of hours of observation belonging to each K interval are indicated on the diagram. As before, the first half of each K interval represents returns coming from the NW, and the second half from the NE. The sample size becomes

rather small for K indices ranging 7-9. It is very obvious from this graph that the E-layer backscatter is a very sensitive function of the K index. Between K indices of 0-3 there is the usual E-W asymmetry in the incidence of echoes, but the percentage occurrence remains small. Beyond  $K_{PT} \geq 4$ , the percentage occurrence increases with each integral increase of K. It finally levels off for  $K_{PT} \geq 6$ , and the degree of asymmetry levels off also, because irregularities appear at all northern azimuths during severe magnetic storms. Figures 24b and 24c show the same data when separated into daytime (0600-1800) and nighttime (1800-0600) hours. Figure 24b shows the total lack of FAE(E) during the daytime for K range 0-3, and a pronounced increase beyond that range. The nighttime hours show a gradual increase for the low indices with the same prominent increase for the high ones.

Similar diagrams for the F-layer backscatter are shown in Figures 25a-c. The total occurrence characteristics are greatly reduced - note the magnified occurrence scale. However it is interesting to note the monotonic increase of occurrence with K index up to a value of  $K=4$ , beyond which the occurrence tapers off becoming zero for  $K \geq 7$ . Now, from scintillation studies (Aarons et al, 1963), it is a well known fact that the incidence of irregularities increases with  $K_{PT}$ . Thus the decrease in the FAE(F) is to be attributed to the depletion in the underlying ionization during severe magnetic storms. The daytime situation alone (Figure 25b) represents the 24 hour picture, as the nighttime occurrence (Figure 25c) is insignificant. We have seen earlier (Figures 19 and 20) that all of this low nighttime occurrence takes place in the pre-midnight hours. The shading within the histograms, which represents supporting F-layer propagated groundscatter echoes, shows a behavior similar to that of the field aligned echoes, i.e., increasing in proportion to the increased echo occurrence and then tapering off during severe storms.

## 8. SOLAR CYCLE DEPENDENCE OF FAE

To study the solar cycle dependence of the field aligned echoes, if any, percentage occurrence contours of both E-layer and F-layer echoes were drawn for the entire five year period of observation. The data base was restricted to quiet magnetic conditions, and the occurrence statistics in the NW quadrant were used for drawing the contours.

The FAE(E) contours are shown in Figure 26. The yearly summer maximum during the evening and nighttime hours is the most distinctive feature. There is a much weaker but quite definite secondary winter maximum. No definite solar cycle dependence is discernible from the contours. A reference to Figures 19 and 20 shows that there were more hours of FAE(E) in 1961 than in 1964. However, it is difficult to come to a definite conclusion with the limited solar cycle coverage available.

The FAE(F) contours (Figure 27), show a positive dependence on the solar cycle. There is a gradual decrease in the incidence of echoes from 1961 to 1964, and then an upward trend is observed in 1965. The rough sinusoidal pattern of echo occurrence is evident as it follows the time of sunset throughout the seasons, the echo onset being much earlier in winter than in summer. The mean monthly Zurich sunspot numbers for the period 1961-65 are shown in Figure 28. Though a general trend is clearly visible, there is much month-to-month variability indicating that this kind of variability should be expected in the FAE data also.

## 9. SUMMARY AND CONCLUSIONS

This detailed study of field aligned irregularities in the E and F layers of the ionosphere has yielded valuable information regarding the diurnal, seasonal, and geomagnetic control of the occurrence statistics. The important characteristics of each



type of echo will be summarized below.

#### 9.1 FAE(E)

1. FAE(E) mostly occur at delays of 3-4 msec and are more numerous in the NW quadrant which contains the magnetic pole.
2. During quiet magnetic conditions ( $K_{PT}$  0-3), FAE(E) are confined to the late evening and nighttime hours.
3. FAE(E) shows a very definite maximum during the summer months. A weaker maximum is observed in the winter. However, the diurnal variation mentioned in (2) is always observed irrespective of season. The summer FAE(E) is mostly accompanied by simultaneous ground-scattered  $E_s$  echoes.
4. Geomagnetic activity increases the occurrence of FAE(E). A great deal of daytime activity as well as increased nighttime activity is seen. No seasonal control is evident. A marked decrease of simultaneous ground-scattered  $E_s$  echoes is observed.
5. There is no clearly defined solar-cycle dependence of FAE(E) observed in the data.

#### 9.2 FAE(F)

1. This type of echo is obtained only when sufficient underlying ionization makes it possible for the ray to achieve orthogonality with the geomagnetic field at F-layer heights. FAE(F) are mostly observed at delays of 7-9 msec and, like the FAE(E), occur mostly in the NW.
2. During quiet magnetic conditions FAE(F) are confined primarily to the sunset hours. Some daytime activity is observed with delay times ranging between 15-25 msec. These long-range echoes can be explained in terms of multi-hop propagation and field alignment.

3. The equinoxes show more activity than the solstices - this can be explained in part by the greater FAE(E) activity seen during the summer and winter, which decreases the amount of energy reaching the F layer. The time of the sunset peak naturally varies from season to season. The FAE(F) is generally accompanied by F-layer supported groundscatter echoes.
4. The dependence of FAE(F) on geomagnetic activity is very interesting. A monotonic increase of the daytime FAE(F) with  $K_{F_r}$  is observed until a threshold value is reached ( $K_{F_r}=4$ ), beyond which the depletion of F-layer background ionization causes it to decrease. Complete cut-off is attained under severely disturbed conditions ( $K_{F_r}\geq 7$ ).
5. The incidence of FAE(F) shows a positive correlation with the solar cycle.

## 10. FUTURE WORK

In the next report the occurrence characteristics of  $E_s$ -layer and F-layer supported groundscattered echoes will be presented. In addition,  $fE_s$  and  $f_oF_2$  of relevant ionospheric stations will be studied in an effort to explain the observed characteristics of field aligned echoes as well as ground-scattered echoes. It is hoped that the FAE(E) can be explained in terms of both the occurrence statistics of  $E_s$  and the equatorward movement of the auroral oval in times of magnetic disturbances. On the other hand, the diurnal pattern of the scintillation boundary under quiet and disturbed conditions, and the change in F-layer ionization as a function of time, latitude, season, and magnetic conditions, will be used to explain qualitatively the observed incidence of FAE(F).

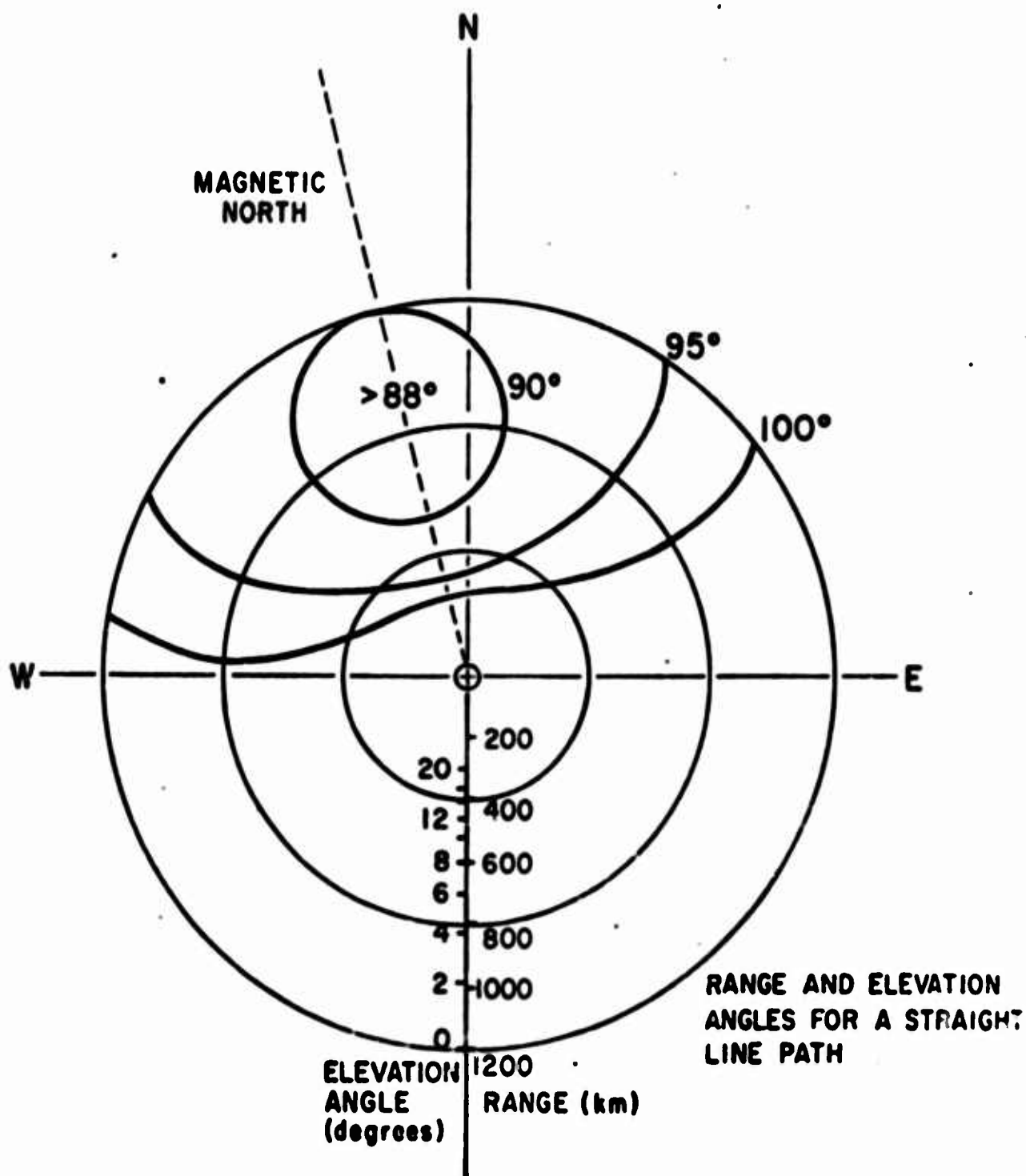


**FIG. 1a PROPAGATION ANGLE CONTOURS FOR PLUM ISLAND MA AT 110 km HEIGHT.**

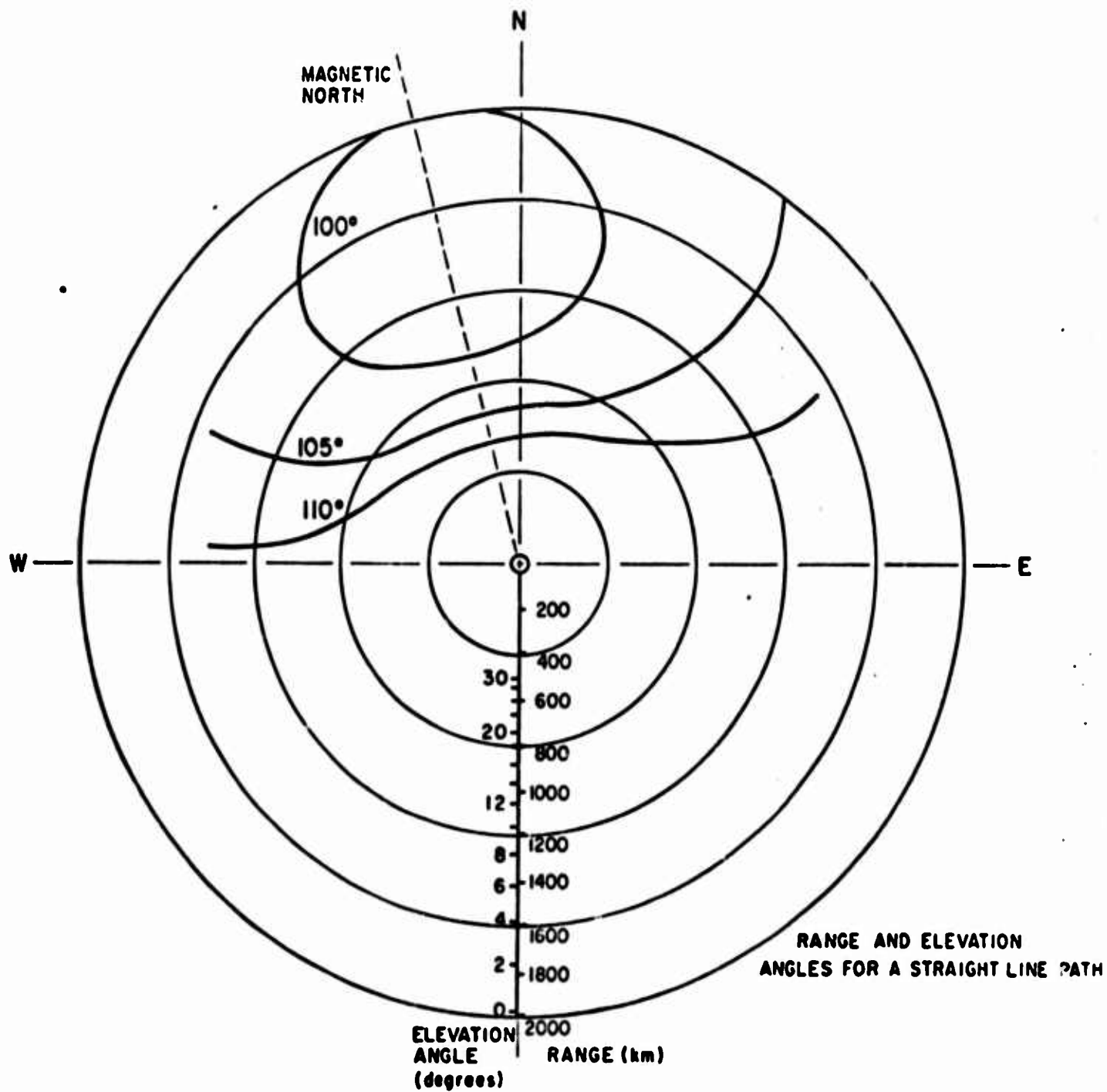


FIG. 1b PROPAGATION ANGLE CONTOURS FOR PLUM ISLAND MA AT 300 km HEIGHT.

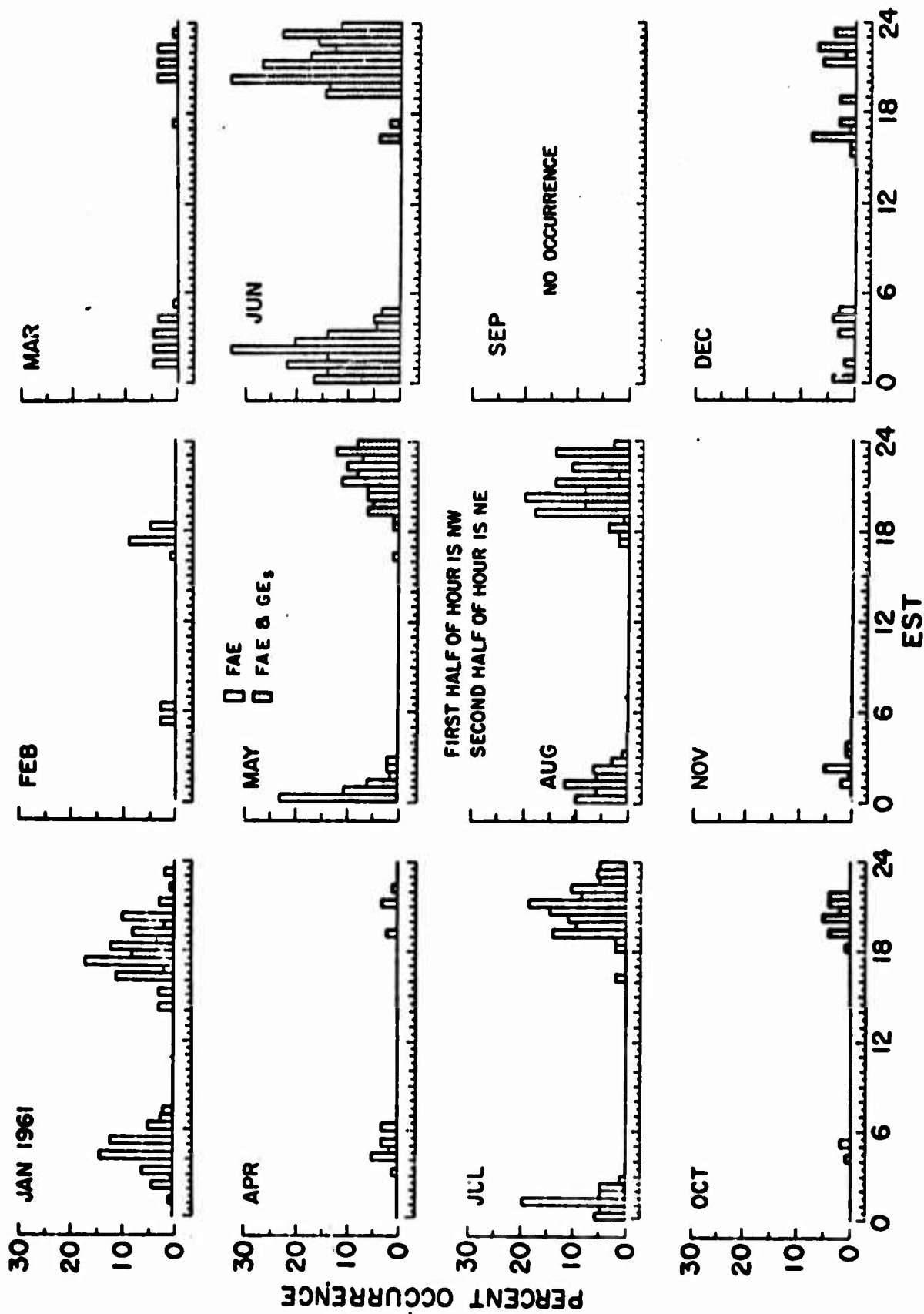


FIG. 2 BACKSCATTER FROM FIELD ALIGNED IRREGULARITIES AT E-LAYER HEIGHTS  
FOR K<sub>F1</sub> 0-3 DURING 1961

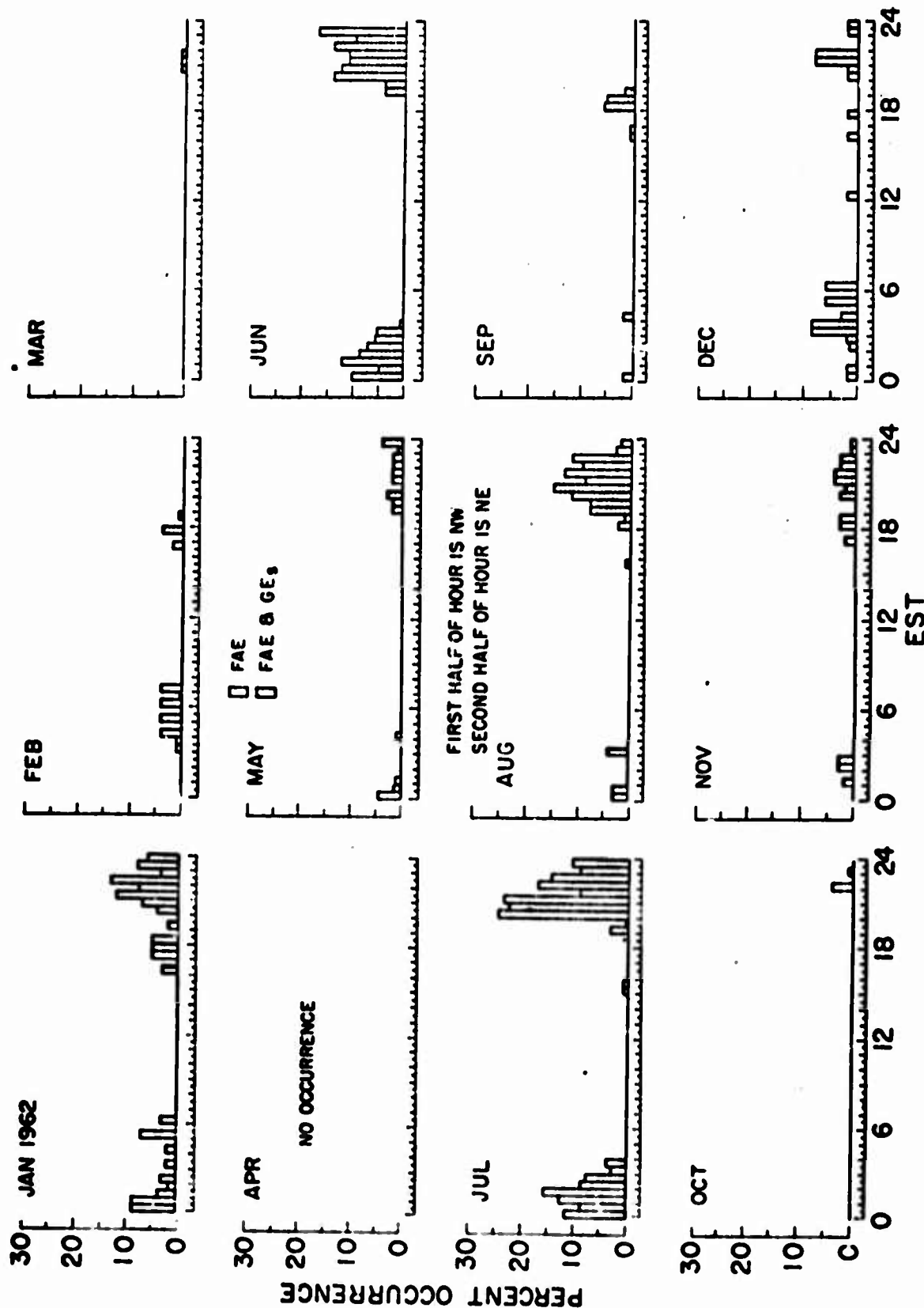


FIG. 3 BACKSCATTER FROM FIELD ALIGNED IRREGULARITIES AT E-LAYER HEIGHTS  
FOR K<sub>F</sub>, O-3 DURING 1962



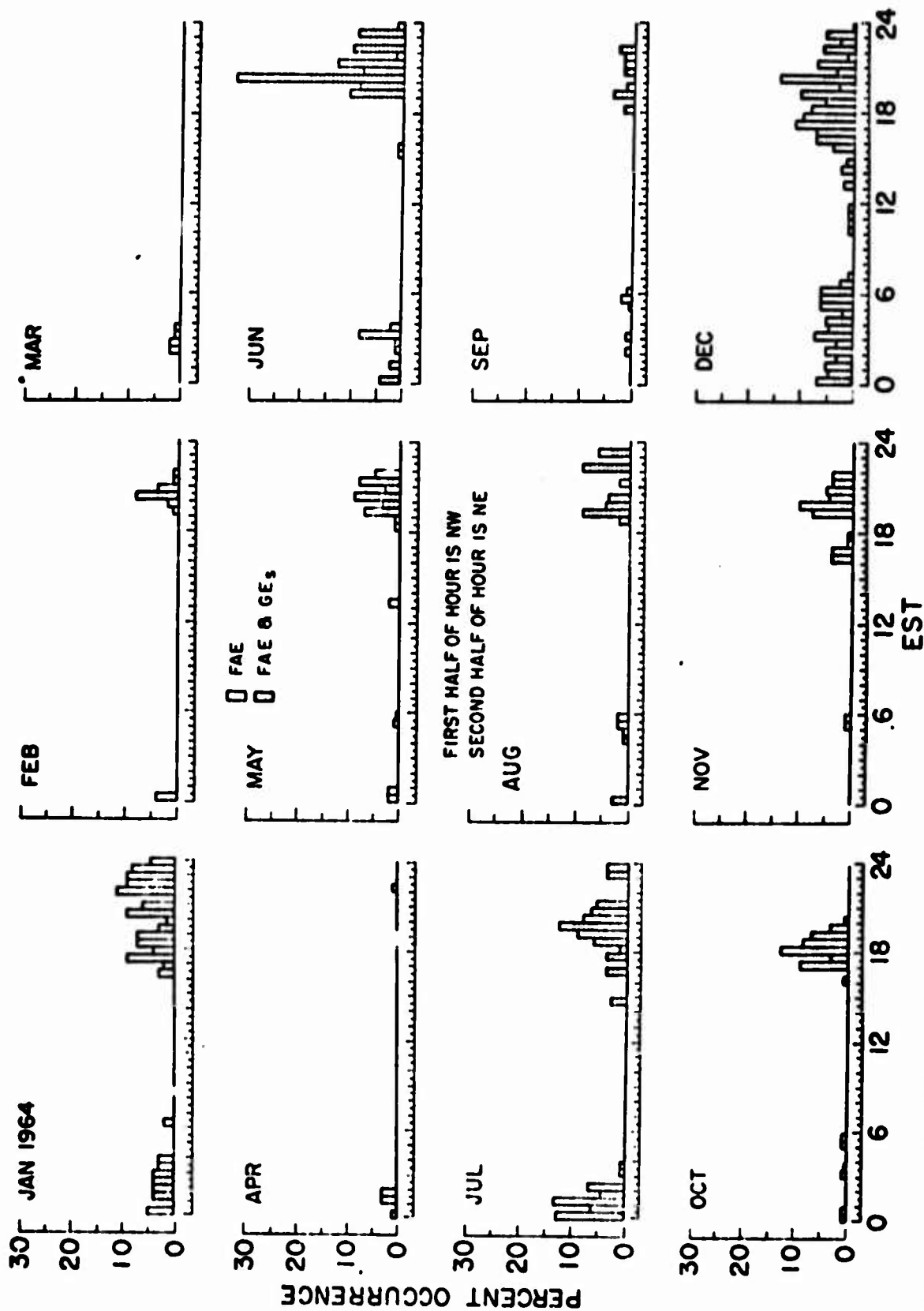


FIG. 5 BACKSCATTER FROM FIELD ALIGNED IRREGULARITIES AT E-LAYER HEIGHTS  
FOR K<sub>F</sub>, 0-3 DURING 1964



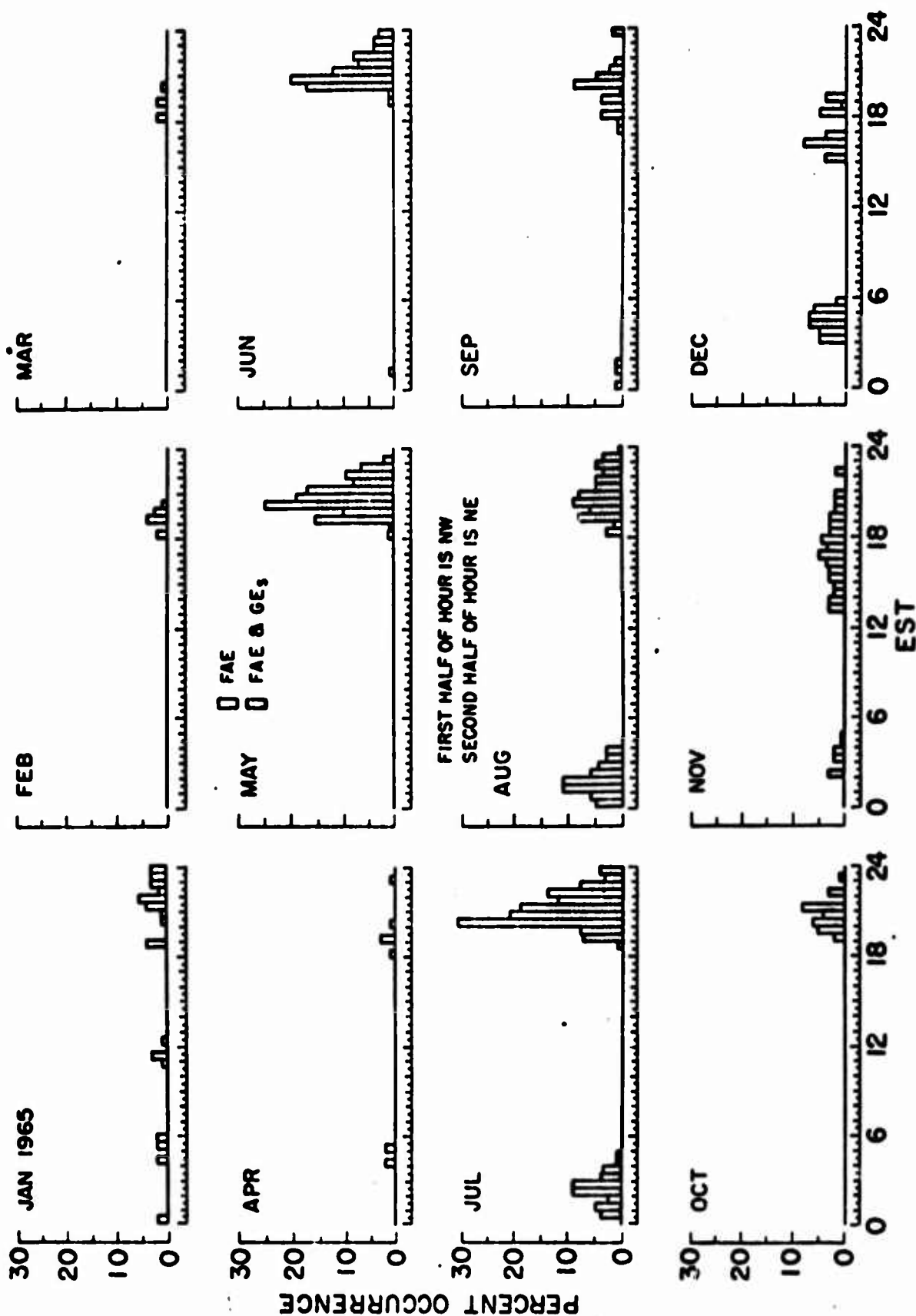


FIG 6 BACKSCATTER FROM FIELD ALIGNED IRREGULARITIES AT E-LAYER HEIGHTS  
FOR Kf, 0-3 DURING 1965

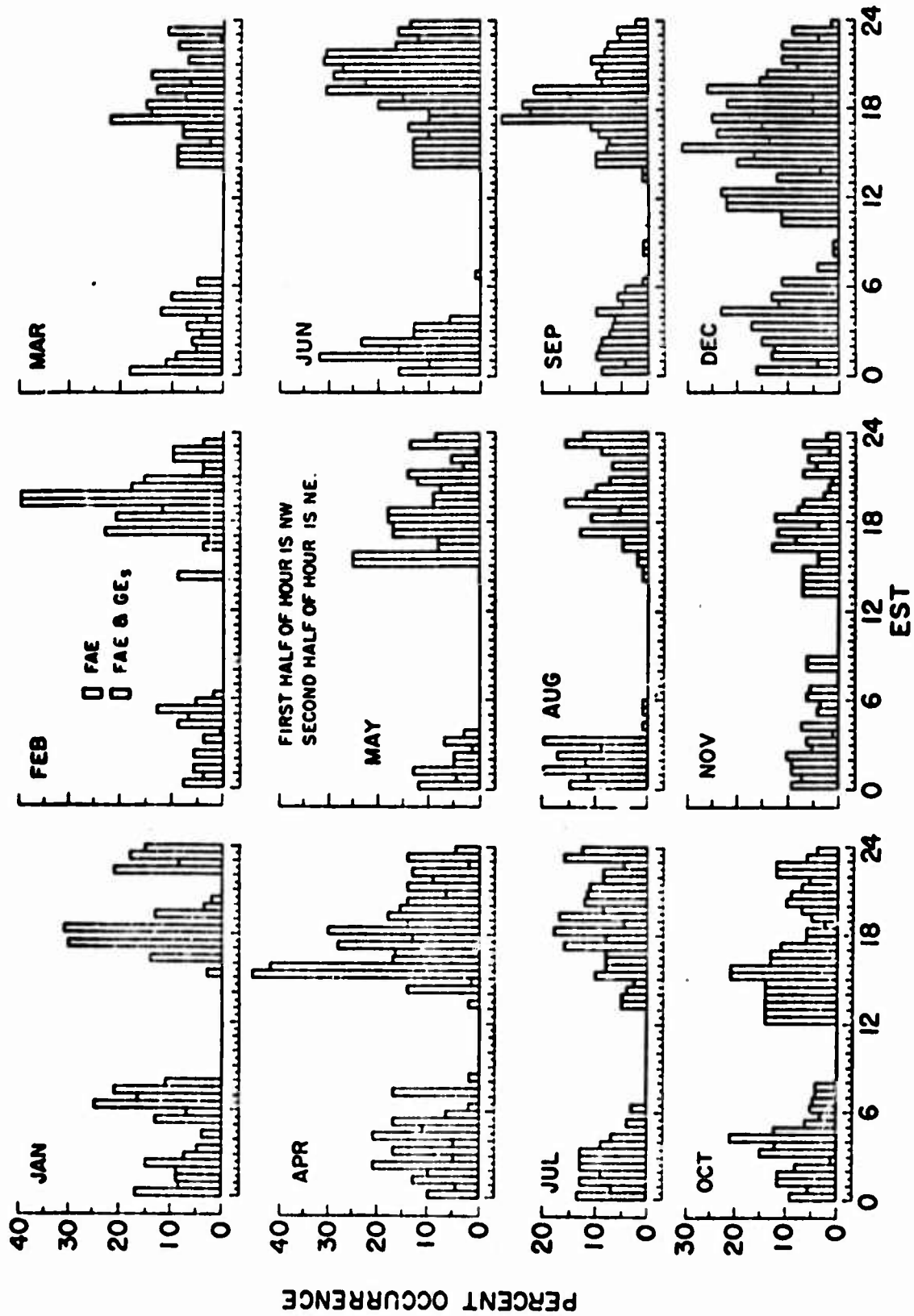


FIG. 7 AVERAGE E-LAYER BACKSCATTER FOR EACH MONTH FOR K<sub>F</sub>, 4-9 DURING 1961 - 1965

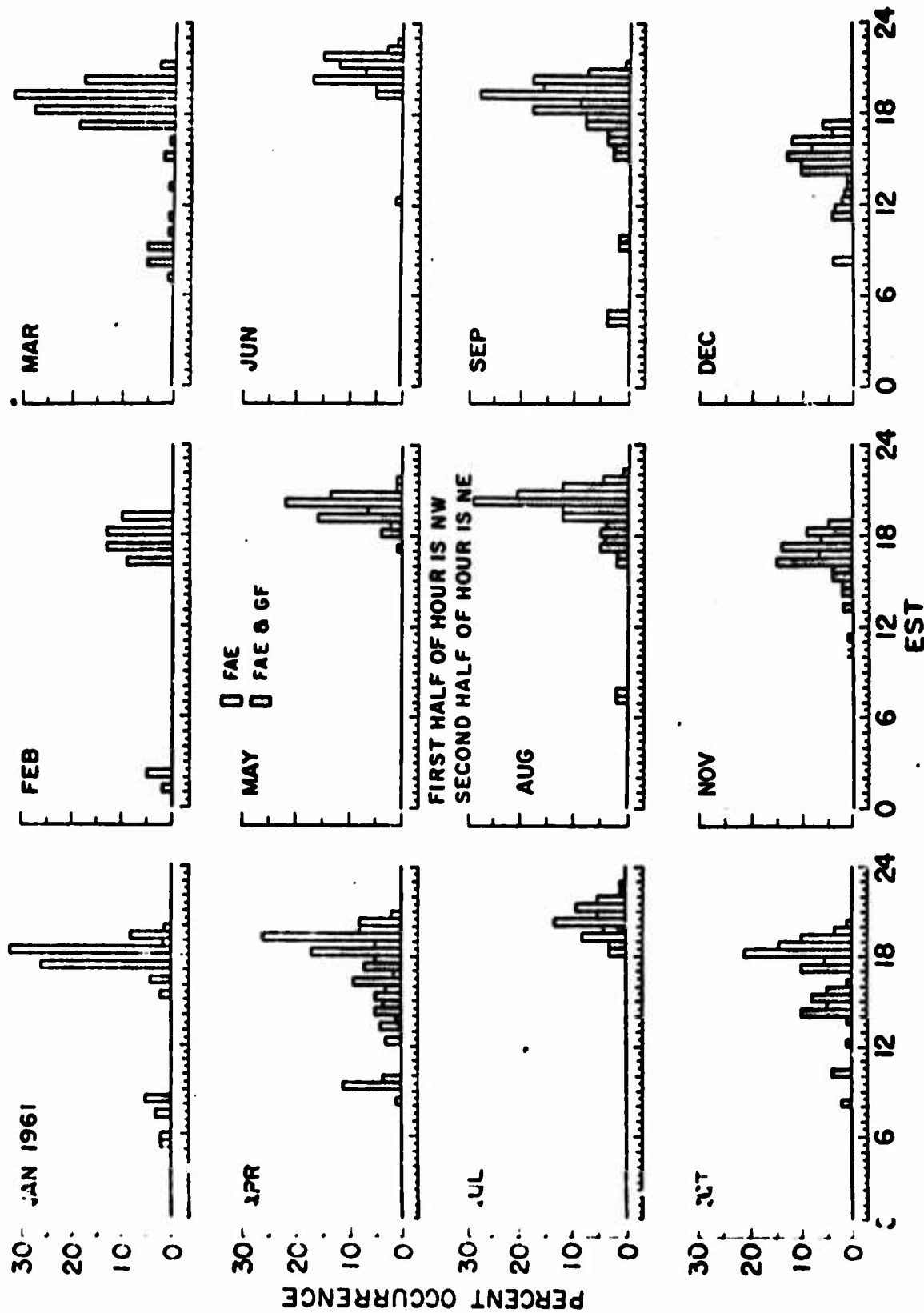
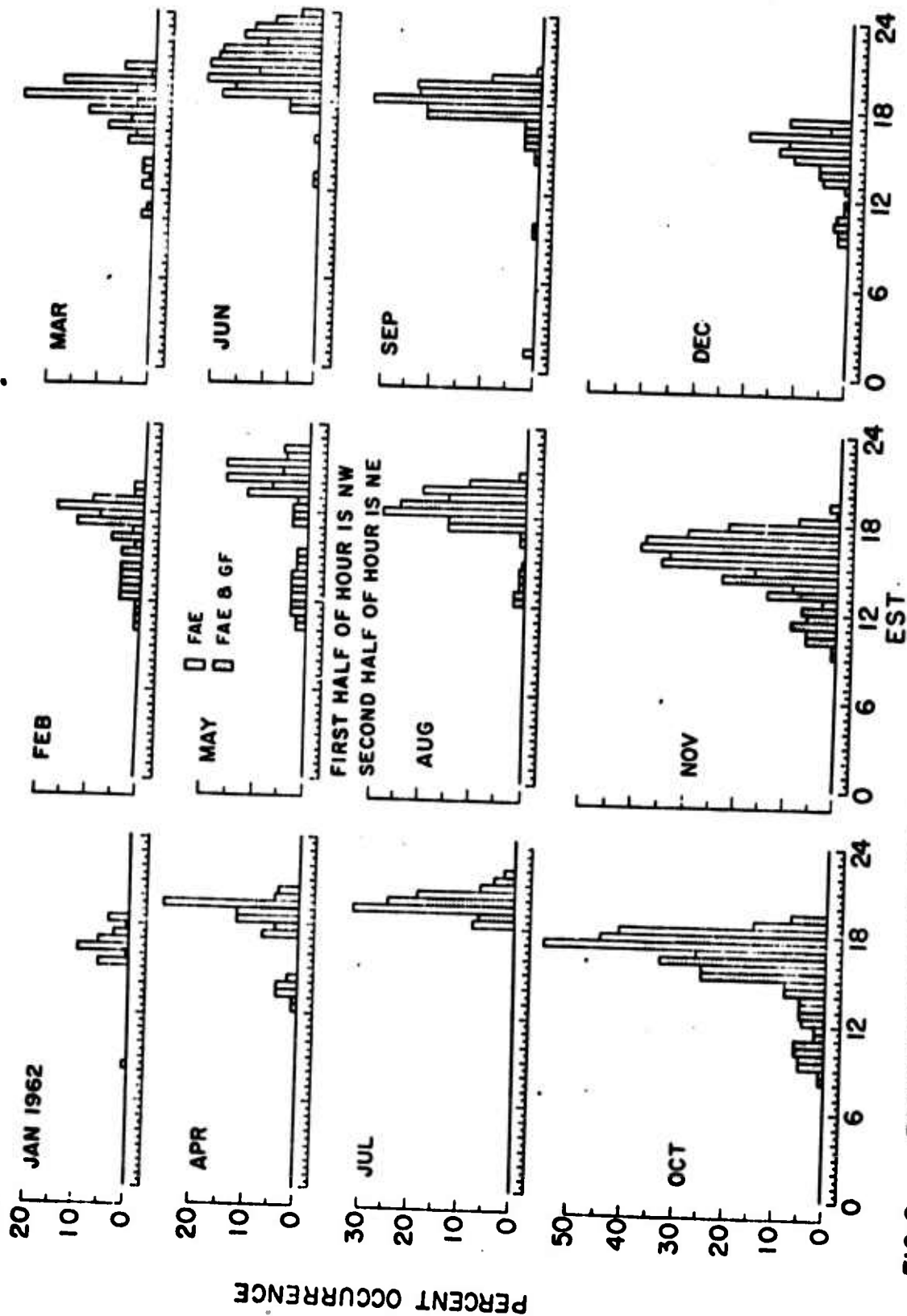


FIG 8 BACKSCATTER FROM FIELD ALIGNED IRREGULARITIES AT F-LAYER HEIGHTS  
FOR KFr 0-3 DURING 1961



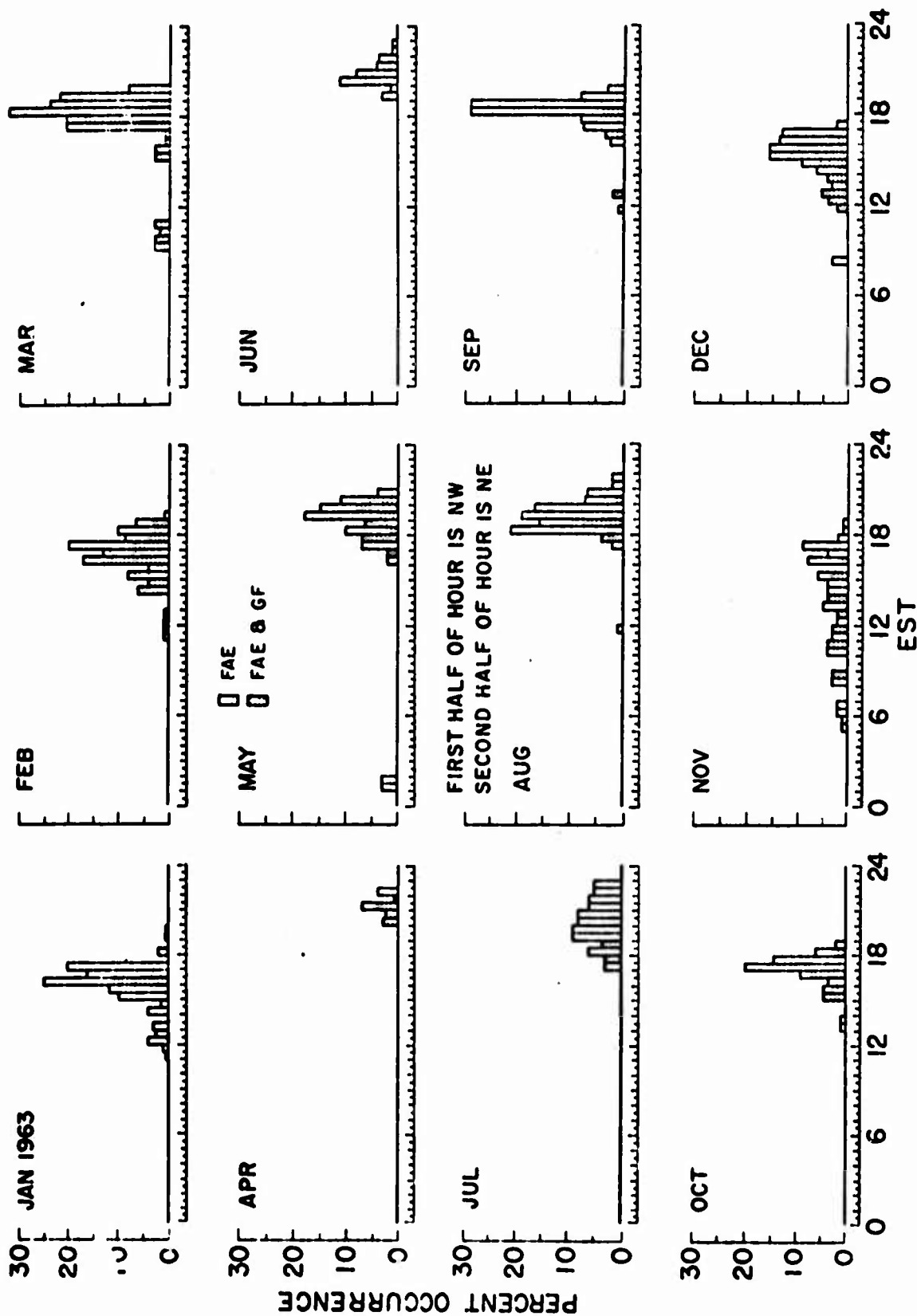


FIG. 10 BACKSCATTER FROM FIELD ALIGNED IRREGULARITIES AT F-LAYER HEIGHTS  
FOR KFr 0-3 DURING 1963

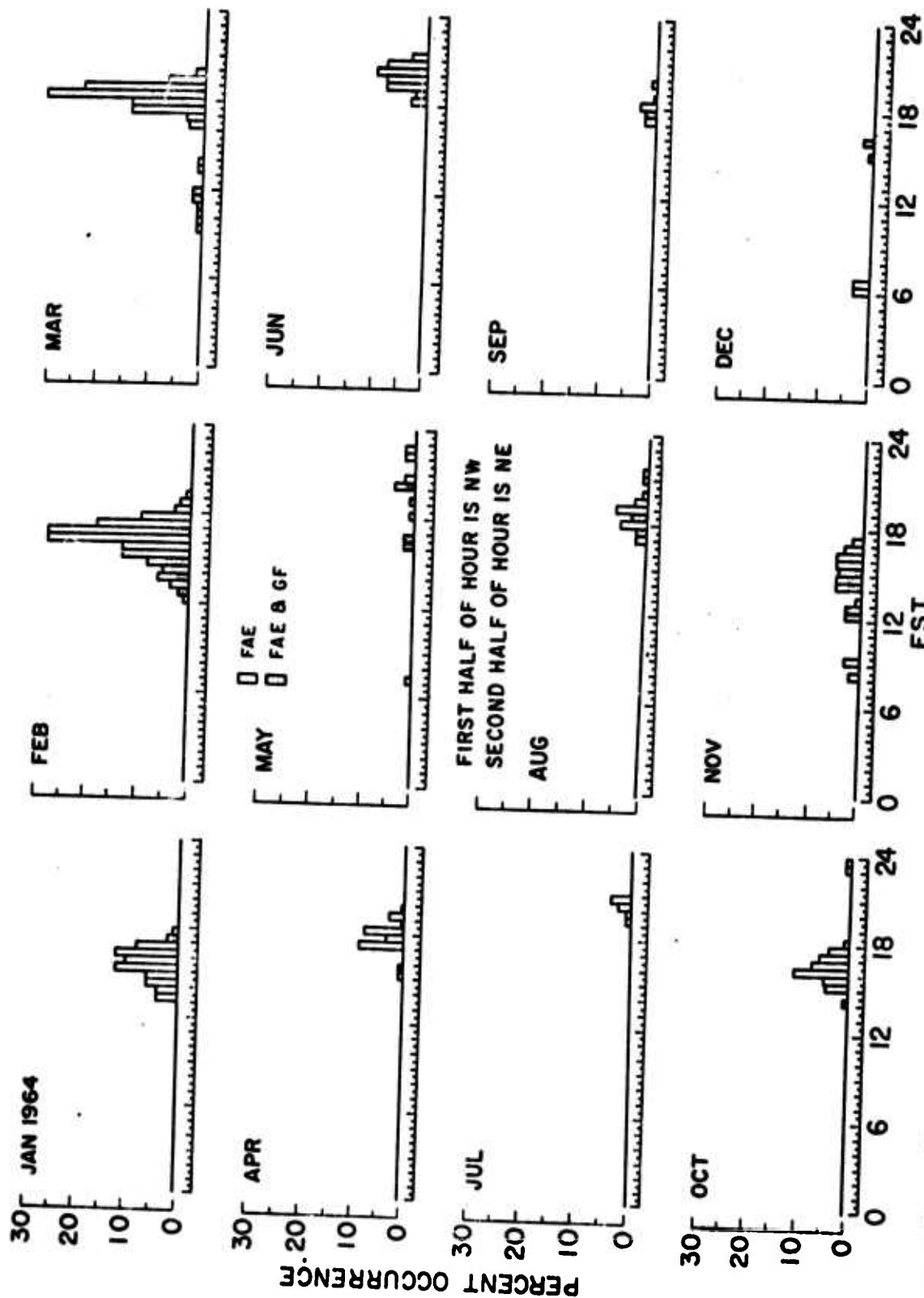


FIG 11 BACKSCATTER FROM FIELD ALIGNED IRREGULARITIES AT F-LAYER HEIGHTS  
FOR KF7 O-3 DURING 1964

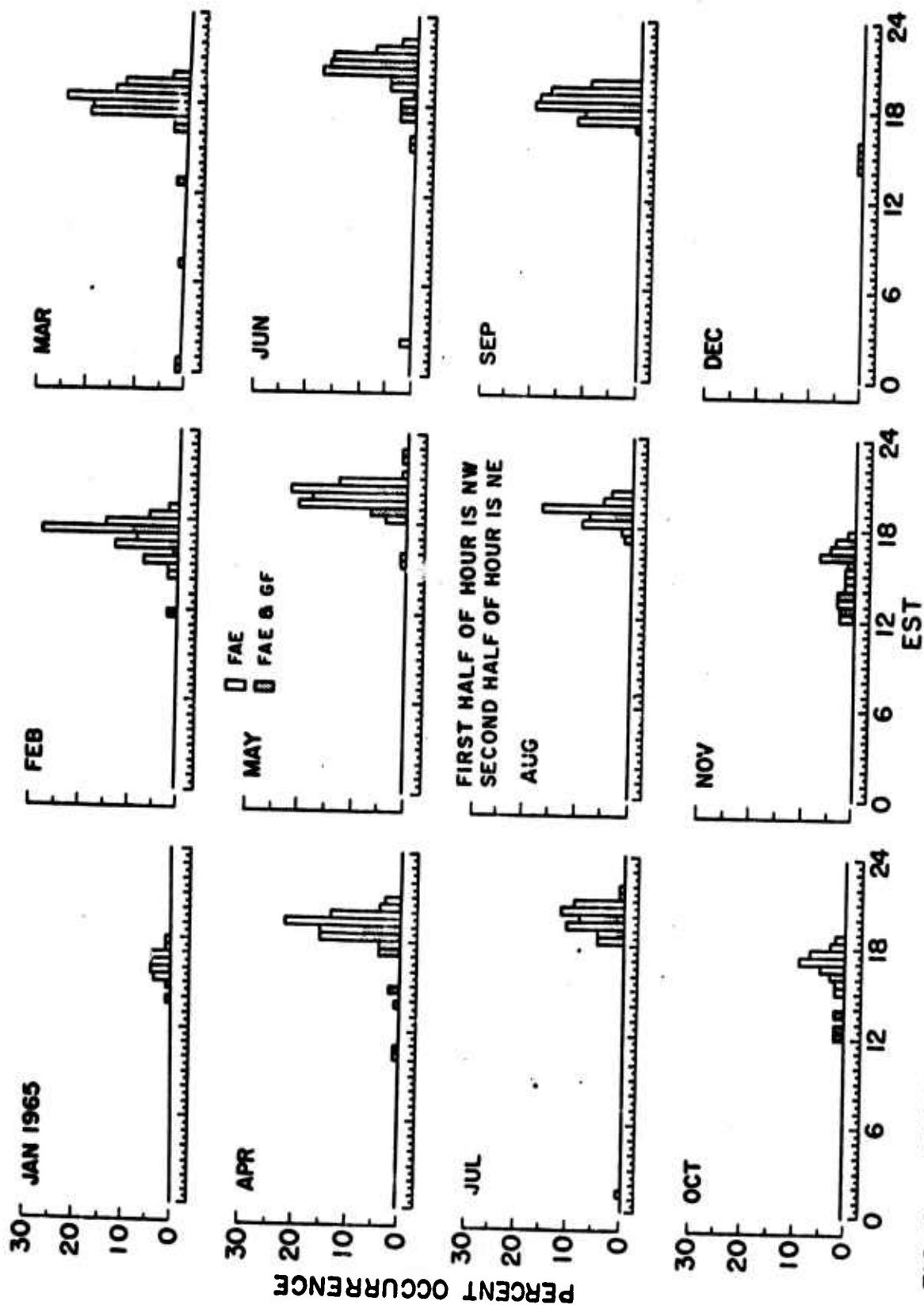


FIG. 12 BACKSCATTER FROM FIELD ALIGNED IRREGULARITIES AT F-LAYER HEIGHTS  
FOR K<sub>F1</sub> 0-3 DURING 1965

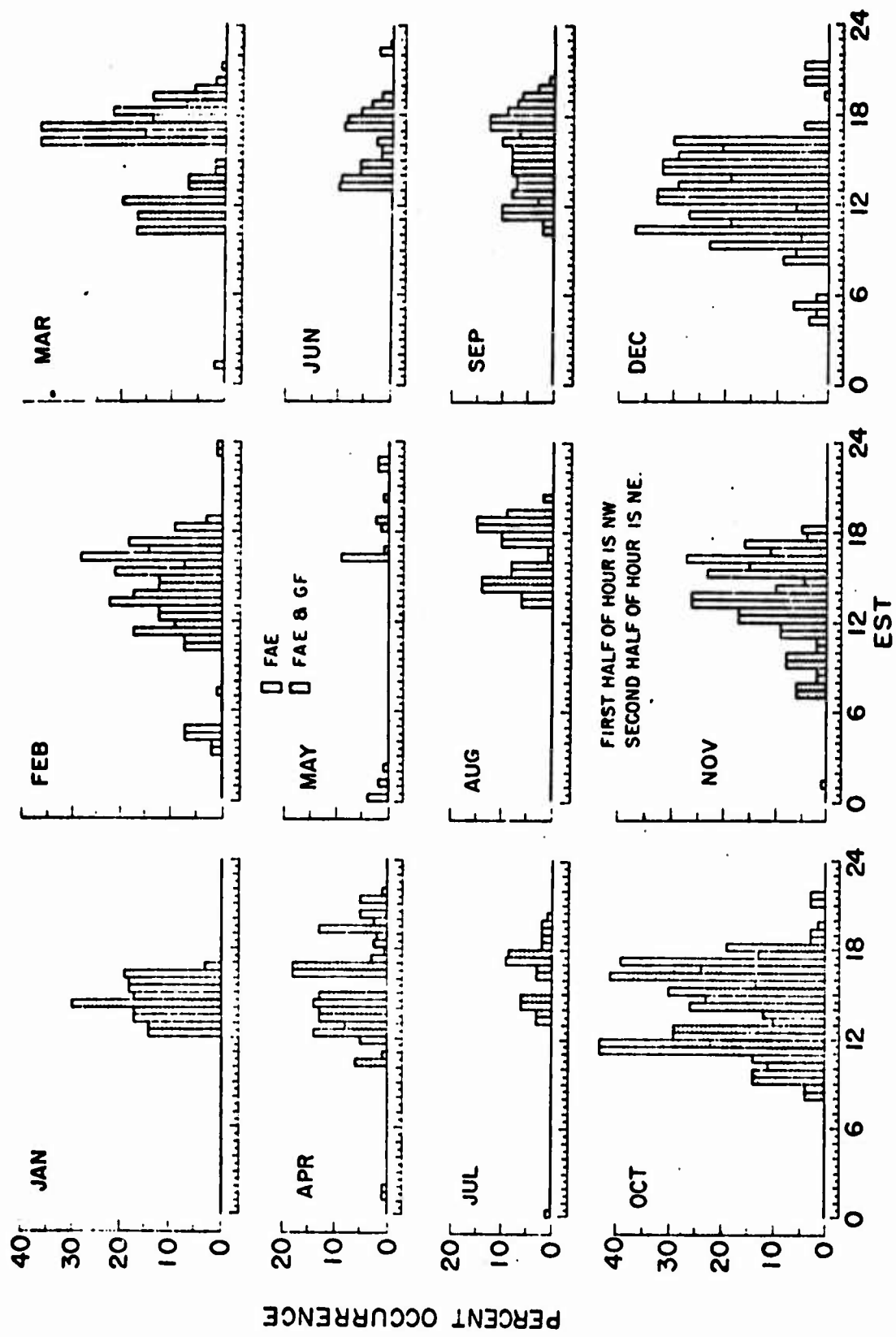


FIG 13 AVERAGE F-LAYER BACKSCATTER FOR EACH MONTH FOR  $K_{F1}$  4-9 DURING 1961 - 1965



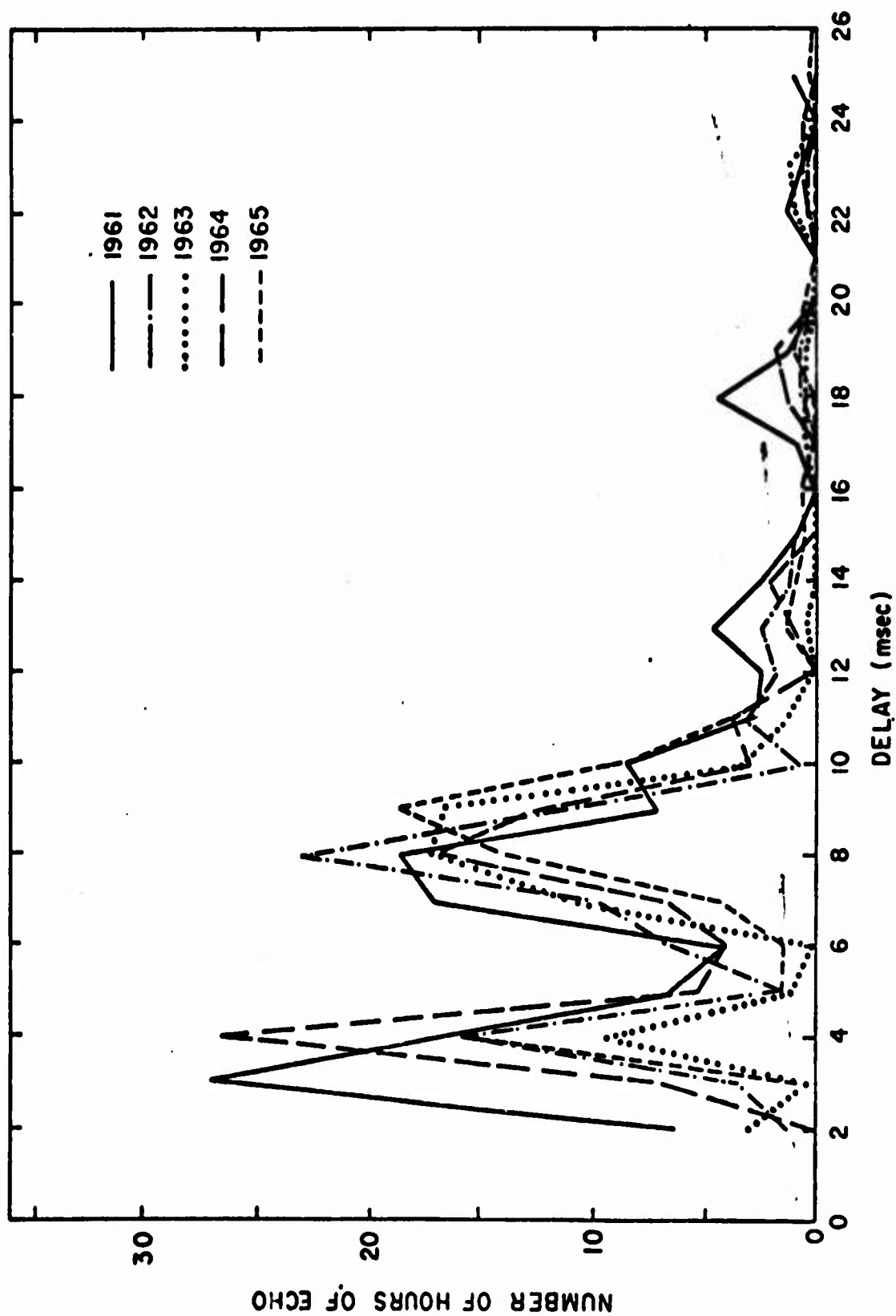


FIG. 14. RANGE DISTRIBUTION OF FAE's DURING THE SPRING SEASON, 1961-1965

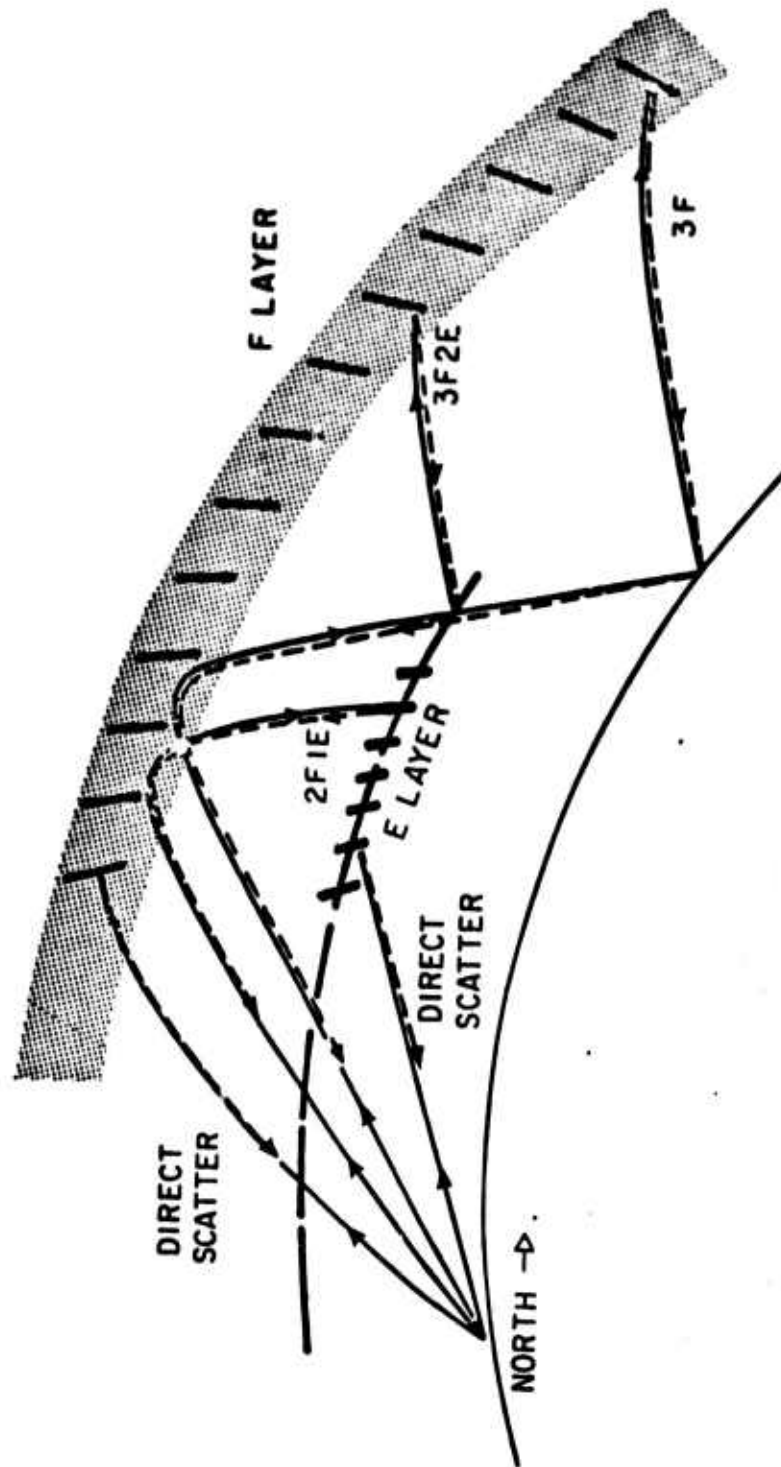


FIG. 15. POSSIBLE MULTI-HOP PROPAGATION MODES AND DIRECT SCATTER FROM  
FIELD ALIGNED IRREGULARITIES IN THE E AND F LAYERS

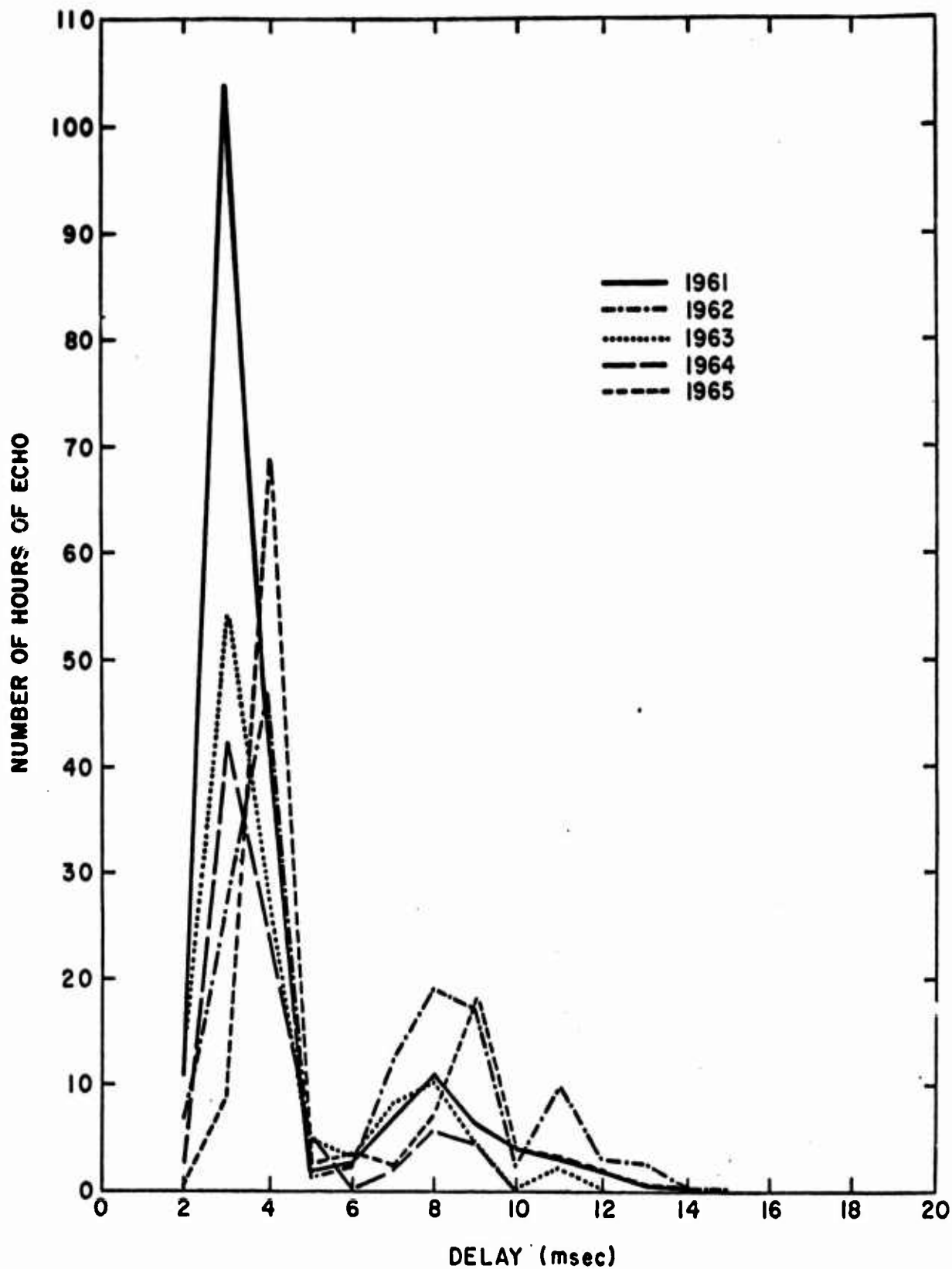


FIG. 16 - RANGE DISTRIBUTION OF FAE's DURING THE SUMMER SEASON, 1961-1965.

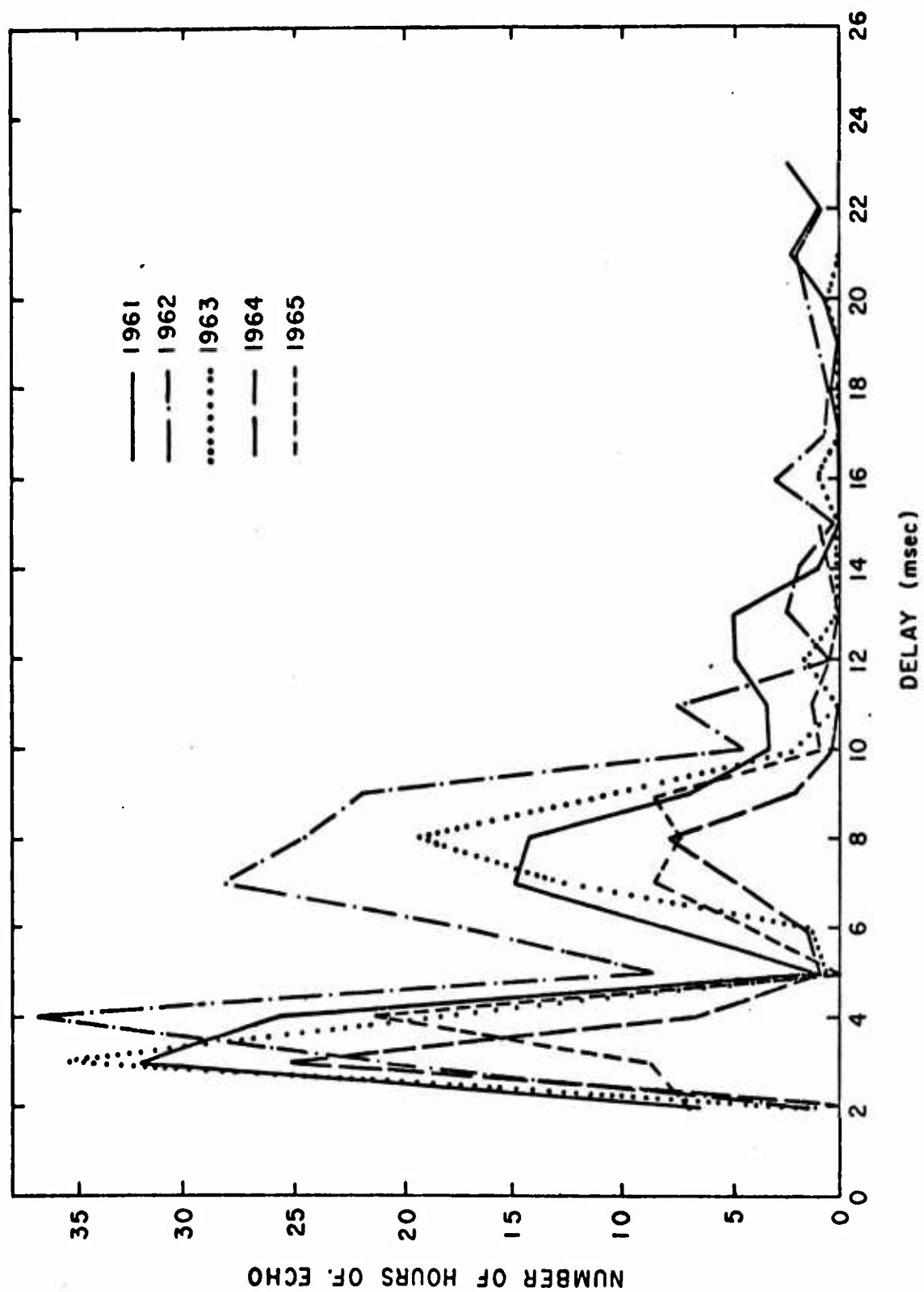


FIG. 17. RANGE DISTRIBUTION OF FAE's DURING THE FALL SEASON, 1961-1965

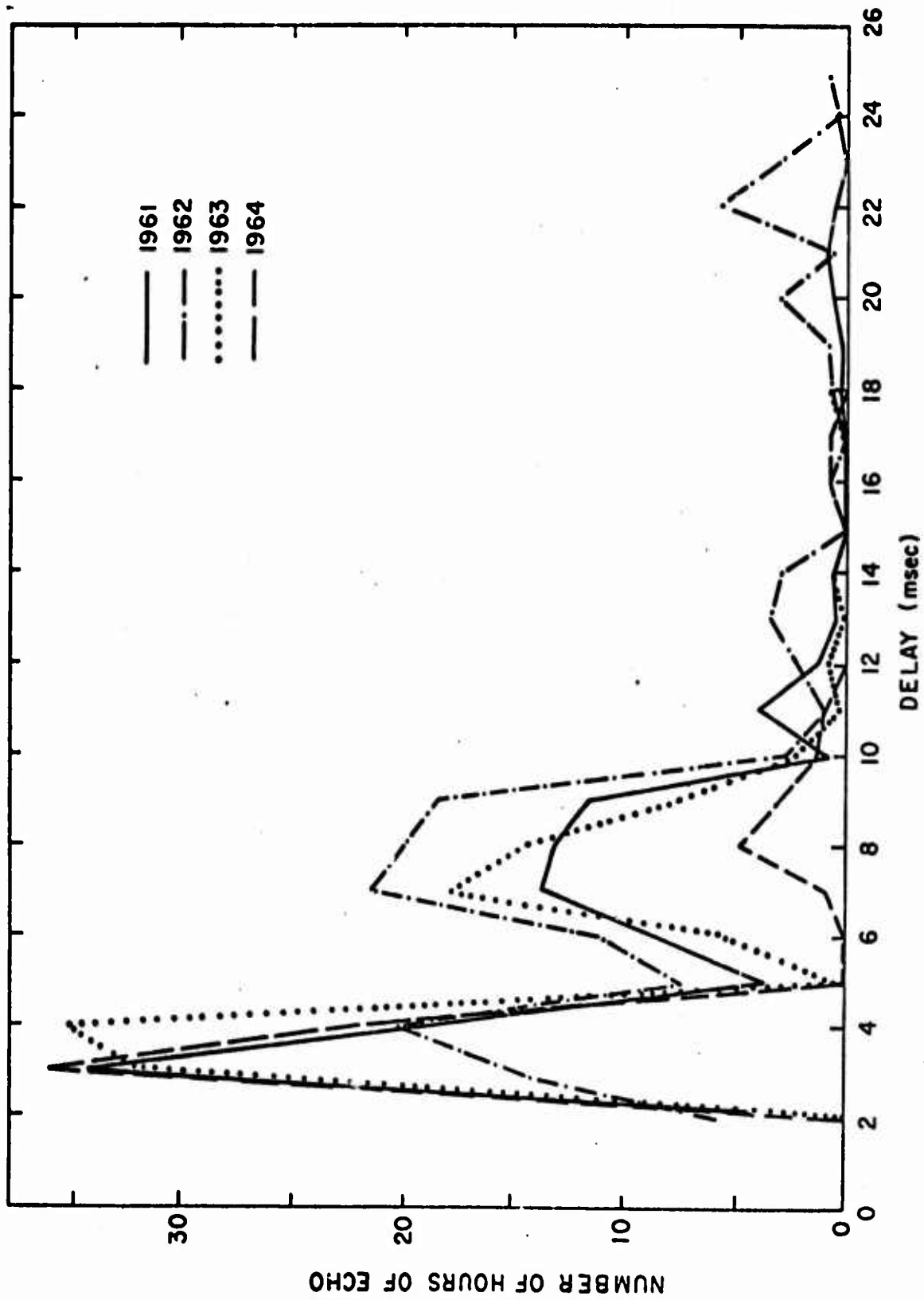


FIG. 18. CHANGE DISTRIBUTION OF FAE's DURING THE WINTER SEASON, 1961-1964

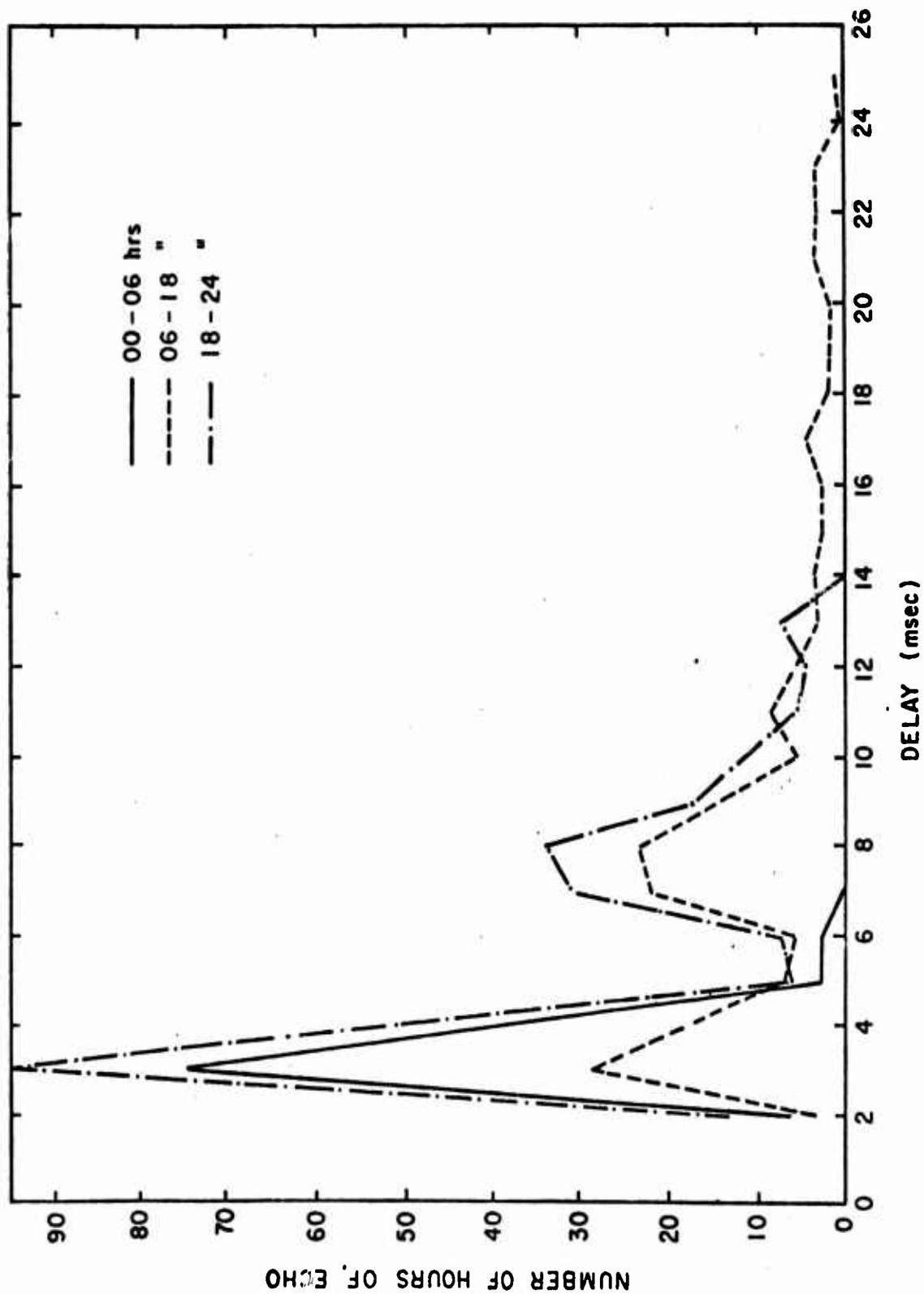


FIG. 19. DIURNAL PATTERN OF THE RANGE DISTRIBUTION OF FAE's FOR 1961

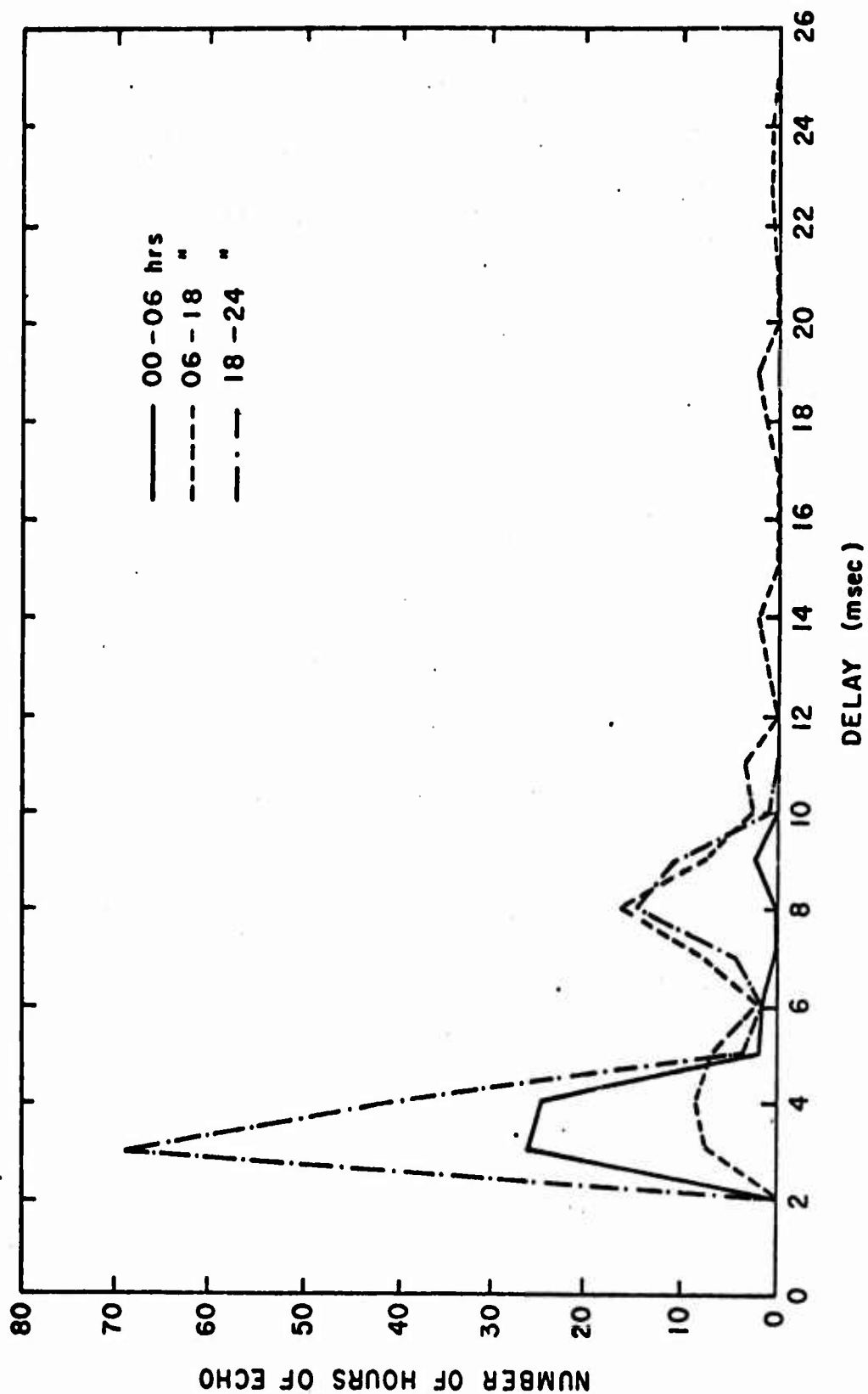


FIG. 20. DIURNAL PATTERN OF THE RANGE DISTRIBUTION OF FAE's FOR 1964

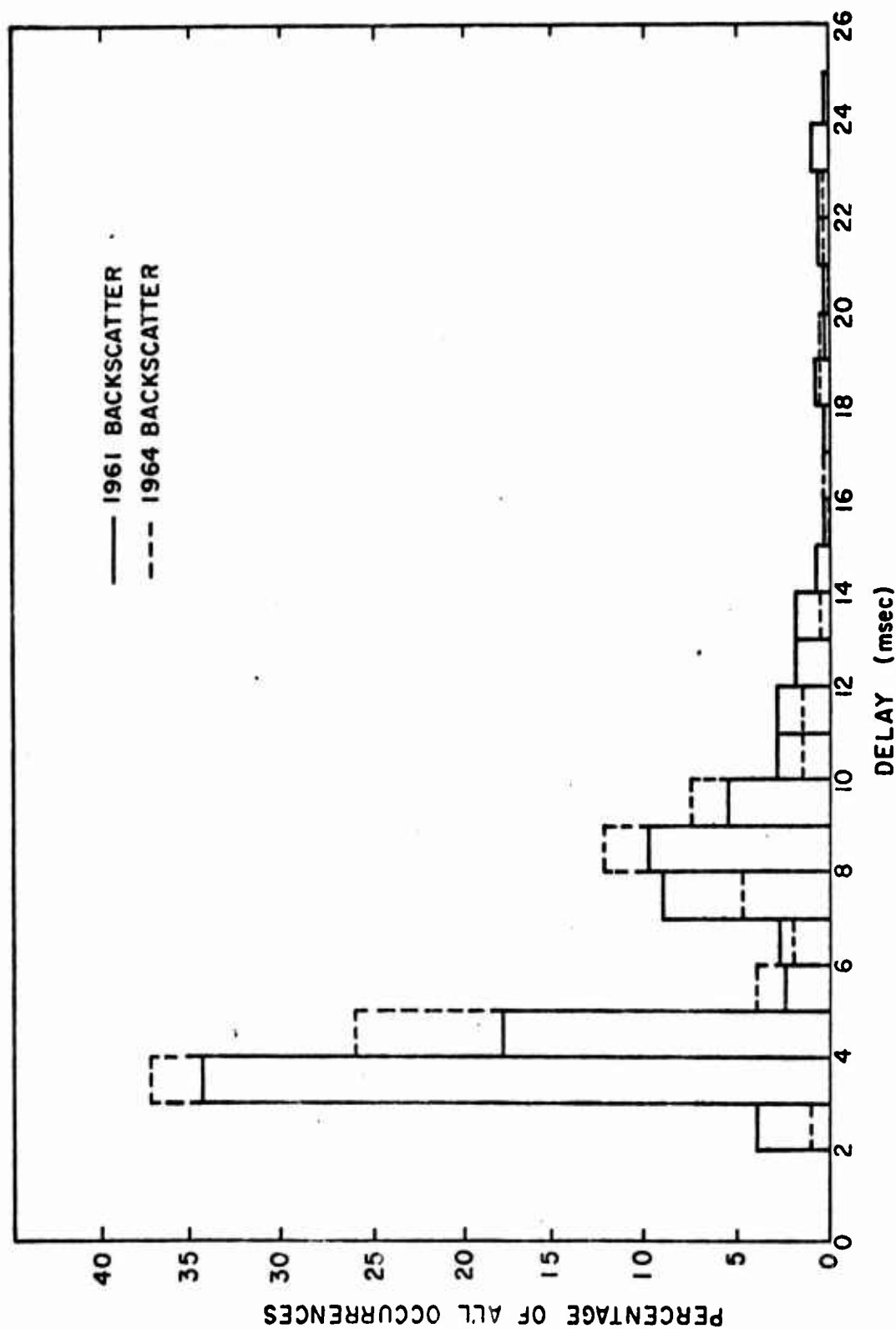


FIG. 21. PERCENTAGE RANGE DISTRIBUTION OF ALL FAE OCCURRENCE FOR 1961 & 1964





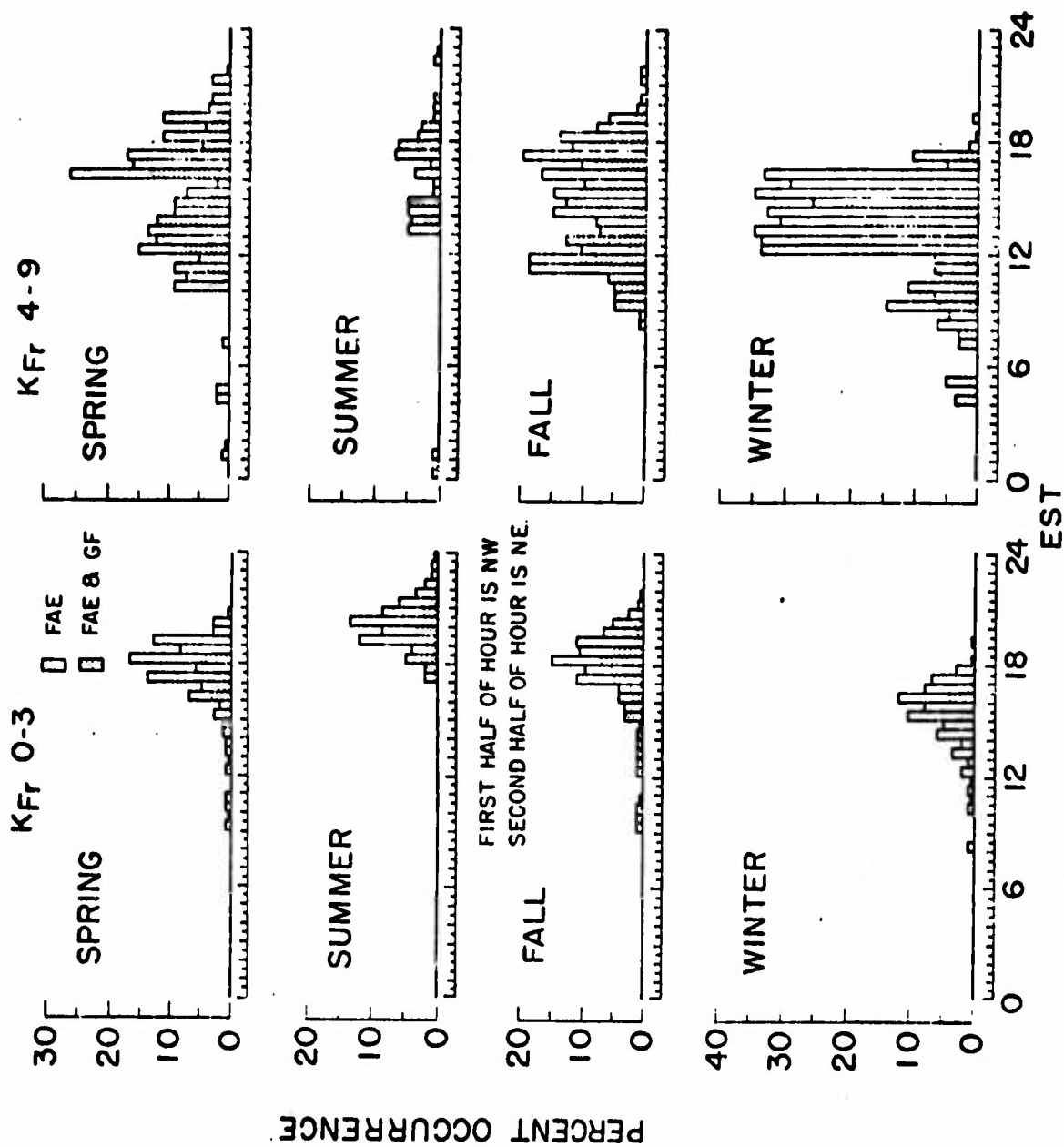


FIG. 23 AVERAGE SEASONAL BEHAVIOR OF FAE (F) DURING  
MAGNETICALLY QUIET AND DISTURBED PERIODS,  
1961-1965

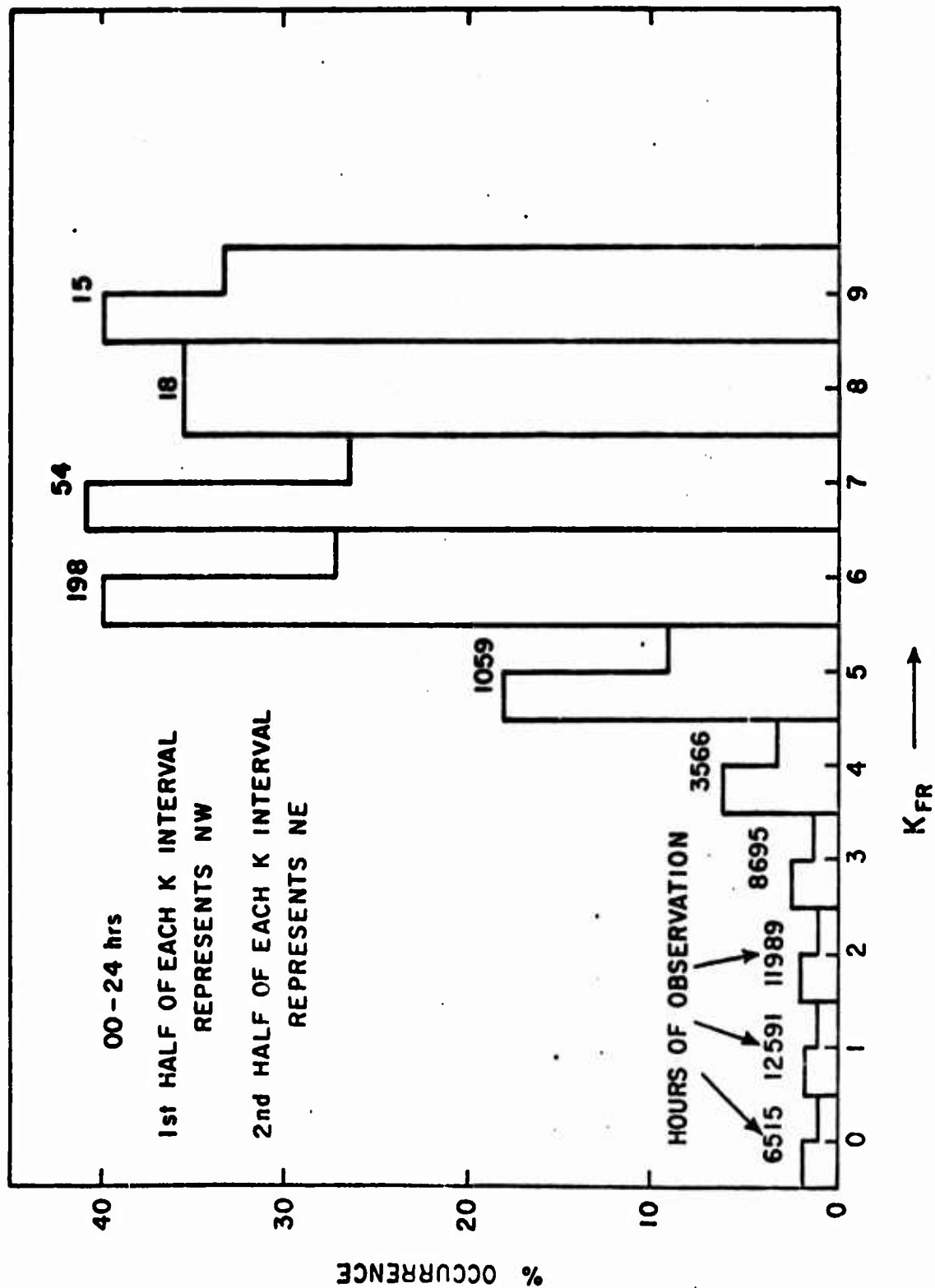


FIG. 24a. FAE (E) AS FUNCTION OF MAGNETIC INDEX  $K_{FR}$

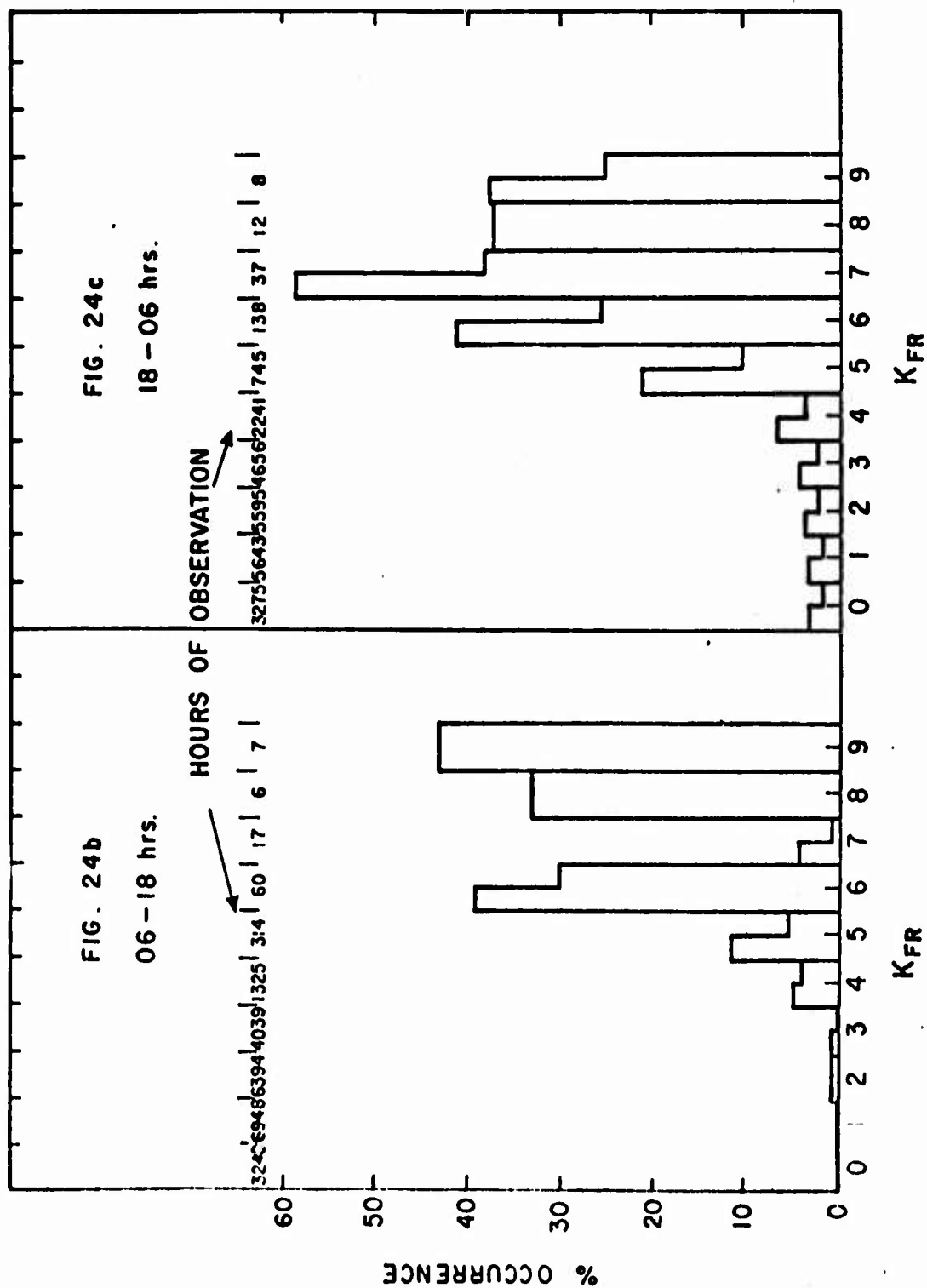


FIG. 24b & 24c. FAE(E) AS A FUNCTION OF MAGNETIC INDEX KFR

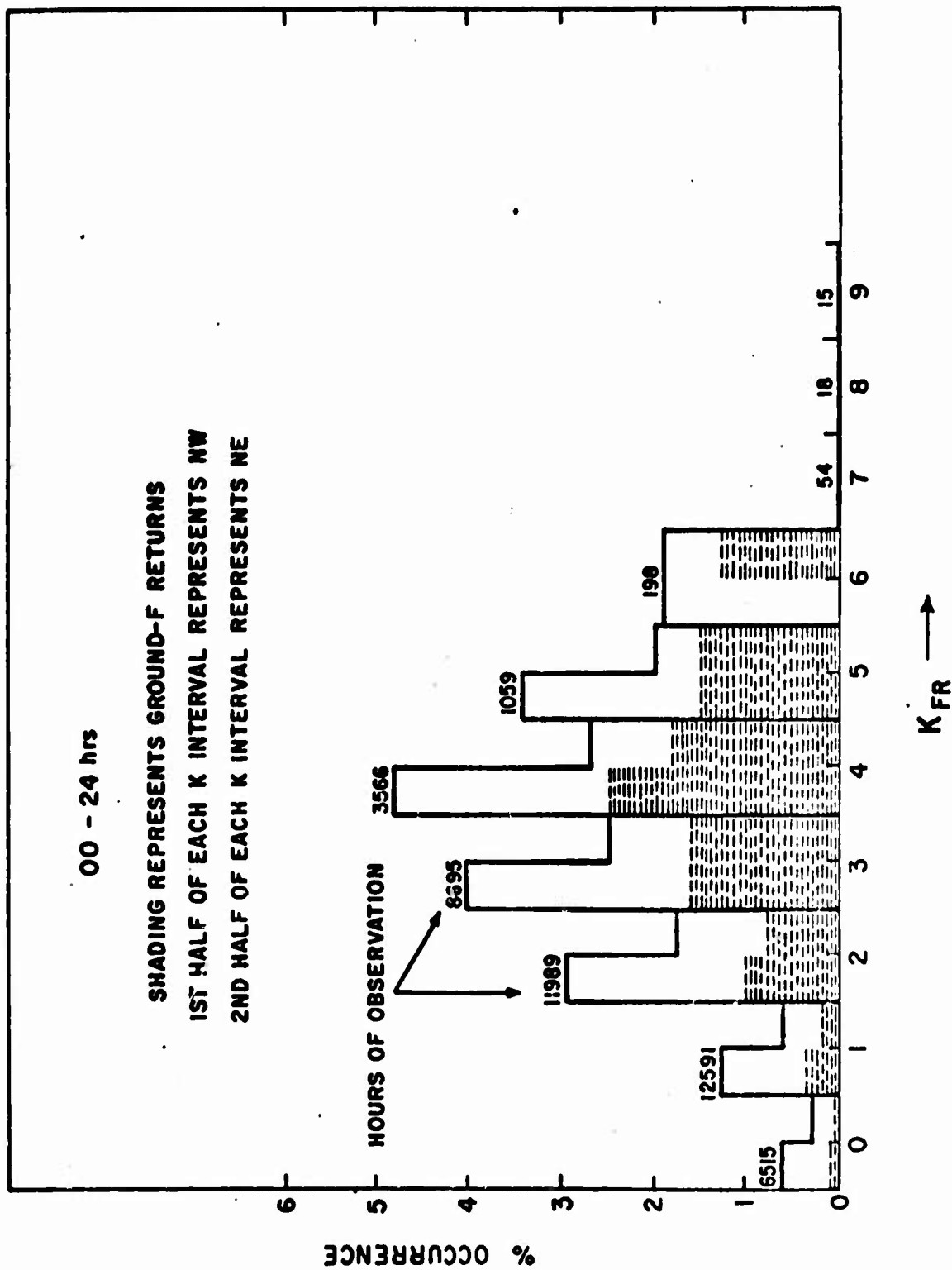


FIG. 25a FAE (F) AS A FUNCTION OF MAGNETIC INDEX KFR

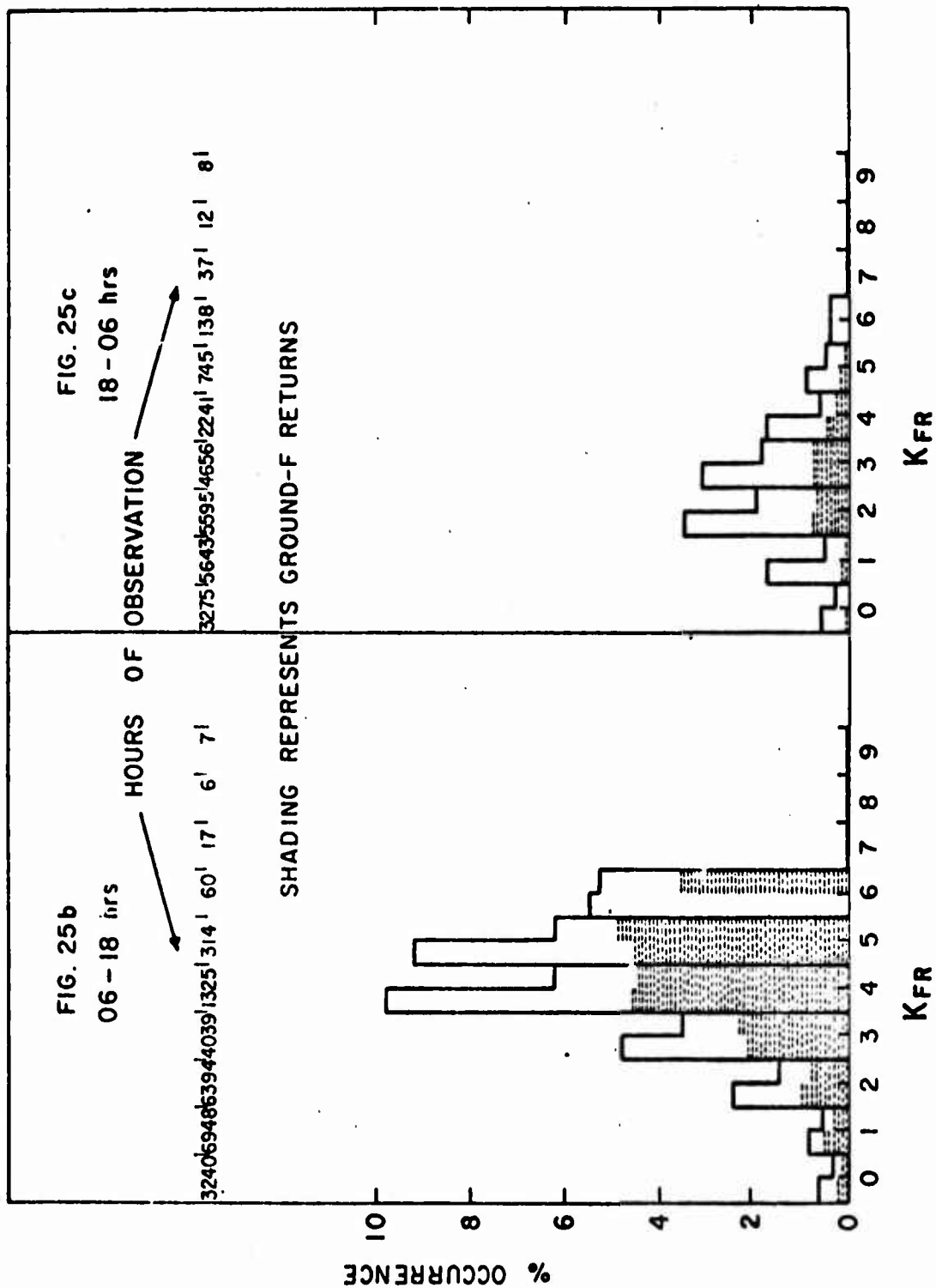


FIG. 25b & 25c. FAE(F) AS A FUNCTION OF MAGNETIC INDEX  $K_{FR}$

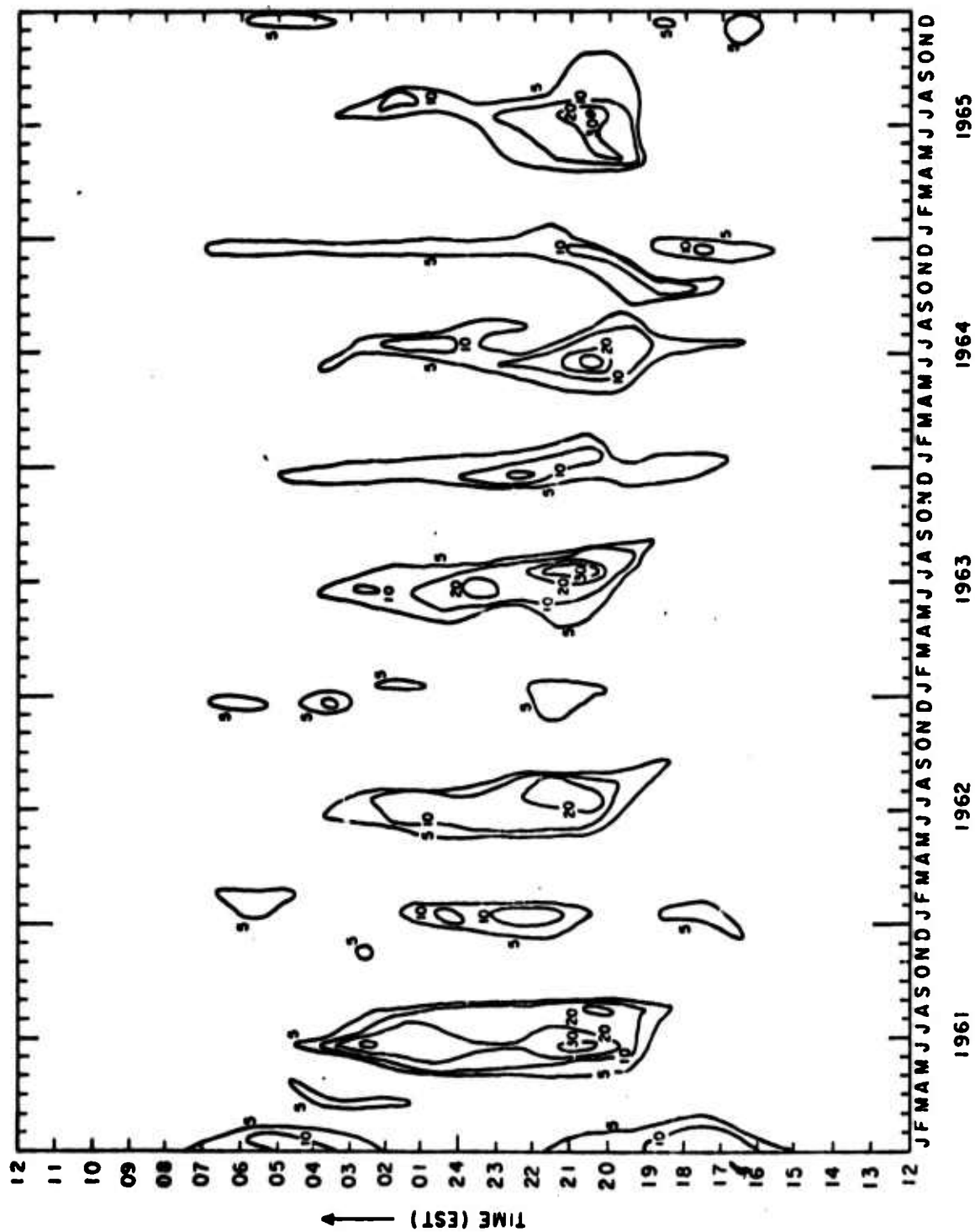


FIG. 26. PERCENTAGE OCCURRENCE CONTOURS OF E-LAYER ECHOES FOR  $K_p$  0-3 FOR 1961-1965

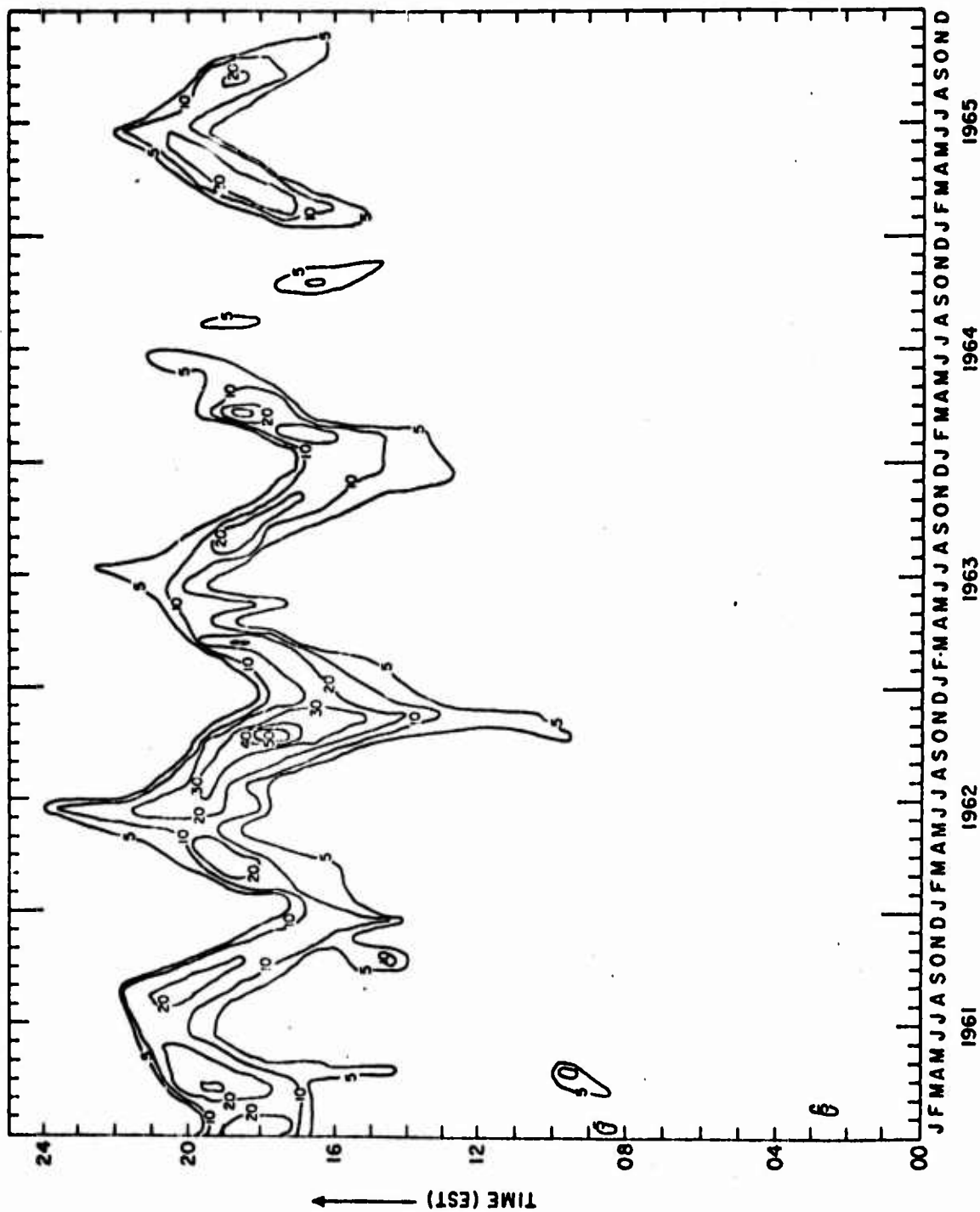


FIG. 27. PERCENTAGE OCCURRENCE CONTOURS OF F - LAYER ECHOES FOR K<sub>fr</sub> 0-3 FOR 1961-1965



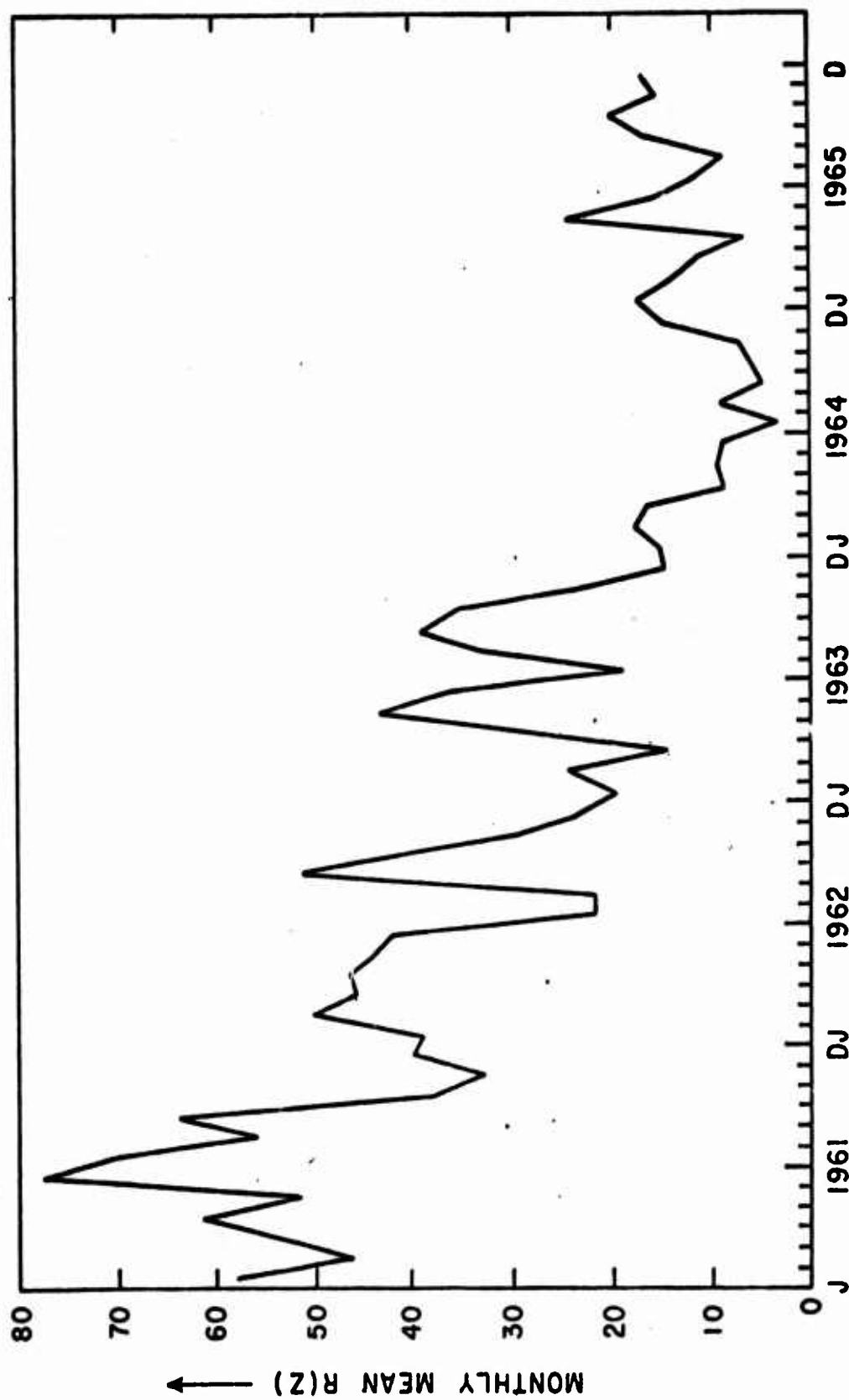


FIG. 28. MEAN ZURICH SUNSPOT NUMBERS FOR 1961-1965

## REFERENCES

- Aarons, J., H.F. Auroral Backscatter and the Scintillation Boundary in "Radar Propagation in the Arctic", AGARD Symposium, Lindau, Germany, Sept., 1971.
- Aarons, J., and R.S. Allen, "Scintillation Boundary during Quiet and Disturbed Magnetic Conditions", J. Geophys. Res., 76, 170, 1971.
- Aarons, J., J.P. Mullen, and Sunanda Basu, "Geomagnetic Control of Satellite Scintillations", J. Geophys. Res., 68, 3159, 1963.
- Agy, V., A Model for the Study and Prediction of Auroral Effects on HF Radar in "Radar Propagation in the Arctic", AGARD Symposium, Lindau, Germany, Sept., 1971.
- Bates, H.H., "The Aspect Sensitivity of Spread-F Irregularities", J. Atmos. Terr. Phys., 33, 111, 1971.
- Booker, H.G., "Radar Studies of the Aurora", Physics of the Upper Atmosphere, edited by J. A. Ratcliffe, Academic Press, New York, 1960.
- Bowles, K.L., "Radio Wave Scattering in the Ionosphere", Advances in Electronic and Electron Physics, edited by L. Morton, Academic Press, New York, 1964.
- Chamberlain, J.W., Physics of the Aurora and Airglow, Academic Press, New York, 1961.
- Keck, R.D., and G. L. Hower, "Backscatter Radar Observations at WSU - 1957-1966", Washington State University, College of Engineering, Research Report 68/16-45, Pullman, Washington, 1968.
- Leadabrand, R.L., Electromagnetic Measurements of Auroras in "Symposium on Auroras", Palo Alto, California, January, 1964.
- Malik, C., and J. Aarons, "A Study of Auroral Echoes at 19.4 Megacycles per Second", J. Geophys. Res., 69, 2731, 1964.

Mendillo, M., M.D. Papagianis, and J.A. Klobuchar, "A Seasonal Effect in the Mid-latitude Slab Thickness Variations During Magnetic Disturbances", J. Atmos. Terr. Phys., 31, 1359, 1969.

Paulikas, G.A., "The Patterns and Sources of High Latitude Particle Precipitation", Rev. Geophys. Space Phys., 9, 659, 1971.